“TIQXMMI” MILLIY TADQIQOT UNIVERSITETI HUZURIDAGI FUNDAMENTAL VA AMALIY TADQIQOTLAR INSTITUTI HUZURIDAGI ILMIY DARAJALAR BERUVCHI DSc.03/31.03.2022 T/FM.10.04 RAQAMLI ILMIY KENGASH

FUNDAMENTAL VA AMALIY TADQIQOTLAR INSTITUTI

XOLIKOV SHUKIRJON SODIKOVICH

QUYOSH ICHKI QATLAMLARI XUSUSIYATLARINI FAZO-VAQT GELIOSEYSMIK USULLAR ORQALI TEKSHIRISH

01.03.01 – Astronomiya
(fizika-matematika fanlari)

E’LON QILINGAN ILMIY ISHLAR BO‘YICHA DISSERTATSIYASIZ FIZIKA-MATEMATIKA FANLARI BO‘YICHA FAN DOKTORI (DSc) ILMIY DARAJASINI OLISH UCHUN TAQDIMNOMA

Toshkent – 2023

UDC 530.12.531.51

Presentation on awarding the scientific degree of Doctor of Sciences (DSc)
in astronomy on the basis of published papers
without a dissertation

Astronomiya ixtisosligi bo‘yicha fan doktori (DSc) ilmiy darajasini olish uchun dissertatsiyasiz, chop etilgan ishlar asosida taqdim etish

Представление по присуждению ученой степени доктора наук (DSc) по специальности астрономия на основе опубликованных работ без диссертации

SCIENTIFIC COUNCIL DSc.03/31.03.2022.T/FM.10.04 ON AWARD OF SCIENTIFIC DEGREE AT THE INSTITUTE OF FUNDAMENTAL AND APPLIED RESEARCH UNDER THE NATIONAL RESEARCH UNIVERSITY "TIIAME"

INSTITUTE OF FUNDAMENTAL AND APPLIED RESEARCH

XOLIKOV SHUKIRJON SODIKOVICH

PROBING THE SUBSURFACE PROPERTIES OF THE SUN WITH TIME-DISTANCE HELIOSEISMOLOGY

01.03.01 – Astronomy
(physical and mathematical sciences)

PRESENTATION
on awarding the scientific degree of Doctor of Science (DSc)
in astronomy on the basis of published papers
without a dissertation

Tashkent – 2023

The subject of the DSc research is registered by the Supreme Attestation Commission of the Cabinet of Ministers of the Republic of Uzbekistan under B2022.3.DSc/FM202.

The research work results have been carried out at Nice University (France), Tsing-Hua University (Taiwan), National Solar Observatory (USA) and Institute of Fundamental and Applied Research, TIIAME National Research University (Uzbekistan).

Presentation abstract of scientific research in three languages (Uzbek, English and Russian (only conclusions)) is posted on the webpage at the address www.ifar.uz and Information-educational portal "Ziyonet" (www.ziyonet.uz).

Presentation of the scientific research will take place on the " _01_ " _august_ 2023 at _16^{00}_ in the meeting of the Scientific Council No. DSc.03/31.03.2022T/FM.10.04 at the Institute of Fundamental and Applied Research under the "TIIAME" National Research University (Address: 100000, Tashkent city, Qori Niyaziy Street 39, Institute of Fundamental and Applied Research, Hall 108; tel.: 71 237-09-61.; e-mail: info@ifar.uz

The DSc presentation abstract can be looked through at the Information Resource Center of the Institute of Fundamental and Applied Research under the "TIIAME" National Research University (registered under № ____). (Address: 100000, Tashkent city, 39 Qori Niyaziy str., Institute of Fundamental and Applied Research, hall 205; ph.: 71 237-09-61)

The presentation abstract of the scientific research was distributed on "___" _____, 2023.

(Registry record № ___ dated "___"_____, 2023)

B.J. Ahmedov
Chairman of the Scientific Council
on Award of Scientific Degrees,
DSc, Professor

E.X. Karimbayev
Scientific Secretary of Scientific Council
on Award of Scientific Degrees, PhD

INTRODUCTION (presentation abstract)

Relevance and necessity of the topic. Helioseismology provides detailed insights into the internal structure and dynamics of the Sun. By studying the propagation of acoustic waves on the Sun's surface, scientists can infer information about the temperature, density, and composition of different layers within the solar interior. This knowledge helps us understand how the Sun's structure evolves over time and contributes to our understanding of stellar evolution in general. Helioseismic investigations allow us to study various physical processes occurring within the Sun. For example, by analyzing the oscillations of the Sun's surface, researchers can probe the convection processes in the outer layers, the rotation rates at different depths, and the magnetic activity associated with sunspots and solar flares. These studies provide valuable information about the mechanisms driving solar activity and energy transport. The Sun's magnetic activity, including solar flares and coronal mass ejections (CMEs), can have significant impacts on space weather. Helioseismic investigations help in understanding the underlying mechanisms and processes that drive these solar eruptions. By monitoring the changes in the Sun's interior through helioseismic techniques, scientists can identify precursor conditions and patterns that may indicate the likelihood of solar flares or CMEs, thus aiding in space weather forecasting and prediction. Helioseismic data serves as a critical benchmark for testing and refining solar models and theories. By comparing observational results with theoretical predictions, scientists can validate or modify models of stellar evolution, energy transport, and magnetic field generation. Helioseismology provides a unique way to test and improve our understanding of the fundamental processes occurring within stars. Helioseismic investigations have broader implications for solar and space research. The knowledge gained from helioseismology contributes to our understanding of other stars, their evolution, and their internal dynamics. Additionally, studying the Sun's magnetic activity and space weather helps us better prepare and mitigate the impacts of solar storms on Earth's technological infrastructure, such as satellite communications, power grids, and astronaut safety. Advanced techniques in helioseismology, such as time-distance helioseismology and ring-diagram analysis, continue to improve our understanding of the Sun's interior. These methods involve studying the propagation of seismic waves on the solar surface and inferring information about the internal structures. Further advancements in seismic tomography techniques may provide the capability to image the solar core with higher resolution and precision. In summary, helioseismic investigations are relevant and necessary for advancing our understanding of the Sun, its internal processes, and its impact on space weather. By providing insights

into solar structure, dynamics, and magnetic activity, helioseismology plays a crucial role in advancing astrophysics, improving solar models, and enhancing our ability to predict and mitigate the effects of space weather.

International context of the research. Helioseismology is a highly collaborative field of research that involves scientists from various countries working together to advance our understanding of the Sun's interior. International collaborations enable the sharing of data, expertise, and resources, allowing researchers to tackle complex problems and achieve more comprehensive results. Helioseismic observations require advanced instruments and facilities to capture high-resolution data of solar oscillations. Several international observatories and space-based missions, such as the Solar Dynamics Observatory (SDO) by NASA and the Solar and Heliospheric Observatory (SOHO) by NASA and ESA, contribute to helioseismic studies. These missions involve the participation of scientists and engineers from multiple countries, emphasizing international cooperation in solar research. International collaboration is crucial for the validation of helioseismic models and techniques. Multiple research groups independently analyze data and compare their results, ensuring the consistency and reliability of findings. This process helps identify potential biases, uncertainties, or limitations, leading to the refinement of models and techniques. The international context of helioseismic studies demonstrates the shared commitment among researchers worldwide to advance our understanding of the Sun's interior. Collaboration, data sharing, and the exchange of knowledge and resources are vital components of this global scientific endeavor.

Current state of the research on the topic. Time-distance helioseismology is a technique used to study the interior of the Sun by analyzing the propagation of acoustic waves on its surface. It provides valuable insights into the structure and dynamics of the solar interior, including the convection zone, radiative zone, and the core. Time-distance helioseismology has been instrumental in mapping the rotation profile of the Sun. By measuring the travel times of acoustic waves across the solar surface, researchers can infer the rotation rate at different depths. This has led to the discovery of differential rotation, where the Sun's equator rotates faster than its poles. Time-distance helioseismology has also been used to study the relationship between subsurface flows and solar activity, such as sunspots and solar flares. Researchers have found that these phenomena are often associated with localized perturbations in the subsurface flow patterns. The technique has provided detailed observations of the Sun's acoustic oscillations, known as p-modes. These oscillations reveal information about the Sun's internal structure, such as temperature, density, and sound speed variations.

Time-distance helioseismology has enabled the measurement of these parameters with high precision. Researchers have used time-distance helioseismology to investigate the meridional flow, which is a large-scale circulation pattern in the solar interior. By tracking the movements of acoustic waves, scientists have been able to study the dynamics and variability of this flow. The emergence of new magnetic fields plays a vital role in the overall dynamo process of the Sun. By studying emerging active regions, scientists can gain insights into how magnetic fields are generated and transported from the solar interior to the surface. This knowledge helps in understanding the Sun's magnetic cycle, which has an approximately 11-year period and influences solar activity over time.

Connection of the research topic with the research activities of the institution. Observational data for DSc research were obtained in frame of three ground base and one space based international projects: International Research on the Interior of the Sun (IRIS), Taiwan Oscillation Network (TON), Global Oscillation Network Group (GONG) and Michelson Doppler Imager (MDI, SOHO/NASA). Computational part and research were performed at facilities of Astronomical Institute of Academy of sciences of Uzbekistan, Nice University(France), Tsing-Hua University (Taiwan), National Solar Observatory (USA) in corporation with different groups of various universities and teams in France, Germany, UK, Spain, Taiwan, USA.

The aim of the research work is to perform analysis of helioseismic observations obtained from ground and space; Study of internal structure of the sun, in particular: subsurface flow structure and its time evolution; active regions and their interaction with solar acoustic oscillations; latitude and depth profile of solar meridional circulation.

The tasks of research are:

develop statistically robust and intercalibrated data analysis pipelines to perform helioseismic analysis of huge amount;

accurate measurements of parameters of low degree solar oscillations, extract scientific outcomes and interpret obtained results;

study of time-distance relations of solar oscillation observations performed using high resolution detectors;

measurements and understanding of mechanism of emerging active regions in the deep solar convective zone;

develop new methods of frequency-space filtering of high resolution doplergramms and implementation them into regular routines of helioseismic data analysis tools;

perform solar meridional flow measurements using all available dataset, construct latitude and depth profile the flow.

The object of the research is helioseismic observables obtained within international projects: sun as a star and high resolution solar dopplergrams obtained both, from ground and space.

The subject of the research is the measured properties and characteristics of solar oscillations, frequency and other parameter tables, developed models of solar internal structure.

Methods of the research are: development of pre-processing and science extraction procedures in modern computational facilities. Enhancing solar acoustic signal by filtering out non-desired source of co-existing components from observables. Probing the local and global scale structures in the sun by measuring acoustic wave parameters. We use our method of reconstruction of solar oscillation image using spherical harmonic coefficients which has been filtered or tuned for specific measurements. Such inverse spherical harmonic decomposition carries in spherical coordinates. Acoustic travel time measurements also we generate only using spherical geometry which is crucial for probing deep layers of solar interior.

The scientific novelty of the research is in the following:

first measurements of frequency tables of solar oscillations of low degree are provided to solar physics community;

for the first time solar internal rotation estimates were obtained using IRIS frequency splitting coefficients;

for the first time the image of the sunspot beneath solar surface is constructed using properties of acoustic waves;

active region emerging from the base of solar convective zone is detected at 40-75 Mm below the surface 1-2 days earlier when it reaches the surface;

new method employed allowed to measure solar acoustic radius with exceptional precision;

we found evidence to suggest that the apparent second-cell structure reported by some members of the solar physics community at high latitudes is not associated with the surface component of the meridional flow;

Equatorward return meridional flow component recovered using ground based GONG observations.

Practical results of the work. Precise frequency measurements of low degree solar acoustic oscillations were performed. It has been demonstrated that measuring the solar acoustic radius with superior precision is possible by helioseismic methods. Moreover, observations from earth provide the same level precision. Low degree helioseismic techniques

can be applied to astroseismology observations. Detecting active regions before they appear on the surface is very potential tool for space weather forecasting. Measurements of poleward and return meridional flow are valuable ingredients for solar dynamo simulations and understanding the solar activity cycle.

The reliability of the research results is demonstrated by analyzing data obtained by four independent instruments. Geographical location and difference in atmospheric conditions and measuring at different height of solar atmosphere provided natural calibrating possibilities of solar acoustic oscillation parameters by having common signal in all observations. Most of the obtained scientific results are generated from at least two independent project data. Majority of recovered internal structure properties reproduced from both, ground based and data obtained in space.

Significance of research results. Most of the presented results here has not been earlier by other scientists or research groups. As an example, an inverse spherical harmonic decomposition of surface oscillations of the sun is developed and applied by author of this work. Active region imaging below the surface and meridional return flow measurements were waiting their discovery for years.

Implementation of the research results. Measurements performed in this study were used as a key ingredient in many solar physics related investigations. Theoretical solar dynamo simulations used return meridional flow profile in order to generate butterfly diagramm in their models. Poleward meridional circulation speed from our measurements is the most important component in the flux transport mechanism based models of polar regions, which play important role to forecast solar activity cycle.

Publications of the research results. The results obtained in frame of this DSc work are presented in 18 peer-reviewed articles published in prestigious scientific journals recommended by the Supreme Attestation Commission of the Republic of Uzbekistan for publication of the main scientific results of DSc thesis and displayed in the Web of Science scientific database.

Structure and volume of presentation. The presentation consists of an introduction, five chapters and a conclusion. The size of the presentation is 116 pages.

MAIN CONTENT OF THE WORK

Introduction. The results obtained here are published by candidate and his co-authors in 18 articles. Covered research observations are obtained within international projects: International Research on the Interior of the Sun (IRIS), Taiwan Oscillation Network (TON), Global Oscillation Network Group (GONG), Michelson Doppler

Imager (MDI, NASA/SOHO). All papers are published in international journals and presented at many related international conferences. The topics of publications cover full disk and high resolution helioseismic data analysis during the last 25 years. Most of the results in these articles are obtained by using time-distance relation of solar acoustic waves trapped in solar cavities. Helioseismology has emerged as one of the most important tools for studying the internal structure and dynamics of the Sun over the past three decades. It utilizes the study of solar oscillations to probe the Sun's interior and provides valuable insights into its physical properties. Here, several contributions of candidate into this field are presented.

Section 1. Global helioseismology using the sun as a star observations.

In this section, scientific results derived from IRIS project are presented. One of the IRIS instruments was installed in Kumbel site, located near the Chimgan mountain (Uzbekistan). Author of this manuscript participated in all phases, building the station, obtaining observations, data analysis and scientific interpretations of results in frame of IRIS project. The first work (Fossat et al., A&A, 1999) is this section is devoted to practical problem of the ground based astronomical observations, gap in the time series. The reason of the gap can be atmospheric conditions, instrumentation malfunctions and et cetera. But more fundamental gap in solar observations which we can not avoid is night time. In particular, the helioseismology requires continuous measurements of very long duration, months to years. This work addresses the specific and limited case of full disk measurements of p-mode oscillations, although it can be generalized, to some extent, to the case of imaged helioseismology. First, a method of mode by mode (or rather pair of modes by pair of modes) interpolation of the signal in gaps is tested, and shown to be efficient for gaps as long as two days, but limited to the frequency range where the signal to noise ratio is good. It is then noted that the autocorrelation function of the full disk signal, after dropping quickly to zero in 20 or 30 minutes, shows secondary quasi periodic bumps, due to the quasi-periodicity of the peak distribution in the Fourier spectrum (first 0.5 hours in Fig. 1). The first of these bumps, at 4 hours or so, is higher than 70 percent and climbs to nearly 90 percent in limited frequency ranges (envelope around 4 and 8 hours). This suggests that an easy gap filling method can be developed, with a confidence of nearly 90 percent across all the frequency range, as long as the gap does not exceed 8 hours, with at least 4 hours of data at both ends. Even a short gap of one or two periods is better filled by the data taken 4 hours earlier or later than by local interpolation. This relaxes quite considerably the requirement of continuity of the observations for the case the full disk p-mode helioseismology.

Applied to 7 years of IRIS data, this method permits the detection of all low frequency p-modes already seen by 2 years of the GOLF (Global Oscillations at low frequencies, NASA/SOHO) instrument data, and makes possible the measurement of their frequencies with an accuracy consistent with the partially filled 7 years of statistics. All helioseismological instrumental programs during the last twenty years have aimed at obtaining the best temporal coverage, 24 hours per day and 365 days per year. This is mainly for the sake of avoiding the presence of "sidelobes" in the Fourier spectra. These sidelobes are produced by the convolution of the Fourier transform of the true signal by the Fourier transform of the temporal window function, which generally contains at least the one-day periodicity when the observations are made from the ground. In the Fourier domain, each peak, signature of a solar oscillation, is then spread over the Fourier transform of the window function, with secondary peaks, or sidelobes, which will unavoidably interfere with other real peaks, thus making accurate p-mode parameters measurements difficult (Fassat et al., A&A, 1999).

The window effect is a convolution in the Fourier space, for which the deconvolution is obviously impossible: by Fourier transform, a convolution becomes a multiplication, and we already know that in the time domain, we have the multiplication of the true signal by the window function made of 1 or 0. The deconvolution in the Fourier space is the division in the time domain, which cannot be done with the zeroes. Several methods of approximate deconvolution have then been attempted, to provide corrected power spectra, without access to the approximation of the true signal in the time domain. See for instance the theses of Loudagh (Loudagh S., 1995, Thesis, Universit de Nice) and Pantel (Pantel A., 1996, Thesis, Universit de Nice). These methods work to some extent, reducing the sidelobe amplitudes and pulling back inside the peaks some of the power which was spread around. However, they are less and less efficient with reduced duty cycle, and they work already badly around 50 percent. An important point is that they completely ignore the specific properties of the solar oscillation signal, so that they are clearly not optimized for our problem. The other approach is to take into account what we know of the solar signal and to see how reliably we can try and imagine the signal which has not been observed. Gaps of a few periods duration can be efficiently filled, provided the signal to noise ratio is high enough and the duty cycle of the observations is not less than 50 percent. Unfortunately, the typical periods of solar oscillations are short (a few minutes), so that many gaps, longer than, say, 15 to 20 minutes, remain unfilled or badly filled, and the signal to noise ratio becomes evidently poor at both ends of the spectral range, where the best possible duty cycle becomes quite crucial.

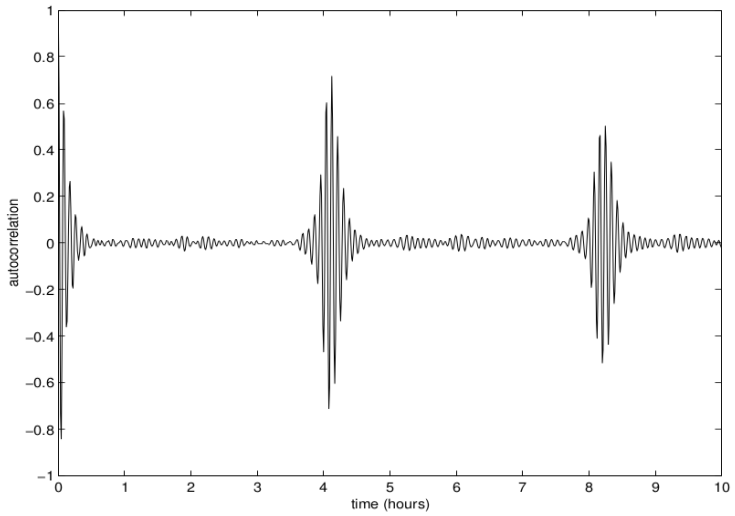

Fig. 1. The first ten hours of the IRIS data autocorrelation (filtered in the p-mode range, from 1.5 to 5 mHz) shows that beyond the quick drop at the beginning, there are secondary bumps around 4 and 8 hours. They are due to the quasi-periodicity of the peaks in the Fourier spectrum. The important point is that the second maximum is higher than 70 percent, and shows that the signal obtained after 4 hours is more correlated than the signal obtained after one period of 5 minutes. An easy and very efficient method of gap filling can be deduced from this simple fact.

However, we know that each individual oscillation has a coherence of several days, even much longer in the lower part of the frequency range. So, if we could isolate the spectrum of one single mode, it would be made of a single peak surrounded by the window function. An inverse Fourier transform would then provide this single mode oscillation, multiplied by the window function, i.e. by gaps. Amplitude and phase are changing slowly, losing memory only after several days. In this ideal case, the signal in gaps could be reliably interpolated up to duration of the order of half the coherence time, a good fraction of several days.

We have then seen that the short gaps (a few periods) can be filled efficiently because the velocity signal has a memory that lasts a few periods, as shown by the autocorrelation function. Now, as shown by (Gabriel et al., A&A, 1998), it is extremely interesting to have a look at this autocorrelation function somewhat further than the first half hour. Fig. 1 shows the first 10 hours of the IRIS autocorrelation function (Gabriel et al. show the same for the GOLF signal). We have filtered the signal in the p-mode frequency range (from 1.5 to 5 mHz). It appears that the signal has a very high level of coherence after a little bit more than 4 hours. It is above 70 percent, and this is significantly greater than its coherence after just one period of 5 minutes. It has been interpreted by Gabriel et al. as the consequence of the almost equally spaced frequency peaks in the Fourier domain. But it has an additional extremely important consequence to be noted here: it means that very much like in many musical songs, or preludes, or sonates, etc, the original signal is almost periodic in time, with a quasi periodicity of a little more than 4 hours. An obvious consequence is that simply replacing a gap by the

signal collected 4 hours earlier or 4 hours later provides a gap filling method with more than 70 percent confidence. Surprisingly, even filling a gap as short as 5 minutes is better done by means of the data obtained (if so) 4 hours earlier than by interpolating the nearby data before and after the gap.

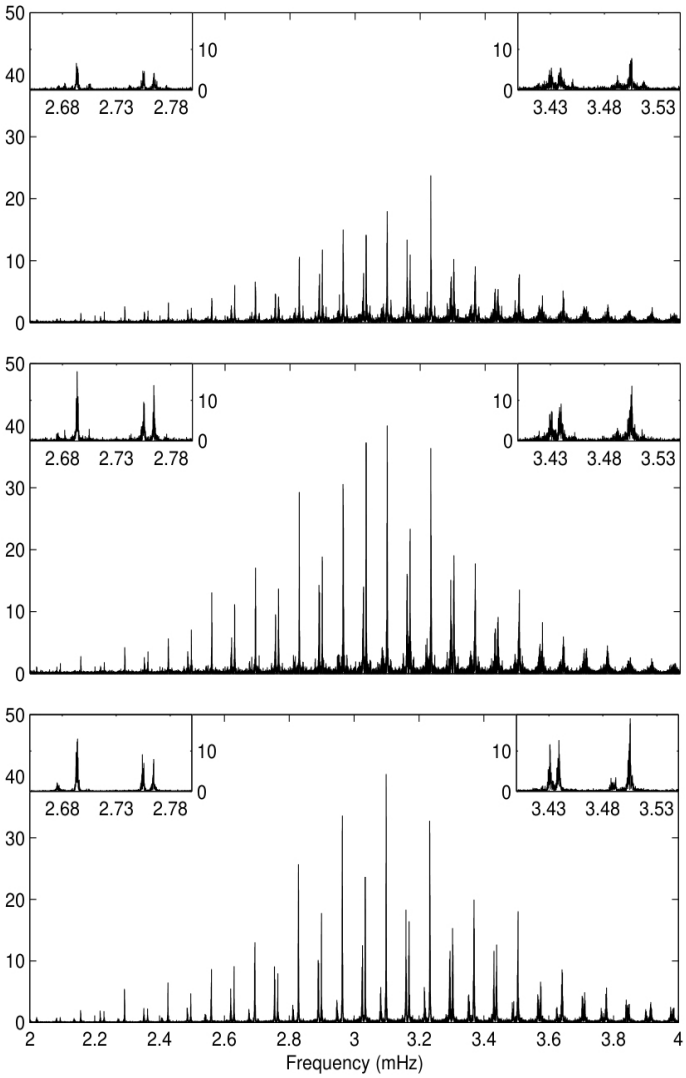

Fig 2. The upper part is the direct (averaged) power spectrum of the 4 summer seasons of the IRIS network data, from 1989 to 1992. Each file has a duration of 136.5 days, so that the frequency resolution is equal to 0.085 μHz. The perturbation of this power spectrum by the window function is clearly visible in the magnified small samples. The middle part is the same power spectrum obtained by means of a Richardson-Lucy deconvolution. Each peak is roughly multiplied by the inverse of the duty cycle, which means that a large part of the surrounding noise was only due to the window function and has been pulled back inside the peak. However, it is not optimized, and the sidelobe structure, although reduced, is still visible. The lower part shows the same power spectrum now obtained after the pairof-modes by pair-of-modes gap filling. The background noise is dramatically reduced, and the sidelobes structure is fully eliminated. See the text for more information on the limits of the method.

Fig. 2 (top) shows the direct power spectrum of this data set. It is an average of the 4 individual spectra, with a resolution of 0.085 μHz. Middle panel shows the power spectrum of the same data obtained after a deconvolution of the window function by means of the Richardson (Richardson W.H., 1972, JOSA 62) and Lucy (Lucy L.B., 1974, AJ 79) algorithm. In lower panel the power spectrum of the same data now obtained after the gap filling method briefly described here above is presented. The improvement is really spectacular. Individual p-mode profiles are much cleaner and most of the sidelobs are gone and peak-fitting procedure can provide more robust and stable measurements of profile parameters. However, main importance of this particular gap filling method in scopus of our future approach is time-distance relations of acoustic waves trapped in solar cavity. In global helioseismology era (projects like IRIS, GOLG, BiSON) time-distance relations were not established yet and no one interpreted the signal at 4 hour in autocorrelation functions as the same signal arrived back traveling about 4 solar radius distance. Most of measurements in the next sections will be based on using time-distance relation of acoustic waves.

In the next two works (Gelly et al., A&A, 1997, Serebryanskiy et al., NewAstr, 2001) here complete details of solar oscillation frequency measurements using groundbased observations. The IRIS network for helioseismology has operated since 1989. In (Gelly et al., A&A, 1997) the tables of solar p-mode frequencies for observations taken during the four summer seasons from 1989 to 1992 are presented. This analysis uses the technique of maximum likelihood fitting and a χ 22 model for the probability density function of the spectrum. The simultaneous fitting of odd and even pairs of peaks strengthens the identification of the $l = 3 - 1$ eigenmodes and improves the error bars on the $l = 2 - 0$ group. The frequencies are in good agreement with other observational results and with theoretical values for the D_0 and the $\Delta\nu$ parameters of the asymptotic approximation. A decrease of 0.25 ± 0.12 μHz is seen between the 1989 and the 1992 data sets. The change is associated with the decrease of solar activity and is comparable with results of previous studies.

The simple model of a solar eigenmode as a damped one-dimensional oscillator has been used. This model allows one to assume that the peaks in the natural Fourier spectrum are asymptotically described by Lorentz profiles. In Fig 3 an example of lorentzian fit of $l = 2 - 0$ (left) and $l = 3 - 1$ (right) pairs is presented. It should be noted that sidelobe peaks located at 11.57 mkHz around the main peaks needs to be taken into account because 24 hour periodical gaps in most ground based observations are common. In (Serebryanskiy et al., NewAstr, 2001) an extra parameter is included into lorentz function to estimation of the peak profile asymmetries.

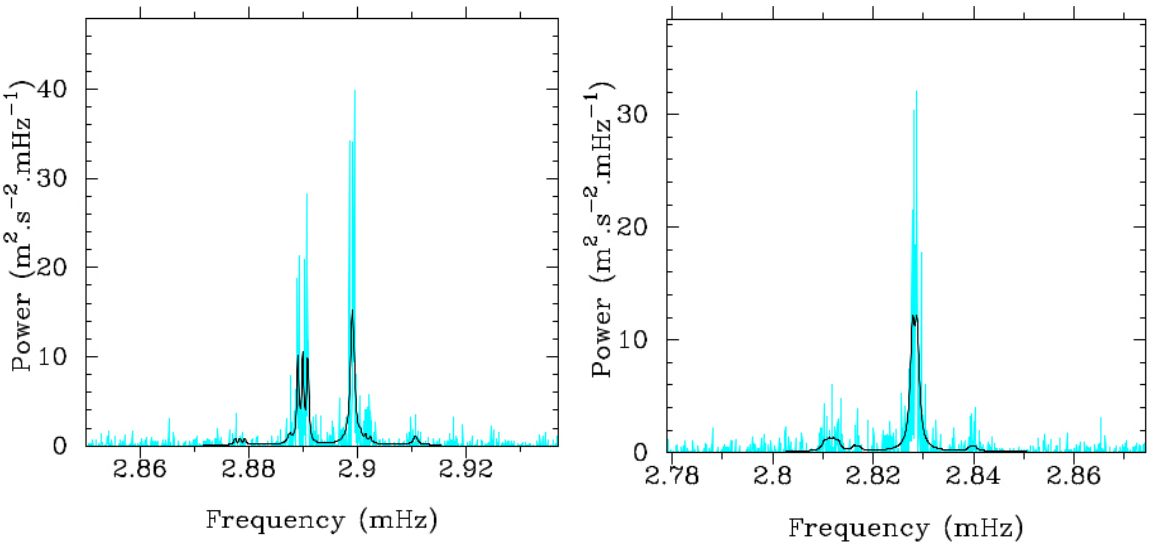

Fig. 3. Power spectra of $l = 2$ and $l = 0$ modes for $n = 20$ and $l = 1$ and $l = 3$modes for $n = 19$.

It has been suggested that this asymmetry could be the result of an interaction between a localised (in depth) source of acoustic power and the resonant cavity of the mode, as well as by a correlation between the resonance and the solar noise (Nigam et al., ApJ, 1998), and would be significantly different for Doppler or photometric data. Moreover, the change of altitude of the upper boundary of the resonant cavity with frequency would also result in a dependence of the asymmetry on the frequency (Unno, Nonradial Oscillation of Stars, 1989). Neglecting the asymmetry in the line profile fitting would then imply systematic errors in the estimation of the mode frequencies.

In (Gizon et al., ApJ, 1997) four time series of IRIS data (4 to 6 months) have been used to obtain improved measurements of the low degree ($l = 1,2,3$) rotational splitting frequencies. Assuming that the rotation law is known in the outer layers of the Sun, we investigate the implications of IRIS splittings for the central regions. Both a one-shell and a two-shell rotation model have been considered in the solar core. A core rotating slightly faster than the outer radiative envelope provides the best fit to the data. Some evidence for the reliability of the observations is shown by the visibility of differential rotation in the $l = 3$ multiplets. This was first confirmation of slow rotating of solar core from real observations!

Section 2. Local helioseismic analysis of high resolution solar observations.

In observational helioseismology, such basic parameters of individual oscillation modes as the frequencies, line widths, and amplitudes have been determined by analyzing their power spectra (Serebryanskiy et al. NewAstr, 2001; Fossat et al. A&A, 2003). By now, all these parameters have been measured with a high accuracy, and their

variations with solar cycle have been studied. The observed frequencies are in good agreement with their theoretical values. These measurements were based mostly on the Fourier expansions of helioseismic time series of intensities or Doppler velocities. With the advent of the new method for analyzing helioseismic data (time–distance analysis) that was first developed by (Duvall et al., Nature, 1993), it became possible to study the physical parameters of local regions near the solar surface by analyzing the perturbations of the travel time of the acoustic-mode wave packets produced by local inhomogeneities. In addition, such methods of local diagnostics of the solar interior as acoustic holography (Roddier, Comptes Rendus, 1975; Lindsey and Braun, ApJ, 1990; Braun et al., ApJ, 1992), acoustic imaging (Chang et al., ApJ, 1997), and other methods (Chou et al., ApJ, 2002) based on time-distance relations have been developed. In contrast to the standard methods of analysis, all calculations in time–distance analysis are performed in the time domain rather than the frequency domain. The main idea of this method is to measure the travel time of acoustic waves on the Sun, which, in turn, provides information about the properties of the matter, the speed of sound, the magnetic field, and the flows. On the Sun, acoustic waves propagate in an inhomogeneous, anisotropic, and dispersive medium. In contrast to terrestrial seismic waves whose source is localized, solar waves are generated stochastically, by many sources in the subsurface layer of the convective envelope, and individual sources cannot yet be observed. The acoustic signal that reaches the solar surface is reflected and propagates back to the solar interior, bends its path due to an increase in the speed of sound with depth, and again returns to the surface, emerging at a certain distance from the starting point. Different waves (with different frequencies and spatial sizes) follow different path and reach the surface in different time intervals and at different distances from the starting point. However, modes with the same angular phase velocity ω/l (where ω is the cyclic frequency, and l is the degree of the acoustic mode) follow approximately the same ray path (Duvall, Nature, 1982). These modes form a wave packet that propagates from point to point on the solar surface. The relationship between the travel time and the angular distance traversed by the wave packet can be obtained by constructing a cross-correlation function (Duvall et al. Nature, 1993). Each point on the time-distance curve corresponds to the wave packet formed by modes with equal values of ω/l.

The cross-correlation function of oscillating signals f for two points with coordinates r_1 and r_2 on the solar surface is defined as

$$C(\tau, \Delta) = \int_0^T f(r_1, t+\tau) f(r_2, t) dt$$

where Δ is the angular distance between the two points, and T is the total duration of the observations. The delay τ specifies the time shift between the two signals.

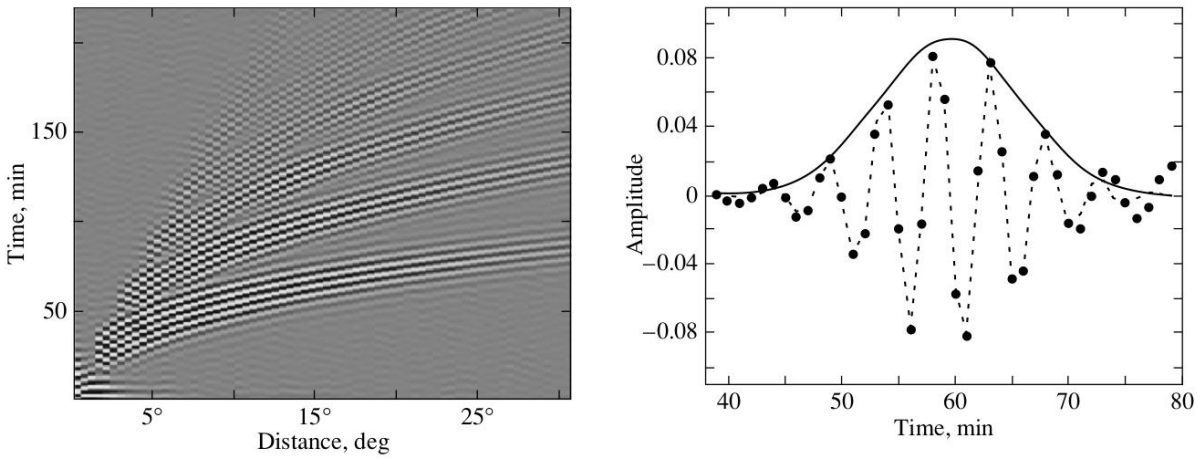

Fig. 4. Cross-correlation function calculated from the TON one-day series (left). Cut of the cross-correlation function for Δ ≈ 15° and its fit by the Gabor function (for clarity, the Gabor envelope is shown).

The cross-correlation function (in Fig. 4) for any fixed Δ has several maxima that correspond to the next appearances of wave packets on the solar surface. These maxima occur at certain values of the time required for a wave packet with a given angular phase velocity to propagate from one point of the surface to the other, following a certain ray path. Since the appearances of a wave packet on the solar surface have a bouncing pattern, these are called bounces. To isolate a certain frequency range of p-modes, the following Gaussian frequency filtering is applied to the data:

$$e^{-0.5\left(\frac{\nu-\nu_0}{\omega}\right)^2}$$

Where ν_0 is the central frequency, and ω is the width of Gaussian filter; as a result, the cross-correlation function $C(\tau, \Delta)$ is described by the Gabor function

$$G = Acos\left[2\pi\nu\left(t-\tau_{ph}\right)\right]exp\left[\frac{-(t-\tau_{en})^2}{2\sigma^2}\right]$$

Here, A, ν, and σ are the amplitude, central frequency, and envelope width of the Gabor function, respectively; τ_{ph} and τ en are the propagation times of the wave-packet phase and envelope, respectively (Duvall et al., Nature, 1993).

Fitting the cross-correlation function at all angular distances, we obtain the time–distance curve (Fig. 5). Each point (Δ, τ) on this curve corresponds to the oscillation modes that have the same angular phase velocity ω/l and that form a wave packet propagating roughly along the same ray path, where τ is the time it takes for the wave

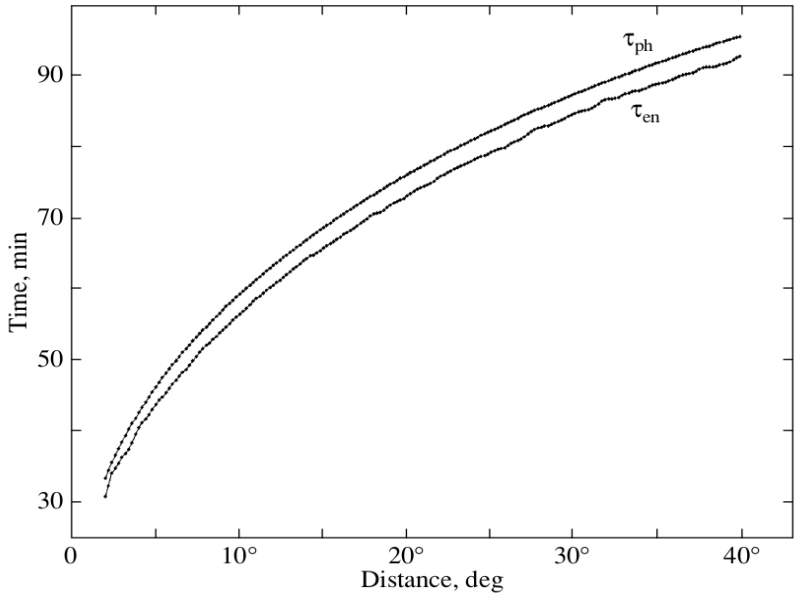

Fig. 5. Time-distance relation derived by fitting the first bounce of CCF in figure 4. Phase time usually can be measured more smoother than group time.

packet to traverse the path in the solar interior between two points on the surface separated by the angular distance Δ. In this work (Kholikov et al., AstLett, 2004) we attempted to determine the variations in the travel time of acoustic waves at the solar maximum and minimum. Our results show that the difference between the wave travel times at the minimum and maximum is $\sim 2s$ down to a depth of $0.8R_{\odot}$; at larger depths, this difference decreases. This probably suggests that acoustic waves penetrating deeper than $0.8R_{\odot}$ are less sensitive to solar activity manifestations; i.e., active structures are localized in the upper layer of the convective zone. The amplitude A measures the degree of correlation of the wave packet of acoustic oscillations that returns to the surface at distance Δ from the starting point after its passage along the ray path. The physical parameters of the medium in which acoustic waves propagate are known to vary with solar magnetic activity. However, these variations are very small, although the parameters of the medium in active regions vary significantly; the variations of the magnetic field are particularly large. As a wave packet interacts with active regions, it must lose part of its energy (Chou et al., ApJ, 1996); therefore, in the years of maximum solar activity, when the number of active structures on the Sun increases, the amplitudes of acoustic wave packets must decrease. Our measurements show relative variations in the correlation amplitudes of wave packets with solar activity, whence we see that the decrease in the correlation amplitudes of wave packets from minimum to maximum solar activity is $10-20\%$. In (Burtseva et al., SolPhys, 2009) variations of the lifetimes of high-l solar p modes in the quiet and active Sun with the solar activity cycle are

investigated. The lifetimes in the degree range $l = 300-600$ and $\nu = 2.5-4.5$ mHz were computed from SOHO/MDI data in an area including active regions and quiet Sun using the time – distance technique. We applied our analysis to the data in four different phases of solar activity: 1996 (at minimum), 1998 (rising phase), 2000 (at maximum), and 2003 (declining phase). The results from the area with active regions show that the lifetime decreases as activity increases. The maximal lifetime variations are between solar minimum in 1996 and maximum in 2000; the relative variation averaged over all l values and frequencies is a decrease of about 13%. The lifetime reductions relative to 1996 are about 7% in 1998 and about 10% in 2003. The lifetime computed in the quiet region still decreases with solar activity, although the decrease is smaller. On average, relative to 1996, the lifetime decrease is about 4% in 1998, 10% in 2000, and 8% in 2003. Thus, measured lifetime increases when regions of high magnetic activity are avoided. Moreover, the lifetime computed in quiet regions also shows variations with the activity cycle. In (Patron et al., ApJ, 1997) a new method of fitting tridimensional power spectra of solar oscillations is described and compared with a conventional approaches. The new method fits the parameters of the Lorentzian profiles in a bidimensional $k-\omega$ diagram constructed from an azimuthal average of the tridimensional one. The horizontal velocities are then determined keeping these parameters fixed, greatly reducing the computation time. Both methods are compared for two radial orders ($n = 3,4$) of a tridimensional power spectrum obtained for a region of about 15^o square around solar disk center. The images used in this work correspond to a 3 day set of [1080x1080] pixel intensity images obtained at the Observatorio del Teide with the Taiwanese Oscillation Network (TON) instrument. The results of the Fitted velocities agree within the estimated errors for the two methods. The reduction of the computing time obtained with the new method makes it convenient for the ring diagram analysis.

Another successful application of the ring diagramm technique together with time-distance method provide exceptional results of sunspot structure near solar surface (Kosovichev at al., JphCS, 2011). In this article a new results of comparison of the ringdiagram analysis and time-distance helioseismology for active region NOAA 9787, for which a previous comparison showed significant differences in the subsurface sound-speed structure, and discuss systematic uncertainties of the measurements and inversions are presented. New results show that both the ring-diagram and time-distance techniques give qualitatively similar results, revealing a characteristic two-layer seismic sound-speed structure consistent with the results for other active regions. However, a quantitative comparison of the inversion results is not straightforward. It

must take into account differences in the sensitivity, spatial resolution and the averaging kernels. In particular, because of the acoustic power suppression, the contribution of the sunspot seismic structure to the ring-diagram signal can be substantially reduced. It is showen that taking into account this effect reduces the difference in the depth of transition between the negative and positive sound-speed variations inferred by these methods. It seems to be important that both methods indicate that the seismic structure of sunspots is rather deep and extends to at least 20 Mm below the surface, putting constraints on theoretical models of sunspots.

Section 3. Probing different layers of sun's interior.

Time-distance helioseismology is a powerful tool to probe the conditions of small structures below the surface of the Sun. One of the successful applications of this technique was developed by Duvall using South Pole data. Using GONG data we investigate the travel time changes in sunspots. To increase the signal to noise ratio, we applied a phase velocity filter to the time series. In order to increase the signal/noise ratio and to isolate waves traveling along the same ray path down to certain depths (Duvall et al., Nature, 1993), we apply a phase velocity filter to the spherical harmonic SH coefficients and reconstruct the images back into the latitude-longitude domain (inverse decomposition). Since in time distance analysis, the acoustic signal could be used within or outside of active regions separately, it allows us to measure acoustic wave properties and compare active and quite regions. In (Kholikov, SOHO-14, 2004) we address the problem of the acoustic wave propagation time increase within sunspots. The basic method of time-distance helioseismology is the computation of cross-correlations between two points on the solar surface. In this particular case we used center-annulus correlations: the temporal signal at a given target point is correlated with a signal created by summing around an annulus with a given angular distance. The travel time parameters are obtained by using the cross-correlations with a Gabor function described by (Kosovichev et al., ApJ, SCORe, 1996). By varying the separation between central point and annulus we can select different ray paths and probe different depths of the solar interior. The positive time lag corresponds to the travel time of outgoing waves from the center to the surrounding annulus. The negative time lag is interpreted as the travel time of ingoing waves from an annulus to the central point. If the central point is located in an active region or sunspot, then perturbations are expected only in the positive travel times.

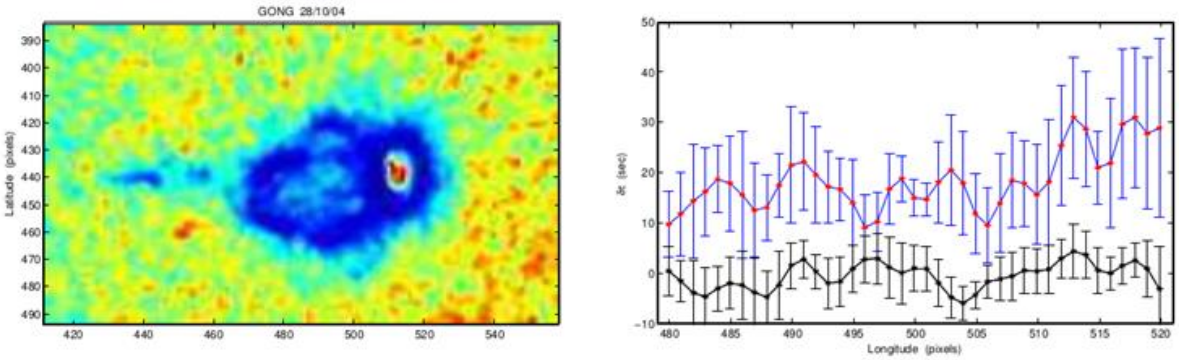

Fig. 6. Acoustic power map (upper panel) and travel time differences between ingoing and outgoing waves (right panel) for the large active region of October 28, 2003. In the travel time plot, the lower curve is computed from a quiet region of the same size. The phase velocity filter was centered at L = 250 and = 3 mHz. The horiizontal axis in the lower panel is the longitude of the sunspot in pixels.

A one minute decrease of phase travel time in active regions was found using South Pole, GONG classic and MDI data. An important result of these analysis was that travel times of outwardly propagating waves are smaller by approximately 1 minute than inwardly propagating waves travel times, suggesting the presence of apparent outflows going from active regions. In this study we use reconstructed images from phase velocity filtered SH coefficients, which significantly improves the signal-to-noise ratio. Using separation distances between the central point and annulus of 1.8 to 4.5 degrees, we found that the phase travel time within sunspots generally decreases by about 20-40 seconds.

In (Hsiang-Kuang Chang et al., Nature, 1997) we have applied a similar approach to map sunspot at deeper layers of the solar interior. In helioseismic ambient acoustic imaging, we form a 'computational acoustic lens'. Each point on the solar surface has a velocity and intensity variation caused by the acoustic waves impinging upon it. We can use a spatial array of solar locations as the elements of an acoustic phased array. The acoustic wave train originating from a target point at the surface propagates inwards to the bottom of the acoustic cavity and back to the surface at a distance from the target point. Different P-modes have different paths and arrive at the surface at different times and different distances from the target point. On the basis of the relation between travel time and distance traveled by acoustic waves in the Sun, we can phase-shift the time series of oscillation signals over the array to coherently detect the intensity of the acoustic signals from a target point in the Sun. Although the P-mode signal at each point in the collecting area includes waves from all other points in the Sun, those signals are expected to cancel in the summation because their phases have different spatial coherence. Other local helioseismic techniques indirectly infer the subsurface

structure by inverting the measured frequency shift, absorption, phase shift and time delay, whereas ambient acoustic imaging can directly image the three-dimensional inhomogeneities below the surface.

We have used a seven-day helioseismic time series, totalling 90 hours of observations, taken with the TON to reconstruct a solar acoustic image at the surface. Images of the intensity of the $Ca_{II}K$-line were taken during the interval 21–27 June 1996, and the sunspot region NOAA 7973 was selected as a test target. The data reduction procedure is as follows. (1) Each observed K-line full-disk image is transformed into coordinates of $sin\theta$ and ϕ, where θ and ϕ are the latitude and the longitude, respectively, in a spherical coordinate system aligned along the solar rotation axis. (2) The differential rotation of the solar surface is removed. (3) The oscillatory amplitude is computed by subtracting the 15-frame running mean from the intensity time series at each spatial point. (4) A temporal filter is applied to isolate the signal in a range of 2.7–6.5 mHz. (5) The signal originating from a target point at time t is phase-matched by summing the signals at different angular distances from the target point measured at the appropriate time delays based on the one-bounce time–distance relation obtained from the quiet Sun. The signals are summed over an annular region 2–26° from the target point, corresponding to travel times of 31–80 minutes after t. (6) The phased summation is repeated for each t in the time series, and then squared amplitudes at different times are added to obtain the acoustic intensity received from the target point. (7) The procedure is repeated for all points in a target region to form a two-dimensional acoustic image. We have applied the time–distance relation of the quiet Sun to both quiet and magnetic regions. The presence of magnetic field in the active region introduces a small change in the total travel time which is much smaller than the period of P-modes (about 5 minutes). Moreover, it should be noted that the differential travel time, which is the difference in travel time of two adjacent points on the time–distance curve, enters our phase-matching technique instead of the total travel time. The change in the differential travel time due to magnetic field is expected to be much smaller than the change in the total travel time. Thus we expect that the presence of magnetic field has little effect on our result.

Fig. 7. shows very important observational phenomena. It is the first acoustic image of the sunspot beneath the surface! Moreover, this is observational confirmation of the deep nature of the sunspot roots in solar convective zone.

Next application of the time-distance technique to deeper layers of the solar interior is devoted to map emerging active region before it emerges to the solar surface (Kholikov, SolPhys, 2013). Solar surface activity is a product of magnetic flux emerged

from the Sun's interior. Emerging strong magnetic fields form active regions of various configurations. The physical properties as well as the evolution of some aspects of active regions have been well studied by various observational and theoretical techniques (Fan, ApJ, 2008; Birch et al., ApJ, 2013). However, the detection of magnetic flux prior to its emergence to the surface remains as one of the most important subjects in this field. Specifically, space weather and solar cycle predictions depend on the outcome of this investigation. (Ilonidis et al., Science, 1011) applied a deep-focusing time–distance technique to detect travel-time perturbations of emerging magnetic flux. They found large travel-time shifts at depths of 40 – 75 Mm. The magnitude of travel-time perturbations found in this study were very large, 10 – 15 seconds.

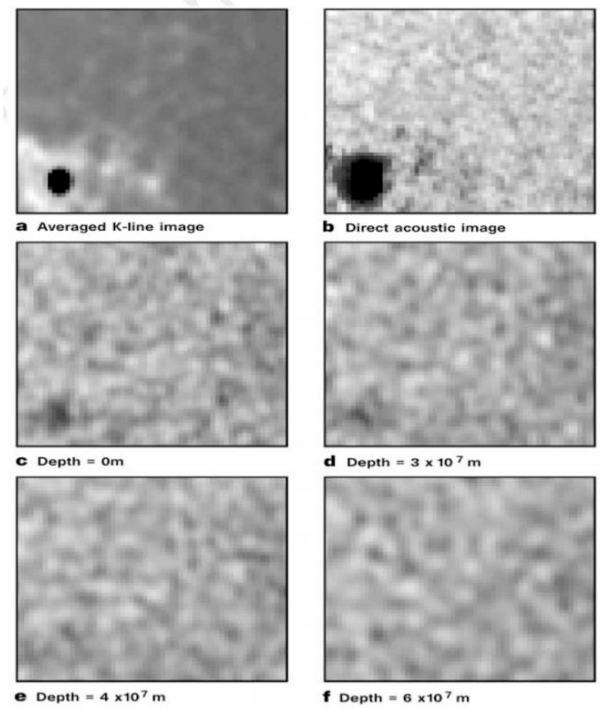

Fig.7. K-line image (a), direct acoustic image (b), reconstructed acoustic images at various depths (c-f). The K-line image is averaged over 7 days of observations. Suppression of acoustic intensity in sunspot region is clear at the surface and decreases with depth.

However, (Braun, Science, 2012) reported that acoustic holography technique measurements of the travel times of the same active regions did not show any travel-time anomalies. According to theoretical simulations, expected travel-time shifts due to the mass-flow caused by emerging Ω-loops at the deep layers should not exceed a few seconds in magnitude (Fan, ApJ, 2008). Modeling buoyant magnetic flux, (Birch et al., ApJ, 2010) also suggested that the travel-time perturbations are approximately one second for flow speeds of 40 m s^{-1} at depths of 30 Mm. Since the sensitivity of travel

times at lower turning points is higher for horizontal flows, the large time-shifts observed by (Ilonidis et al., Science, 201) are not related to strong magnetic field changes. Moreover, magnetic field perturbations alone may not be responsible for such large travel-time perturbations. According to (Chou et al., ApJ, 2002), an estimated travel-time shift of about 0.015 second at the base of the convective zone (≈ 200 Mm below the surface) is equivalent to a magnetic field strength of $(4–7)\times10^5$ G.

Our aim was focused on reproducing the results of (Ilonidis et al., Science, 2011) by using an independently developed technique and additional measurements from the GONG helioseismology network (ground-based) while they used data obtained by NASA's SOHO/MDI space mission. We used MDI and GONG Doppler velocity images for three active regions (AR): NOAA 10488, 8164 and 10132. They were observed in different time periods between 1996 and 2003. For each AR, we analyzed data for the period of 2 – 3 days preceding their emergence. Although the processing steps we used differ from those used by (Ilonidis et al., Science, 2011) in detail, the basic outcome remained the same.

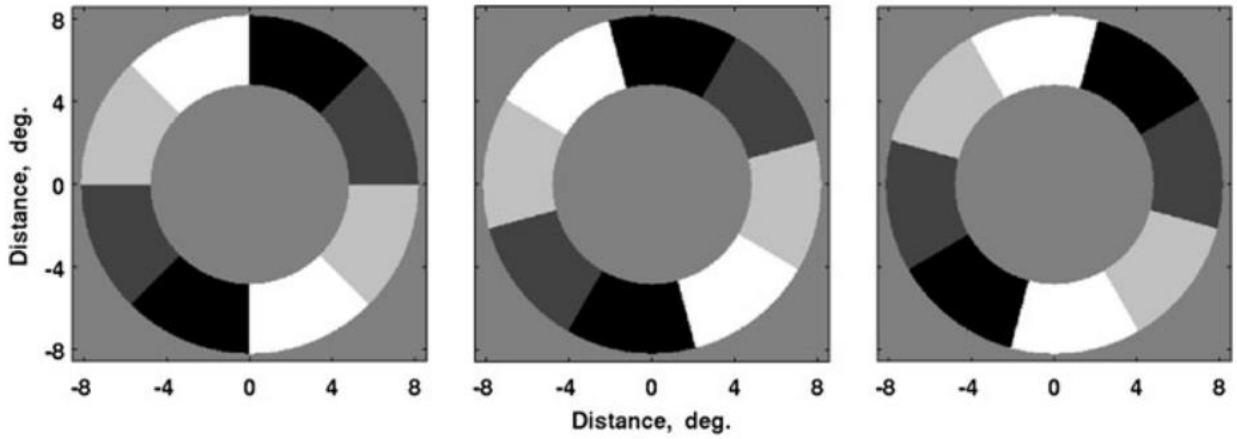

Fig. 8. Configurations of the 45° arcs for the deep focusing cross-correlation measurements. Each arc is divided into 22 separation distances relative to the central point. The cross correlations of solar oscillation signals are computed between averaged diametrically opposite sub-arc locations.

In the standard time–distance analysis, the data cube is filtered by transforming it into Fourier domain, applying a filter to select acoustic waves with certain phase-speed parameters (phase speed and temporal), and transforming back to the time–space domain. The size of data cubes is usually 30 × 30 degrees in latitude and longitude with durations of nearly 8 hours. The phase-speed filtering with specific parameters isolates acoustic waves with approximately the same raypath and lower turning point at a selected depth range. In order to increase the signal-to-noise ratio, (Ilonidis et al., Science, 2011) used a modified phase-speed filter, replacing the Gaussian shape filter by a Π-shape filter, which is flat at the center and Gaussian at the edges; in our study

the same phase-speed filter was employed. The flat part of the filter corresponds to the phase velocity range of 21 – 29 km s^{-1}. The main steps of the filtering procedure are as follows:

– Decompose individual Doppler velocity images into spherical harmonics (SH) coefficients using the central 120×120 degree in latitude and longitude part of the disk.

– Apply the phase-speed filter to all individual (l, m) SH coefficients of the observed time series.

– Reconstruct the oscillation velocities using the filtered coefficients; they can be reconstructed using the relation

$$V(\theta, \phi) = \sum_{l=0}^{l_{max}} \sum_{m=0}^{l} C_l^m P_l^m(\theta) e^{im\phi + \delta\phi}$$

Here C_l^m are SH coefficients, P_l^m is the associated Legendre polynomial of degree l and order m, θ and ϕ are latitude and longitude, respectively. $\delta\phi$ is a differential rotation profile (Libbrecht et al., Solar Interior and Atmosphere, 1991), function of latitude and time (relative to the middle of the data cube) to remove the surface differential rotation. The range of l for the chosen phase-speed parameters is $l = 70 - 200$, implying that it is not necessary to use very high degrees of SH coefficients, therefore $l_{max} = 300$ covers all our needs.

– Tracking of the reconstructed images is done by introducing the surface differential rotation profile angular velocity into the argument of the complex exponential in the right-hand side of the equation above.

Deep focusing cross-correlation calculations of these reconstructed data are produced using the scheme discussed in (Ilonidis, Science, 2011). The maximum peak of the cross-correlation function for the phase speeds ranging in 21 – 29 km s^{-1} corresponds to separation distance $\Delta = 12\text{–}13^0$. For any given central target region position, the annulus diameters used in these calculations are $D1 = 9.6^0$, $D2 = 16.32^0$. The annulus is divided into an even number of arcs. For this analysis we use the arc sizes of 60º, 45º, 36º, 30º, 25.71º, 22.5º, 20º. In each case, we have an even number of arcs to cross correlate the signal between the diametrically opposite pairs. Each arc configuration is rotated left and right by 1/3 of its length which makes 21 independent configurations. Fig.8 demonstrates a diagram of three configurations of the 45º arcs. The annulus width is divided into 22 equidistant sub-annuli relative to the central position. The cross correlations are computed between the opposite sub-annuli for each arc configuration. The individual cross correlations are difficult to fit with the Gabor wavelet, therefore, instead of fitting every cross correlation, we combined the cross correlations for the different travel distances. Before averaging these 22 cross

correlations, we shifted them into one of the central travel distance locations using the mean time–distance relation which is obtained by averaging measurements over the entire target region. This operation can be done by interpolation. To avoid interpolation artifacts, we used the Fourier shift theorem:

$$\psi(t-\tau_{\Delta}) = F^{-1}\{e^{-i\omega\tau_{\Delta}}\Psi(\omega)\}$$

Once cross correlations are computed and averaged over all travel distances, travel-time maps for selected target regions are constructed by the standard Gabor wavelet fitting procedure (Duvall et al., Nature, 1997). In order to cover a typical active region in size, 13°×13°, travel-time maps centered at AR locations where emergence was expected were produced. Measurements were carried out for the 2 – 3 days time periods that preceded the emergence of the AR to the solar surface.

Nine consecutive travel-time maps prior to the emergence time are presented in Fig. 9; each map is produced using an 8-hour data cube at the times shown on each panel. The travel-time perturbations on these maps range from 0 (blue) to −15 (red) seconds. Despite a few minor features, the strongest perturbations occur at two locations and remain for 7 hours. It should also be mentioned that the first map is 11 hours away from the time when the AR started appearing on the surface. MDI magnetogram and continuum images of corresponding AR locations are shown in the last three panels of the bottom row. There is no significant surface magnetic field during the time period when the travel times are computed. In the magnetogram of 15:30 UT on 27 October, the AR is clearly seen at the surface and starts to evolve. The continuum image taken two days later displays two separate components of the AR. Our study shows that the deep focusing time–distance helioseismology measurements indeed provide evidence of some emerging ARs, with time shift magnitudes significantly larger than estimated predictions from simulations (Fan, ApJ, 2008). The work (Kholikov et al., SolPhys, 2008) is a successful application of local helioseismology technique to problems of global oscillations of the sun. Solar radius changes over the solar cycle during the past ten years have been investigated with different techniques. However, the results were often controversial (Laclare et al., SolPhys, 1996; Noël, A&A, 2004; Kuhn et al., ApJ, 2004). In contrast, acoustic-radius measurements provided by helioseismic methods (Schou et al., ApJ, 1997) based on f-mode frequencies are quite consistent (Antia, A&A, 1998; Dziembowski at al., ApJ, 2005). The properties of the autocorrelation function (ACF) of global solar oscillations have been analyzed by several authors. Estimates of p-mode lifetimes have been obtained from the ACF of 70 days of GOLF data (Grec et al., Sounding Solar and Stellar Interiors, 1997). A long sequence of 500 days of observations was studied in detail by (Gabriel et al. A&A, 1998).

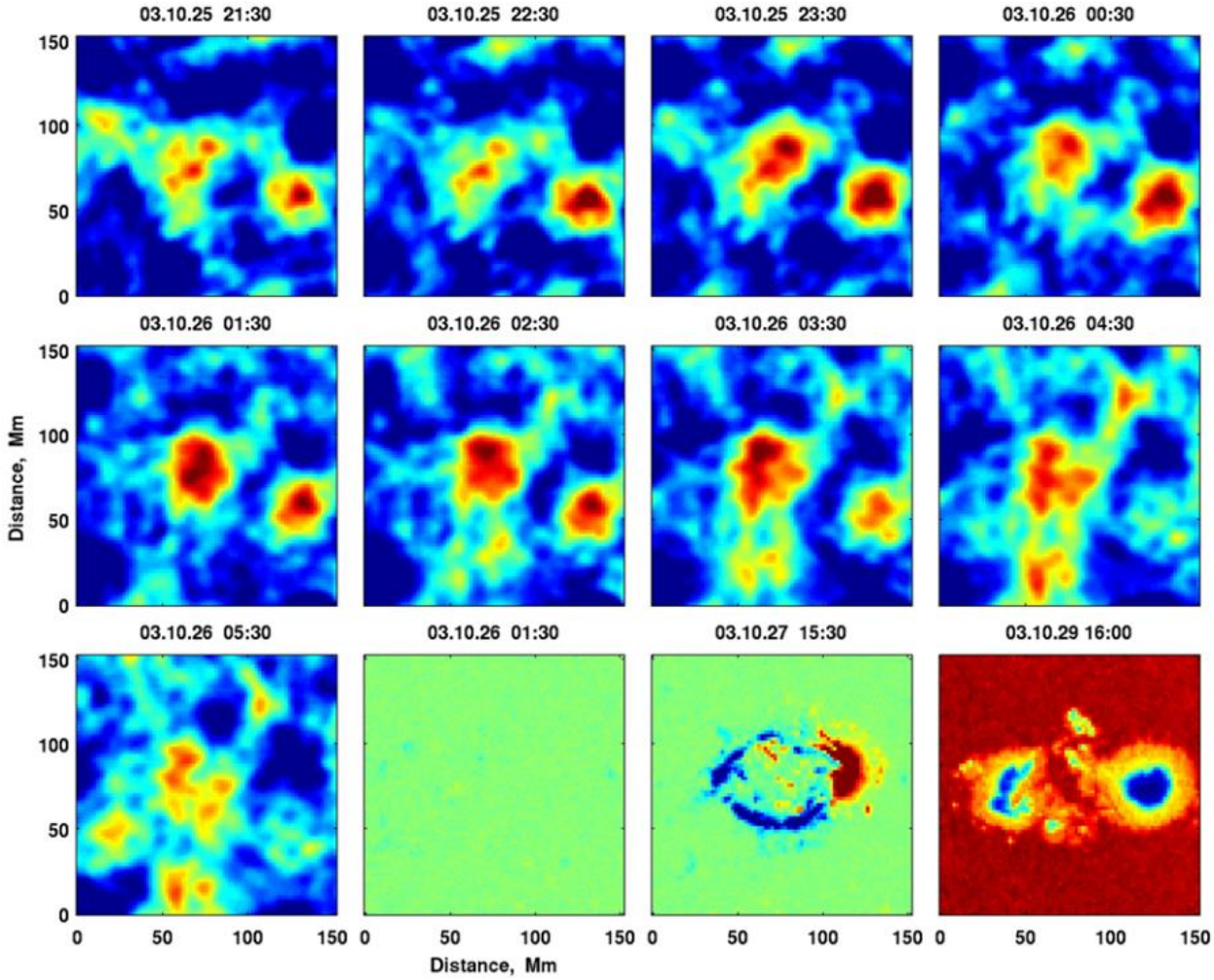

Fig. 9. Deep focusing travel-time maps of the Active Region 10488 (top two rows and left image in bottom row). The focus depth for these measurements covers 40 – 70 Mm. Each map is created using 8-hour duration MDI data cubes centered at the emerging active region location (dates and times are displayed at the top). The magnetic fields before and after the emergence time and a continuum image for a later time are presented in the last three panels of the bottom row. The active region location shows significant double structure travel-time perturbation on below the surface prior the emergence on 25 – 26 October, and after emergence on the surface on 29 October.

They found that variations of the lag of the ACF peaks are not related to the damping time but are a consequence of the nonconstancy of the so-called large frequency separation, $\Delta\nu = \nu(n+1,l) - \nu(n,l)$, where ν is the frequency, l is the spherical harmonic degree, and n is the radial order of the mode. Measuring the large and small frequency separations [where the small frequency separation is defined as $\delta\Delta\nu_l = \nu(n,l) - \nu(n-1,l+2)$] from the ACF and its modulation has been proposed by (Kholikov et al., Stellar structure and habitable planet finding, 2004). Using the ACF as a diagnostic tool for stellar oscillations has been proposed by (Roxburgh et al., MNRAS , 2006), who

also developed a method of measuring the strength of acoustic-wave refraction in the stellar core from the modulation of the ACF (Roxburgh et al., MNRAS, 2007).

We have used GONG and MDI monthly spherical-harmonic (SH) coefficient time series for $l = 0–3$. These time series are computed by projecting individual full-disk Doppler velocity images onto the spherical-harmonic functions. The decomposition of an image, acquired every minute, provides a set of numbers that represent the relative strengths of the SH with different (l, m)values for that image. These numbers, known as spherical-harmonic coefficients, are then rearranged to form a set of time series for each (l, m). Typical SH time series lengths are 36 days for GONG and 72 days for MDI. Our data set covers the time period from 1995 to 2007. The time series were filtered with a Gaussian filter of FWHM = 2.0 mHz centered at $\nu = 3.3$ mHz. The filtering was done by applying a Fourier transform to the SH time series, applying the filter in the frequency domain, and then transforming the filtered power spectrum back into the time domain to give the ACF. The ACF was computed separately for each l and m. Figure 10 shows an example of the ACF for the $l = 0$ time series of 36 days duration. The most dominant peak, with a lag of about four hours, arises from the solar value of $\Delta\nu$ of ≈ 135 μHz. This value is the inverse travel time of sound from the solar surface to the center and back. Since the acoustic wave undergoes multiple reflections from the solar surface, the peak appears at delays of four, eight, . . . hours.

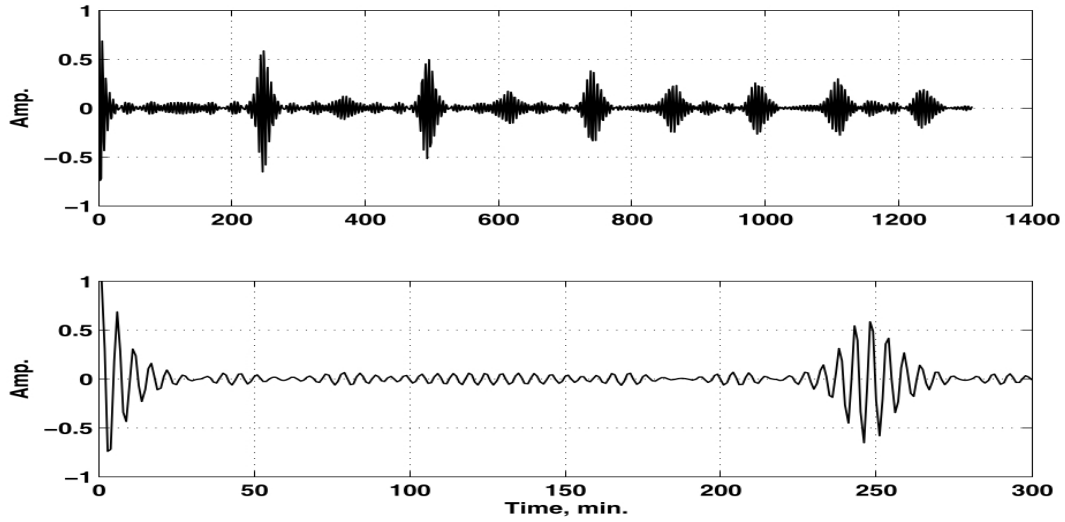

Fig.10. The autocorrelation function computed from a GONG 36-day $l = 0$ time series. The dominant peak corresponds to the large frequency separation $(\Delta\nu)$

The location of the ACF peak is an estimate of the acoustic radius (T) of the Sun multiplied by four owing to the propagation of the wave through the Sun from the observation point to the far side and back, traveling a distance of four radii. The units

of T are seconds, as it is expressed as the sound travel time. To obtain the location of the peak we use a technique from time – distance helioseismology, where it has been shown that the correlations of the waves can be approximately represented in the form of a Gabor function. We thus fit the peak around its maximum to the Gabor wavelet. As mentioned in previous section, the phase travel time can be measured more accurately than the envelope travel time. Figure 11 shows phase travel times obtained from $l = 0$ and $l = 3$ time series for a set of five-day-long time series. The measurements are smoothed by a 1.5-year running window by using the Savitzky – Golay method.

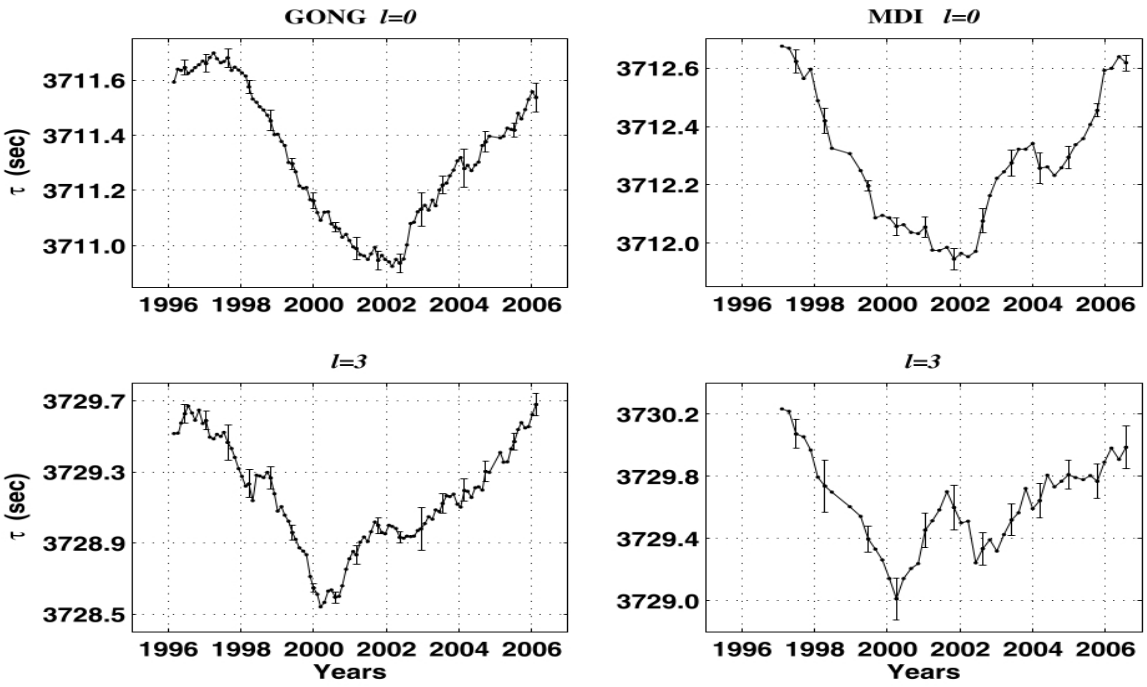

Fig.11. The acoustic radius of the Sun as a function of time from GONG (left) and MDI (right). The individual autocorrelation functions were obtained from five-day time series. The measurements are smoothed by a 1.5-year running window. A significant anticorrelation with the solar activity level can be clearly seen.

The large separations obtained from the ACF have very small error bars. In Fig. 11 the typical error bars are about 0.1 seconds. These errors are estimated from the scatter of the averaged measurements computed from the five-day time series, not from formal estimations of the Gabor fitting procedure. The origin of the one-second difference in acoustic radius between the GONG and MDI results is unknown. We also analyzed measurements of $\Delta\nu$ from GONG and BiSON frequency tables. Time series of T obtained from fitted frequencies do not show any changes with solar activity cycle because of the much larger errors resulting from the peak-fitting analysis. The typical

errors in frequency differences from peak fitting are typically about 0.5 μHz, corresponding to an error in T of approximately 25 seconds.

The most important features of Fig. 11 are the clearly visible variations of the acoustic radius, which are anticorrelated with the solar activity cycle. For all low-degree modes ($l = 0–3$), the magnitude of the change between the minimum and maximum activity phases is less than one second. These small changes cannot be seen from individual frequency separations, where the precision of the determination is poorer by more than a factor of 100. Variations in the solar acoustic radius arise either from changes in the density scale height, which affects the depth of the upper reflecting point, or from variations in the internal sound speed. From our measurements we cannot infer the depth dependence of radius changes, but it clearly is anticorrelated with the solar activity cycle.

Section 4. Solar meridional flow measurements.

One of the most important goals of solar physics is to understand the origins of quasi-periodic solar activity and its relationship to the solar dynamo. A key process of the interior dynamics in the Sun is the meridional circulation, which is a crucial ingredient in dynamo models. The classical picture of this large-scale circulation is a near-surface poleward flow in each hemisphere of about 10−20 m s^{-1} , and a "return" equatorward flow at the bottom of the convection zone with an amplitude an order-of-magnitude weaker [Giles, PhD thesis, Stanford, 2000]. In this section we describe our efforts and contributions to the meridional flow measurements from GONG and MDI observations carried since 1995.

Early studies using magnetic-feature tracking (Komm et al., SolPhys, 1993; Snodgrass et al., SolPhys, 1996) and surface Doppler measurement (Hathaway, ApJ, 1996; Nesme-Ribes et al., A&A, 1997) found evidence of poleward meridional flow at the solar surface and variations of the flow with the solar cycle. Helioseismic observations, which are able to infer the depth profile of the flows, confirmed the existence of such a flow (Giles et al., Nature, 1997). An average poleward flow at the surface and upper layers of the convection zone of 10 – 20 m s^{-1} seems to be the consensus. (Giles, PhD thesis, Stanford, 2000) was the first to use a local-helioseismology technique, time – distance (Duvall et al., Nature, 1993), to study the temporal evolution of the meridional flow. The results showed a variation of the amplitude of the flow which decreased towards solar maximum during cycle 23. (Chou et al., ApJ, 2001) extended the results also finding an increase on the amplitude towards solar minimum using data obtained during the previous cycle. Ring-diagram analysis

of Michaelson Doppler Imager (MDI) data (Haber et al., ApJ, 2002; Basu at al., ApJ, 2003), during the rising phase of cycle 23, and Global Oscillation Network Group (GONG) data (González Hernández et al., ApJ, 2006; Zaatri et al., SolPhys, 2006), in the declining phase of the same cycle, confirmed the overall variation of the meridional flow with the solar cycle, with larger amplitude toward solar minimum. (Ulrich et al., ApJ, 2005) show temporal variations of the meridional flow for almost two solar cycles using a technique that tracks points at the surface. They also found an anticorrelation between the amplitude of the meridional flow and the solar cycle.

The particular behavior of the meridional flow around the latitude of magnetic activity concentration has been noted by most of these authors. A steep gradient of the flow around the Equator toward the activity latitudes, which increases with increasing surface magnetic activity, has been a common factor in these observations. (Gizon, PhD thesis, Stanford, 2003) analyzed two Carrington rotations eliminating the contribution from areas of high magnetic activity and found a marked difference from the meridional flow calculated using only quiet areas in the activity latitudes. This result suggested that the organized inflows that had been shown to exist surrounding large active region complexes (Zhao et al., ApJ, 2001; Haber et al., SolPhys, 2004; Komm et al., ApJ, 2004; Braun et al., Helio- and Asteroseismology: Towards a Golden Future, 2004) were responsible for this observed component of the meridional flow that converges towards the active latitudes. (Zhao et al., ApJ, 2004) pointed out that there may be an extra component in the active belts beyond the inflows surrounding active complexes, since they found residual flows below the maximum depth of the flows associated to the activity.

First work in this section [Subsurface merflow_in_activi_belts] describes meridional flow measurements derived ring-diagramm approach. Six years of high-resolution observations from GONG (http://gong.nso.edu/data), during the declining phase of solar cycle 23, give us the unprecedented opportunity to study the meridional flow using local helioseismology with continuity. It also allows us to study the effect of the surface activity on the inferred flow with statistical significance. Figure 12 shows the yearly-averaged meridional flow obtained by applying the standard ring-diagram analysis (Haber et al., ApJ, 2002) to the continuous set of GONG high-resolution data. The bumps or inflows around the active belts are clearly visible in the figures. In this work we discriminate between measurements of meridional flow averaging all available data and those obtained by using only areas of quiet Sun to investigate how the surface magnetic activity affects the inferred flows. We apply standard ring-diagram analysis (Hill, ApJ, 1988) to GONG high-resolution Dopplergrams from July 2001 to December

2006 to infer the meridional flow from the solar surface to a depth of approximately 16 Mm for the declining phase of cycle 23. The ring-diagram method studies high-degree waves propagating in localized areas over the solar surface to obtain an averaged horizontal-velocity vector for that particular region. By analyzing a mosaic of these patches, it is possible to develop a three-dimensional velocity map in the depth range where the waves propagate. Typical ring-diagram analysis uses 1664-minute series of full-disk Dopplergrams with a resolution of about 1.5 Mm per pixel at the center of the disk. Patches of 16^0 square, apodized to 15^0 -diameter areas, are tracked at the surface rotation rate. A three-dimensional FFT is applied to a tracked area, and the corresponding power spectrum is fitted using a Lorentzial-profile model that includes a frequency shift term due to the horizontal-velocity flow (Haber et al., ApJ, 2002). Finally, the fitted velocities are inverted using a least-squares method to recover the depth dependence of the velocity flows. The GONG ring-diagram pipeline has been used for the work presented here. Details of the pipeline can be found in (Corbard et al. SOHO 12 / GONG+ 2002, 2003). A single horizontal-velocity vector (v_x, v_y) at several depths is obtained as the result of analyzing a single patch.

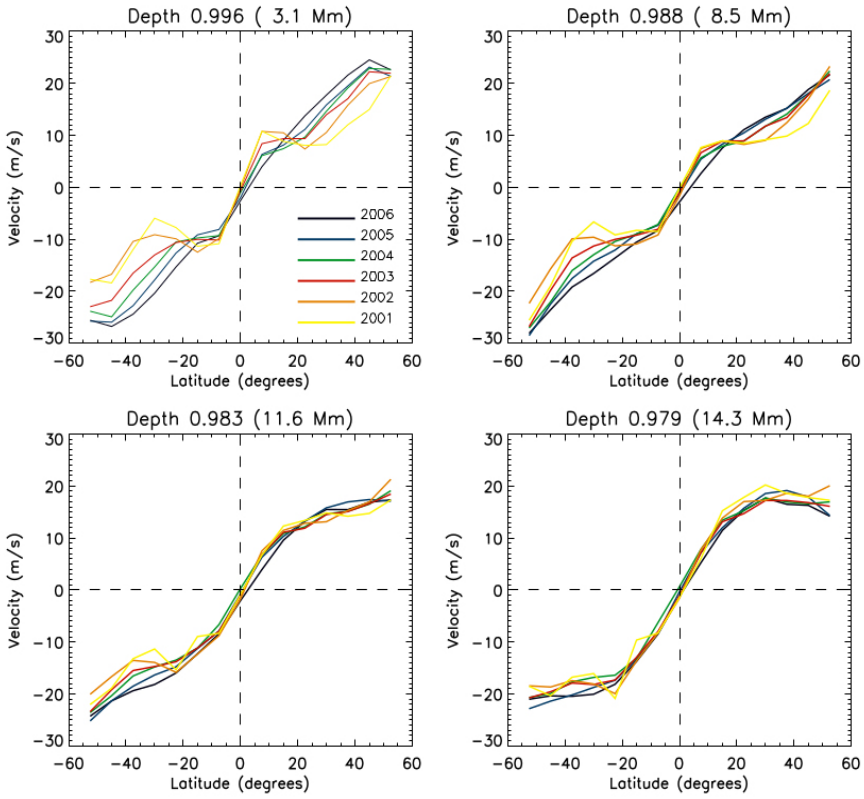

Fig. 12. Yearly averages of the meridional flow obtained by ring-diagram analysis of GONG continuous set of data at four different depths. The variation with the solar cycle clearly observed at the superficial layers is less pronounced at deeper layers.

To study the meridional circulation, we concentrate on the v_y component of the calculated flows. Local-helioseismology inferred flows at high latitudes have been shown to be affected by the periodic variation of the solar B_0-angle (González Hernández et al., SolPhys, 2006; Zaatri et al., SolPhys, 2006). We do not yet have a full understanding of the effect. (Beckers, Astronomische Nachrichten, 2007) analyzed the problem and showed that a different correction can result in substantially different results. Hence, we have decided to not correct the inferred flows. Since the B_0-angle effect will affect equally the yearly averages of all calculated flows, the temporal variations that we are interested in should still be valid. Thanks to the continuous stream of data provided by the GONG instrument, we have obtained velocity flows for 5.5 uninterrupted years. The yearly-averaged meridional flow at four particular depths can be seen in Fig. 12. Close to the surface, at approximately 3 Mm depth, the marked increase in the amplitude of the flows as the solar cycle progresses towards minimum can be seen, confirming previous results. The bumps around the active belts are very pronounced at this depth, and the amplitude decreases with decreasing magnetic activity. With the limited resolution attained by using a standard ring-diagram analysis, the variation of the flows at high latitudes could also be interpreted as an effect due to the contribution of organized flows around active regions.

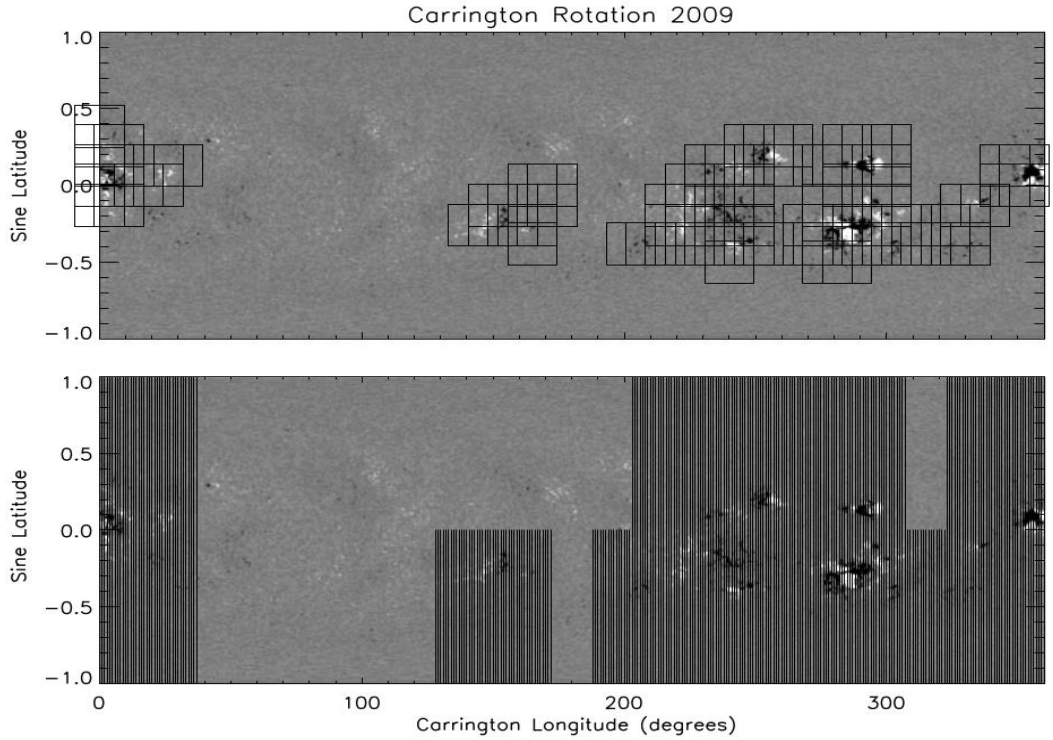

Fig.13. Two different approaches to eliminate data associated with surface magnetic activity applied to Carrington rotation 2009. Top panel shows mask 1: only those patches associated with surface magnetic activity are eliminated. Bottom panel shows mask 2: all patches in the same hemisphere and at the same longitude as a particular patch with surface magnetic activity are eliminated.

With the spatial resolution of the standard ring-diagram analysis, removing areas of surface magnetic activity to measure meridional circulation in the quiet Sun is complicated, especially in periods of high activity. However the period from 2003 to 2004 of the complete data set presents areas of high activity combined with large areas of very low activity, allowing for statistically significant comparison between meridional flows averaged over all areas versus those obtained only from quiet regions. Our first attempt to isolate quiet areas from active ones was based on removing all of the patches with an averaged magnetic-field strength above a certain threshold (mask 1). For our purposes, ten Gauss seemed to account for most of the surface activity. The top panel of Figure 13 shows the areas removed using this approach. The square patches corresponds to the ring-diagram standard areas. After removing these patches, the residual meridional flow was practically the same as that obtained by including all areas (Figures 14).

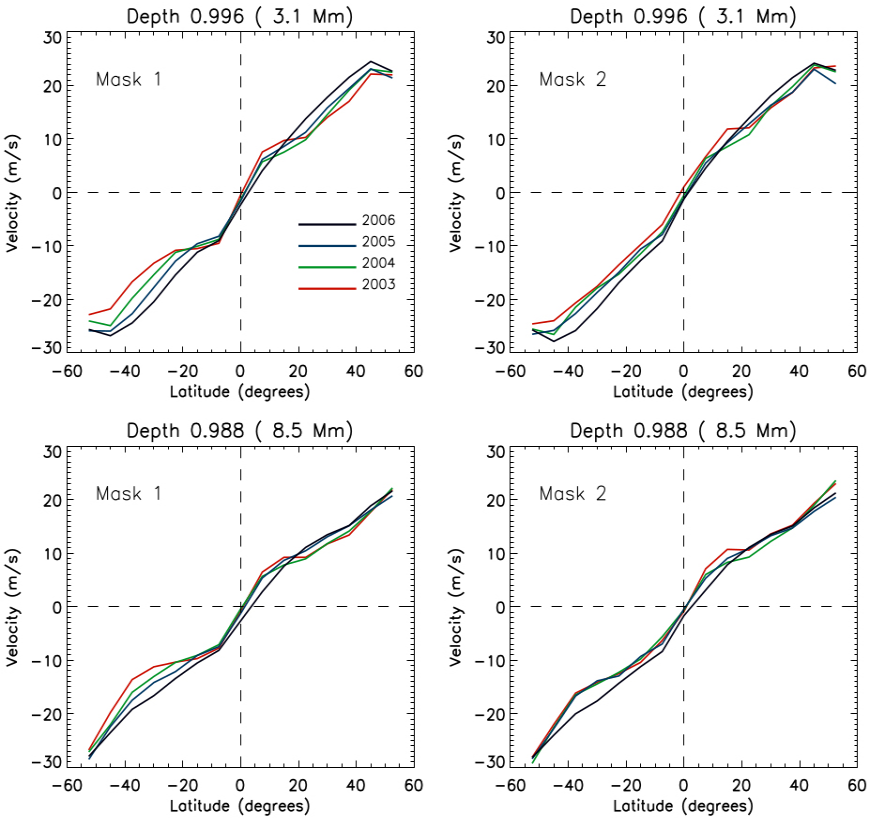

Fig. 14. Yearly averages of meridional flows obtained by ring-diagram analysis of GONG continuous set of data at two different depths after applying mask 1 (left) and mask 2 (right). The variation with the solar cycle is attenuated after applying the more aggressive masking procedure.

The second attempt removed data associated with surface activity more aggressively. It consists of removing the patches with average-magnetic field strength

above ten Gauss and all the patches at the same longitude and in the same hemisphere as the masked one (mask 2) (see bottom panel of Figure 2). In this way, flows associated with surface activity that extend for long distances will be completely removed. We made the assumption here that organized flows around a particular active region do not cross the Equator. This is not completely accurate when the activity is very near the Equator, but statistically we expect the flows crossing the Equator in both directions to cancel out. The removed areas are dark colored in the bottom panel of Fig. 2 for Carrington rotation 2009. In both cases, the averaged magnetic field for a particular patch has been calculated using MDI magnetograms.

The meridional flow obtained for years 2003 to 2006 at two particular depths before and after removing the surface areas of activity is presented in Fig. 14. The overall trend of the flow, increasing as the activity decreases does not change. Still, the trend is less prominent after applying mask 2. However, not all of the extra circulation goes away when applying even the most aggressive masking procedure, especially at depths around 6.0 Mm.

When averaging all of the available data, including areas of surface magnetic activity, the temporal variation depends on latitude and presents a maximum difference of ≈ 10 m s^{-1} around 40^{o} between solar minimum and solar maximum. Towards the interior of the Sun, the variation is less pronounced, with a maximum difference of approximately 5 m s^{-1} at a depth of 10 Mm. The variation is greater in the southern hemisphere, coinciding with the surface activity. Even after removing all of the surface activity (mask 2), the variation of the flow towards solar minimum persists, but the acceleration is smaller. We confirm the extra circulation in the active belts previously reported by other authors. (Spruit, SolPhys, 2003) presented a model that explained the torsional oscillation as a geostrophic flow due to the lower subsurface temperature in active regions. This model predicts the appearance of flows from the edges towards the center of the main latitude of magnetic activity, a meridional version of the torsional oscillation with a maximum amplitude of ≈ 6 m s^{-1} at the surface. The model also predicts a rapid decline of these oscillations with depth, which would disappear below 30 Mm. However, our results show a more rapid attenuation of the inflows in the active belt, which disappear around 10 – 14 Mm.

The observed extra circulation in the active latitudes varies with the solar cycle, decreasing towards solar minimum. These inflows towards the center of activity do not disappear when the contribution of the surface activity is removed, although the amplitude is reduced when only data from the quiet Sun is used for the calculation of the flows. In a preliminary study of two single Carrington rotations (González

Hernández et al., JphCS, 2008) the meridional flow obtained in the active latitudes when using only the quiet Sun differs from that calculated using all available data. This confirmed the results from (Gizon, PhD thesis, Stanford, 2003). These limited studies suggested that the extra circulation was due to the inflows that have been shown to exist surrounding large active complexes (Zhao, et al., SolPhys, 2001; Haber et al., SolPhys, 2004; Komm et al., SolPhys, 2004; Braun, et al., Helio- and Asteroseismology: Towards a Golden Future, 2004). However, the systematic study that we present here shows that this extra circulation cannot be accounted for exclusively by localized inflows associated with surface activity, since it persists even when using only data from the quiet Sun.

Second work of this section is devoted to deriving and analizing meridional travel-time differences using GONG data for 1995-2001 time period [Merflow GONG data]. We use the entire Global Oscillation Network Group (GONG) data set taken with the original low-resolution GONG "Classic" (May 1995 – August 2001) designed for global helioseismology and the more recent GONG+ local-helioseismology data acquisition system (August 2001 – December 2010) to obtain travel times for northward and southward propagating acoustic waves. The main idea in time–distance helioseismology is to compute travel times between two locations on the solar disk separated by some distance (Δ) using cross correlation of velocity signals at each location (Duvall et al., Nature, 1993). Waves with the same phase speed form a wave package and propagate along the same ray path in the solar interior penetrating to the same depth. Applying the phase-velocity filter increases the signal-to-noise ratio in cross-correlation measurements.

The standard procedure of phase-velocity filtering is simple. After remapping and tracking a series of velocity images, the data cube is transformed into the Fourier domain and phase-velocity (ω/k_h) filter with a specific phase speed is applied, and transformed back into the time domain. Thus filtered images contain only waves corresponding to a certain range of phase speed. Since we produce a spatial Fourier transform in the above procedure, we need to assume that waves are plane parallel. This assumption is approximately true only for high-degree modes, because waves that penetrate deeper are no longer plane parallel. This means that measurements for deep layers need to be analyzed with phase-velocity filtering in spherical geometry. Therefore, to be able to isolate waves penetrating to any depth, we use time series of spherical harmonics (SH). In this case we can apply a phase-velocity filter ω/L instead of ω/k_h $[L \approx \sqrt{l/(l+1)}]$. Then using filtered SH coefficients we reconstruct velocity images in the time domain.

To infer the meridional flow, it is necessary to measure wave travel times in opposite directions along the same ray path that lies between two locations at constant longitude. In this case, the travel-time difference between two directions is sensitive primarily to the meridional (north–south) component of the flow (Kosovichev et al., SolPhys, , 1997). To achieve this in the above reconstruction process we can use only near-zonal modes ($m \ll l$). In our first measurements we used only $m = 0$ coefficients (straight north–south direction). Later we found that using additional low-m coefficients improves the signal-to-noise ratio in cross-correlations. In this particular analysis we have used 30 % of the lower-m coefficients.

The steps to obtain travel-time differences are:

- Eight different l-ranges were selected to cover all depths 0.97 – 0.67 $R_\odot$. Phase-velocity filter parameters corresponding to each l range defined .
- Velocity images were reconstructed using only low-m coefficients for 142 GONG-month (36 day) time series.
- The cross-correlation functions (CCFs) were computed.
- Cross-correlations were averaged over longitude $-30^\circ \leq \varphi \leq 30^\circ$.
- Northward and southward travel times were obtained by fitting positive and negative lags of cross-correlations to the Gabor wavelet.
- The difference between two oppositely directed travel times is computed for travel distances (Δ) corresponding to each phase-velocity filter. Averaging of travel-time differences over 15 years resulted in very low uncertainty levels.

Fig. 15 demonstrates how the high-m filtering improves the signal-to-noise ratio of cross-correlation functions. Especially at high latitudes up to 65°, it is important to be able to fit a Gaussian envelope by a Gabor wavelet. Due to the better signal-to-noise ratio, the high-m filtered CCFs provide significantly more successful fittings than either phase–velocity filtered or raw only CCFs. Without this filtering, no CCF fit can be obtained above 50° in latitude. Forward and inverse computations have shown that the travel-time difference is approximately linearly proportional to the flow speed averaged over the mode cavity: a time difference of one second corresponds to a flow speed of about 10 – 20 m s^{-1} (Giles et al., SOHO 6/GONG 98, 1998). In Fig. 16, north–south travel-time differences for two particular separation distances obtained from GONG SH time series are presented. Blue and red correspond to the flow propagating southward and northward, respectively. The one-year quasi-periodic signal in both hemispheres (opposite phase) suggests the influence of the annual variation in B_0. At high latitudes, sign changes of the time differences occur during extreme tilt-angle periods, giving rise to an apparent second-cell structure, which may be spurious.

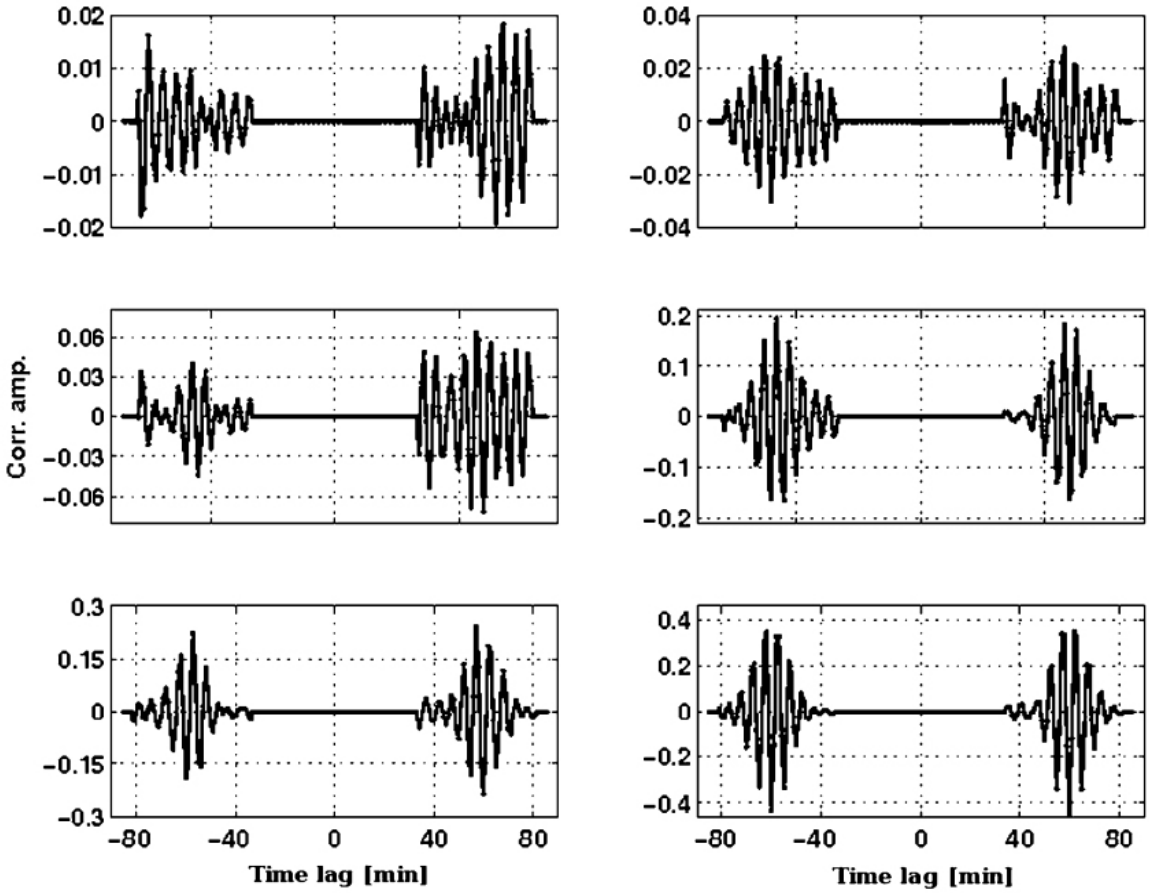

Fig. 15. Cross-correlation functions computed with three different filtering techniques at two latitudes: $\theta = 60^0$ (left column) and $\theta = 0^0$ (right column). Top: without any filtering, middle: phase-velocity filter, bottom: phase-velocity filter plus high-m filter. A significant increase in the strength of the cross-correlations are seen.

Our measurements cover two minimum and one maximum phases of cycles 22 and 23. Interpretation of temporal variations in time differences is difficult due to possible artifacts related to the solar B_0 angle. Fig. 16 clearly shows a one-year periodicity at high latitudes. This periodicity is strongly correlated with the B_0 angle. Moreover, this periodicity is present at all latitudes, and even visible around the equator. Evidence that the cause of this artifact is the tilt angle (increased magnitude of tilt) in the GONG-Classic time period when images were obtained with lower spatial resolution, which produces stronger projection effects. To see the general pattern of temporal variation, we strongly smoothed (3° in latitude and 1.8 years in time) time-difference measurements for a small range of separation distances (Fig. 17). The mean time difference for the 2007 – 2010 time period was subtracted and both hemispheres were averaged (with sign reversal). The butterfly-like structure of changes is correlated with the solar cycle and systematically shifted relative to the activity belt. These

changes are most likely associated with outflows from active regions and are not a global change of meridional flow speed with the activity cycle. The smallest travel distances used in this paper are larger than typical sunspot size; therefore inflows in active regions do not significantly affect our measurements.

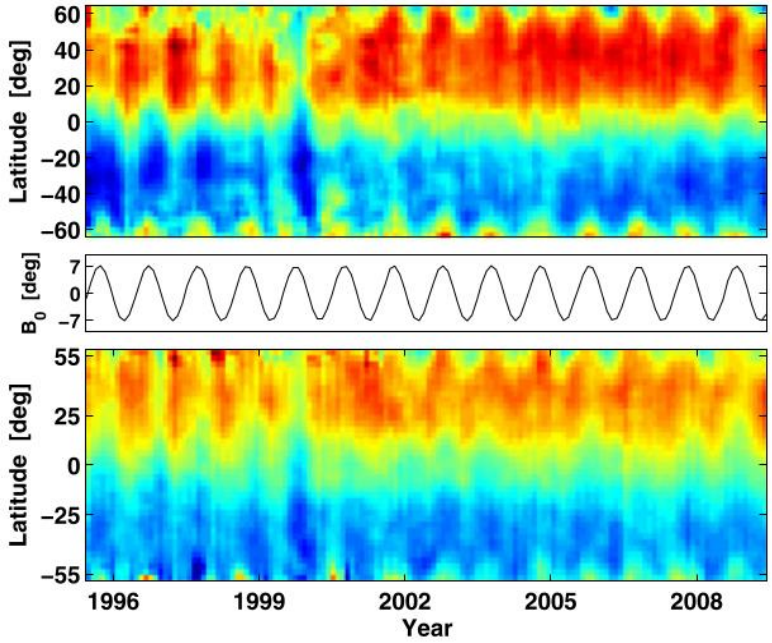

Fig. 16. Travel-time differences using a phase-velocity filter plus a high-m filter for separation distance $\Delta = 7^0$ (top) and $\Delta = 15^0$ (bottom). Individual daily travel-time differences were averaged over a 36-day interval. Middle panel shows variations of solar B_0-angle versus time. The 1-year periodicity is much stronger during the GONG Classic time period.

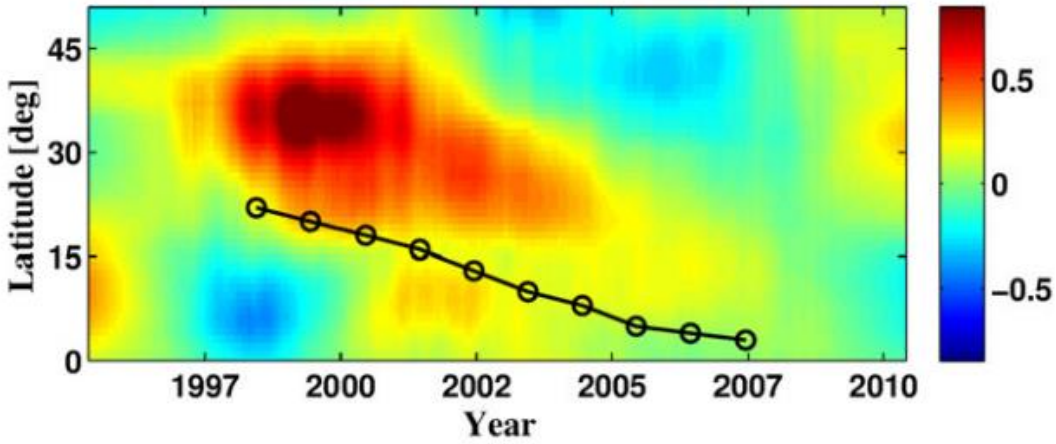

Fig. 17 Temporal variations of time-differences for separation distances $\Delta = 6 - 9^o$, corresponding to a lower turning point of about $0.92R_\odot$. The map is the average for both hemispheres. Time differences were smoothed by two-dimensional Gaussian running window 3° in latitude and 1.8 years in time. The rough location of the magnetic-activity belt is drawn in black circles.

The primary focus of this study was to construct the depth profile of time differences. Averaging measurements over 15 years substantially decreases systematic and realization noise, especially the annual periodicity due to the B_0 angle. In Fig. 18, the average time differences for 3658 daily measurements from 1995 to 2010 are presented as a function of latitude and separation distance (left panel). The latitude grid corresponds to the midpoints of the ray path connecting the two locations in the north–south direction. At small separation distances, the measurements can be made for latitudes as high as 63°. For large separation distances, one of the endpoints lies above 70° latitude which can not provide enough signal-to-noise ratio for the Gabor-wavelet fitting procedure. A decrease in the magnitude of the time difference for small distances around 60° is visible in both hemispheres, but it does not change sign, which is the case in small separation measurements. There is evidence of a decreasing magnitude of time differences towards high latitudes, but we do not see any signs of countercells.

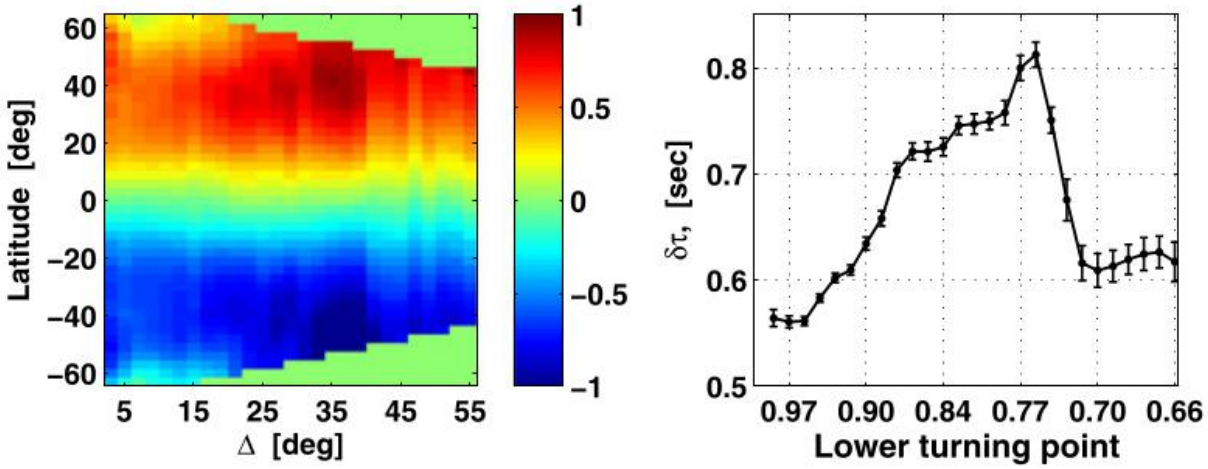

Fig. 18 Travel-time differences as a function of latitude and separation distance (left panel). The colormap shows the range of travel-time measurements in seconds. Right panel: a symmetrized horizontal cut corresponding to latitudes around 35°– 40°. The abscissa indicates the lower turning points of the separation distances used in the left panel. A sharp drop at approximately $0.76R_\odot$ is apparent.

The main behavior of this averaged map is an increase in time difference with depth. Figure 18 (right panel) shows the average time difference for the 35°– 40° latitude range as a function of the lower turning point. A monotonic increase up to $0.76R_\odot$ is followed by a sharp decrease at deeper depths. This could be an artifact related to the speed-of-light problem discussed by (Duvall et al., GONG 2008/SOHO 21, 2009), or other projection-based issue. On the other hand, this is not able to explain why it drops at this particular depth: the artifacts should be even stronger for larger

distances. One possible reason could be the presence of a reverse flow (equatorward) below $0.76R_{\odot}$. Measurements for travel distances $\Delta = 51 - 57^{o}$ correspond to waves with the lower turning point of about $0.68R_{\odot}$. These waves propagate mostly vertically in the upper layers, which makes them less sensitive to the poleward flows. Since the time shifts obtained from cross-correlations are integrated measurements over the whole ray path, some contributions of meridional flow in the upper convection zone might be present in such large separation distance measurements.

Section 5. Latitude and depth profile of meridional circulation.

Meridional circulation plays a critical role in models of solar dynamo, magnetic flux transport, and the solar cycle (Glatzmaier et al., ApJ, 1982; Wang et al. Science, ApJ, ApJ, 1989, 1991, 2002; Choudhuri et al., A&A, 1995; Dikpati et al., ApJ, 1999; Nandy et al., Nature, 2011). It is well established observationally that meridional flow is poleward in each hemisphere with an amplitude of about 10–20 m s −1 in the near-surface layers, peaking in strength at mid-latitudes (Duvall, SolPhys, 1979; Hathaway, ApJ, 1996; Braun et al., ApJ, 1998; González Hernández et al., ApJ, 1999, 2006; Basu et al., ApJ, 1999; Basu et al., ApJ, 2010; Hathaway et al., Science, 2010; Ulrich, ApJ, 2010).

Since mass does not pile up at the poles, it is believed that a return equatorward flow in both hemispheres is operating somewhere in the convection zone, likely near its base. One of the most promising and complete attempts to measure this meridional circulation was during the graduate work of (Giles et al., Nature, 1997; Giles, PhD thesis, Stanford, 2000). Using the Solar and Heliospheric Observatory spacecraft's Michelson Doppler Imager helioseismic data, Giles found that the poleward meridional flows continued throughout almost all of the convection zone and that there was indirect evidence of a return equatorward flow near the tachocline of a few m s^{-1}. His methods and analysis imposed a constraint of mass conservation. Thus, the picture that emerged was of two closed circulating flows, one cell in each hemisphere, that diverge from the equator at the surface and converge toward the equator in the deep interior.

Since then, other helioseismology studies using a variety of techniques have offered many differing views. For example, (Chou et al., ApJ, 2001; Beck et al., ApJL, 2002; Chou et al., ApJ, 2005) observe an additional "cell" of meridional circulation at mid-latitudes near the location of the active sunspot latitudes, which is divergent and varies in time. Also, (Zhao et al., ApJ, 2004) and (González Hernández et al., ApJL, 2010) found that such a cell has a convergent flow field (Cameron et al., ApJ, 2010). Indeed, large-scale flow profiles (in both meridional and zonal directions) have been

found to vary rather strongly with the solar cycle, and several studies have found that the amplitude of the flow is anti-correlated with the strength of the cycle (e.g., Komm et al., SolPhys, 1993; Chou et al., ApJL, 2001; Haber et al. ApJ, 2002; Basu et al., ApJ, 2003; González Hernández et al., SolPhys, 2008; Gizon et al., SolPhys, 2008). The latitudinal extent of the surface poleward flow has widely varied in the two previous cycles, and some helioseismic measurements indicate a high-latitude, reverse equatorward surface component (Dikpati et al., ApJ, 2012). To add to the complexity, recent observations have shown an increasing polar flow magnitude as one probes deep into the convection zone (Kholikov et al. SolPhys, 2011), and (Hathaway, ApJ, 2012) place the equatorward return flow at a depth of 70 Mm.

(Zhao et al., ApJL, 2012b) observed a new systematic center-to-limb signal in time–distance measurements (Duvall et al., Nature, 1993), which may play a key role in obtaining reliable deep meridional flow measurements and be one of the sources of the discrepant results mentioned above. The approach of (Zhao et al., 2012b) was to remove the systematic travel-time shifts found in the east–west measurements, after rotation is removed, from the meridional (north–south) measurements. This correction led to consistent helioseismic measurements using several different observables. While the source of this signal is not completely understood, it could be related to existing observational limitations like changes of the line formation heights across the solar disk, which produce additional acoustic travel-time shifts in cross-correlation measurements between different locations. (Baldner et al., ApJL, (2012) showed that the effect of the vertical flows from convection in the outer solar convection zone can similarly affect travel-time measurements.

Subsequently, (Zhao et al., ApJL, 2013) applied their local techniques to measure two meridional circulation cells in the solar convection zone, while (Schad et al., ApJL, 2013) implemented a new global helioseismic analysis that resulted in evidence of a complex multicellular velocity structure. These new and exciting findings from space-based data present a potentially revised view of these important large-scale flows.

In (Kholikov et al., SolPhys, 2014 we explore meridional circulation using time–distance helioseismology applied to Global Oscillation Network Group (GONG) data. Here we describe in detail the travel-time measurement procedure we implement, which is non-standard and differs from the methods of (Zhao et al., ApJL, 2012a) and (Hartlep et al., ApJ, 2013), for example. We use more than 600 daily sets of GONG velocity images to probe deep into the convection zone. In order to decrease possible geometric and observational artifacts, we have selected dates with a duty cycle of more than 85% and time periods when the solar tilt angle $B_0 \leq 4^o$. These strict requirements

substantially decrease the amount of data that can be used. We assume that the center-to-limb systematic mentioned above is the same in any direction on the solar disk and we compute it only using the equatorial region of the observations. Travel-time differences are computed for north–south flows and corrected by subtracting the east–west signal.

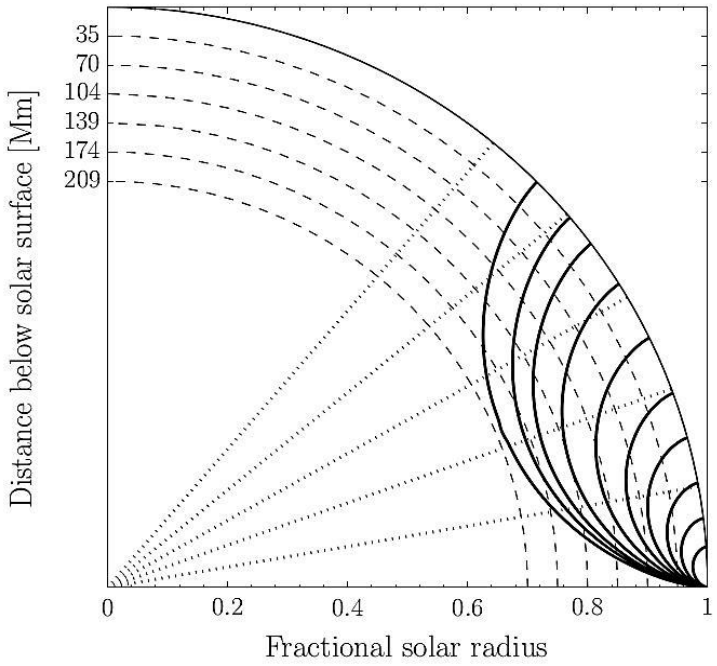

Fig.19. Illustration of approximate ray paths for the 10 phase-speed filters we employ. A realistic solar model is used to trace the paths. We only plot the point-to-arc separation distance for the central distance considered. The five dotted lines are plotted in 10° increments. The depth scale in Mm for the lower turning point of the rays is given on the y-axis for reference.

In this study, we utilize GONG Doppler velocity images, and have selected 652 daily sets of observations with duty cycle higher than 85% during the 2004–2012 time period. The typical travel-time measurements are based on cross-correlation function analysis between two locations on the solar surface separated by certain distances (Δ) (Duvall et al., Nature, 1993). It is well known that waves with the same phase speed form a wave packet and propagate along approximately the same ray path. In order to increase the signal-to-noise ratio of CCFs, phase velocity filters are used to isolate particular wave packets. To infer the meridional flow signal we measure wave travel times for waves propagating in opposite directions along the same ray path that lies between a pair of points (more precisely, a point and an arc) at constant longitude. In this case, the travel-time difference for waves propagating in the two opposite directions is sensitive only to the meridional (north–south) component of the flow.

Ten different phase speed filters are employed and designed to cover the approximate depths of $0.98-0.70R_{\odot}$. Only modes within temporal frequencies between 1.8 and 4.5 mHz are retained. The approximate ray paths of the filtered wave packets considered here are illustrated in Fig. 19. The CCF between a point and the signal averaged over a 30° arc for a given longitude. Arcs in the four cardinal directions are considered. For each filtered set of data the cross correlations were computed for some range of travel distances with increments of 0.75° around the maximum of the first bounce in the CCF. In total, 72 correlation functions are computed for travel distances covering $\Delta = 2.75–47°$.The cross correlations were averaged over about 250 longitude bins in the range $-45^{o} \leq \phi \leq 45^{o}$. Using smaller bands in longitude provides more proper center-to-limb corrections, but leads to a decrease in the signal-to-noise ratio of cross-correlation measurements. Simple comparison using narrower bands showed significant increase of the variance of individual measurements. Since we are interested in travel time differences of about 1 sec, we decided to use a wider longitude range. Northward and southward travel times were obtained by fitting a Gabor wavelet function to both the positive and negative lags (τ) of the cross correlations. The difference between two oppositely directed travel times is computed for travel distances Δ corresponding to each phase velocity filter. We use the convention of "south minus north" (S-N) travel-time differences. In addition, travel-time differences in the "east minus west" (E-W) direction have also been computed using all of the exact steps of the data processing procedure outlined above. The travel times for these measurements were averaged over ±20° in latitude. A constant shift due to internal solar rotation is observed and removed for each travel distance measurement. These measurements are used to correct the systematics for the meridional observations. The top left panel of Fig. 20 shows an average over 652 days of S-N travel-time differences presented as a function of latitude and travel distance. Each point at a given travel distance corresponds to the middle position between a point and an arc in our cross-correlation scheme. To avoid very high latitude information where the endpoints of the cross correlations lie, the measurements are cut off as a function of distance. The uncertainties are given in the second column, computed from the dispersion in individual measurements for each longitude and each day. These are typically a very small percentage of the averaged signal.

Signatures of poleward meridional flow in each hemisphere are clearly seen in Fig. 20(a). The color convention in this figure is such that blue is consistent with a flow toward the north pole, and red a flow toward the south pole. Indeed, in addition to a peak at mid-latitudes as expected, an increase in the travel-time difference with depth

(i.e., travel distance) is also observed. We expect this to be due to one or several systematics. To explore this further, E-W travel times computed from the same data set are shown in the middle panel of Fig. 20 as a function of longitude on the x axis. The E-W map has been symmetrized about the central meridian, as we expect there to be no significant differences between the two (east/west) hemispheres since the data have been tracked to account for differential rotation. These measurements show a similar pattern of center-to-limb variation as the S-N map.

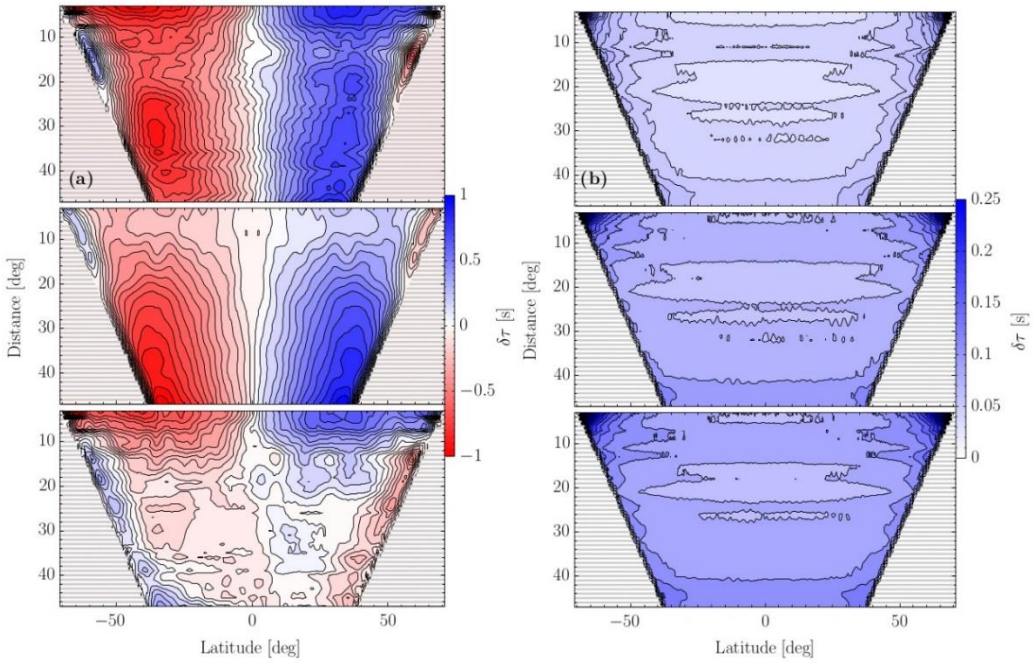

Fig. 20. Travel-time difference maps obtained using 652 daily sets of Doppler velocity images. Column (a) shows the S-N, E-W, and S-NE-W contour maps from top to bottom, respectively. Column (b) plots the corresponding measurement uncertainties associated with each panel in column (a). Note the x-axis in the middle panel in each column is the longitude, with the same numerical scale values as shown for latitude (±75°). Hatched regions show where no measurements were computed due to limb constraints.

(Zhao et al., ApJ, 2012a) reported a very detailed analysis of travel-time measurements from different observables. Since they found that the shape and magnitude of center-to-limb variations is quite different for Doppler, continuum, line core and line depth of Helioseismic and Magnetic Imager measurements, one might conclude that these variations are not caused by any large-scale sub-surface flow of solar origin. Here we follow the same procedure and "correct" the S-N measurements by subtraction of the E-W measurements, the result shown in the bottom panel of Fig. 20(a). This correction removes the tendency of the travel times to increase with depth. Furthermore, some evidence of sign changes can be seen.

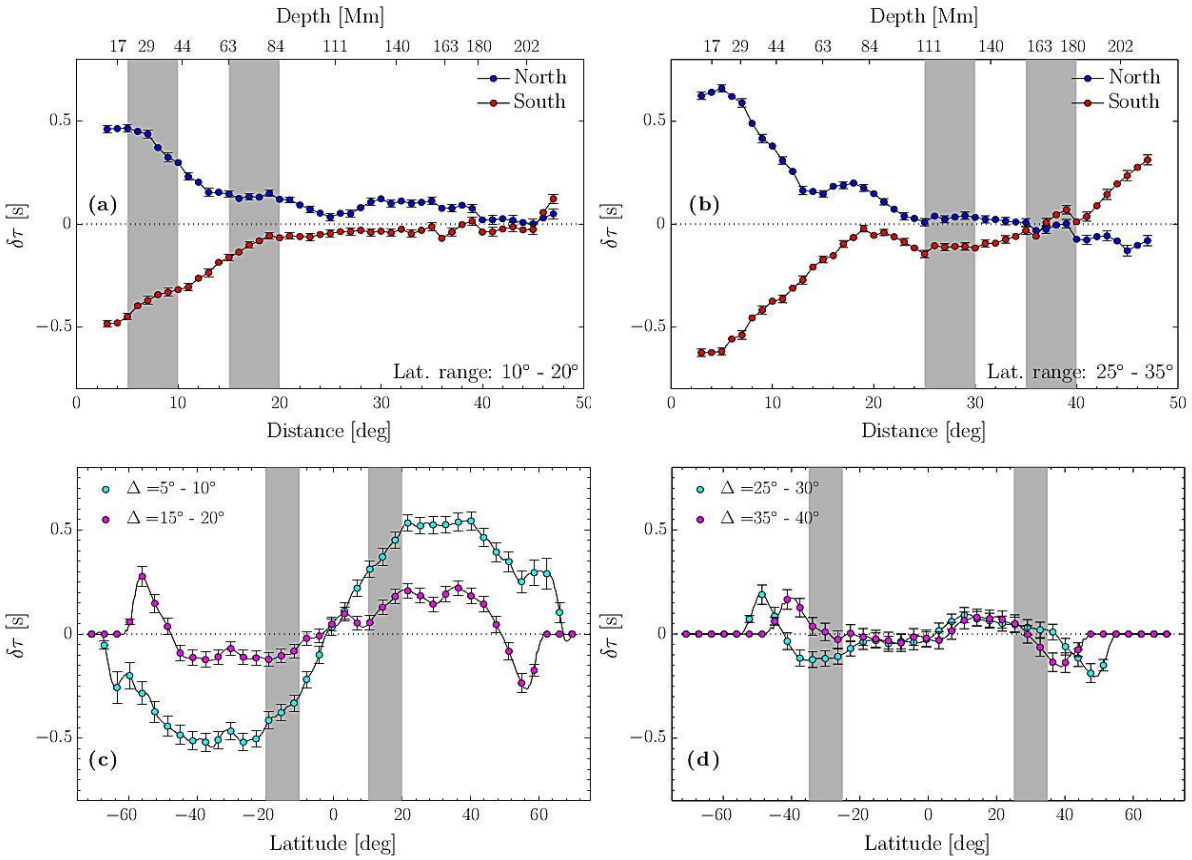

Fig. 21. Cuts through depth and latitude of corrected S-N travel-time differences. The top row panels (a) and (b) show the travel-time differences in each hemisphere as a function of measurement distance (Δ) for the latitude range averaged over the 10° band noted in the figure. A proxy for the lower turning point depth for each travel distance is shown on the upper x-axis. Highlighted in gray are the travel distances shown in the corresponding plots below. Panels (c) and (d) shows travel times as a function of latitude averaged over an interval in distances of 5°. The latitude ranges in panels (a) and (b) are given in the gray boxes of panels (c) and (d). The uncertainties are shown for all cases and are plotted only at staggered data points for clarity.

Figure 21 shows various cuts through the travel-time difference maps. Panels (a) and (c) are cuts at lower latitudes and shorter travel distances, while panels (b) and (d) are for mid-latitudes and larger travel distances. These figures confirm that travel-time differences are strongest at mid-latitudes around 30° for a range of depths, as has been observed in past studies. This representation shows a clear yet peculiar asymmetry between the northern and southern hemispheres. Most importantly, we also observe evidence that a change in sign occurs in the measurements for two cases: (1) at high latitudes in each hemisphere for travel distances greater than about 15° and (2) for large distances for most latitudes greater than about 20° in each hemisphere.

Indeed, if large-scale flows are responsible for these signals, Fig. 21(a) and (b) show a tendency for the flow to approach a change of sign at skip distances of 15° –20°

for a broad latitude range. At larger distances, this signal then resurrects its poleward sense, eventually reversing again at the deepest probe depths. This very broadly suggests a multicellular structure as discussed in (Zhao et al., ApJ, 2012a, 2013), who found poleward flows down to $0.91R_{\odot}$, equatorward flows in the $0.82 - 0.91R_{\odot}$ range, and then poleward again beneath that. Th work by (Schad et al., ApJL, 2013) reports yet another measurement of multicellular structure of the meridional flow using a different, global approach. We caution that the change in sign at all distances at the maximal latitudes considered here (most evident in Fig. 20) could be due to a systematic caused by the solar B_0 variation, as demonstrated recently in (Kholikov et al., SolPhys, 2014). However, in the measurements here such an artifact is somewhat puzzling since we have restricted the data coverage to epochs when this angle is small. Another possible cause could simply be the use of the ad hoc correction method and any of its inherent systematics. The real origin of the center-to-limb variation across the solar disk is not well understood at present. Most likely, this effect is possibly due to the increase of spectral-line formation height with the distance from the disk center. The (Jackiewicz et al., ApJ, 2015) work describes inversion results of meridional flows using travel-time measurements obtained in (Kholikov et al., ApJ, 2014). Usually, helioseismic measurements inverted in terms of acoustic ray theory (e.g., Kosovichev et al., SCORe'96, 1997), whereby travel-time differences $\delta\tau$ of waves propagating in opposite directions are assumed to be caused only by slowly varying interior flows along a given ray path. Working in a coordinate system where r is the distance from the Sun's center and θ the latitude, requires to solve well known inverse problem:

$$\delta\tau = \int K(\theta, r) \cdot u(\theta, r) ds$$

where $\delta\tau$ is time-differences measured as a function of delta and latitude, u is the flow and K represents sensitivity kernels. To interpret the GONG travel times, we compute kernels for each measurement, namely for all 45 values of Δ in the range of 3°–47°, using 3300 μHz for the value for the central frequency. We solve above equation by inverting the travel-time differences and obtain the meridional flow as a function of latitude and depth using the subtractive optimally localized averaging, or SOLA (Pijpers et al., A&A,1994; Jackiewicz et al., SolPhys, 2012) technique. In order to test and validate the inversion procedure we apply it to reproduce well known solar differential rotation profile as a function of depth and latitude.

In addition to the E− W measurements discussed in (Kholikov et al., ApJ, 2014), we also made travel-time measurements of untracked data that preserve rotation information. The geometry is such that cross correlations for a given latitude and separation distance are computed from point to arcs, where the point is always on the

central meridian and the arcs lie in one of the hemispheres centered on that latitude. The westward signal (prograde) is subtracted from the eastward signal (retrograde), leaving behind the expected influence of rotation that is subsequently free from the CTL effect described earlier. In other words, since a purely symmetric CTL effect has the same sign in each hemisphere with this measurement geometry, upon subtraction it is canceled out. These calculations are then done for many distances and latitudes, for about 360 days of data.

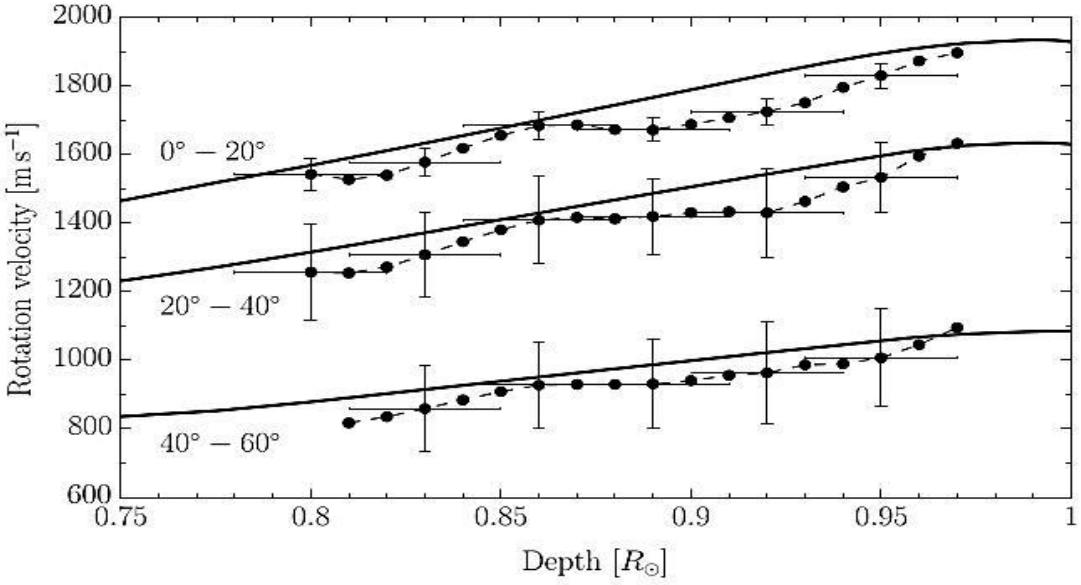

Fig. 22. Comparison of the solar (differential) rotation velocity estimated from inverting travel-time differences (dashed lines with circles) with global helioseismic results (solid lines). Averages are computed over three latitude bins as labeled.

To invert for solar rotation we use the following set of parameters: the location of the target function in depth is set from $0.8R_\odot$ to $1.0R_\odot$ with steps of $0.01R_\odot$ and in latitude from −60° to +60° with steps of 2.5°; the width of the target function in depth and latitude is FWHM $r = 0.04R_\odot$ and FWHM $\theta = 5^o$, respectively. To make a more meaningful comparison, the global helioseismic results are smoothed to our inversion resolution by convolving with the target function used at each depth. Finally, both sets of results are averaged over three latitude bins from 0°–20°, 20°–40°, and 40°–60°.

The comparison with the time-averaged rotation profile from global analysis of about 1000 days of HMI data (Howe et al., JphCS, 2011) is shown in Fig. 22. Within the uncertainties of our local-helioseismic inversion, the results are in agreement over most depths and latitudes except for the near-surface region around the equator. There are many possible contributions to any disagreement in general, including different

instruments and non-overlapping time series. Despite some discrepancies, this provides more confidence that large-scale flows, albeit strong ones in this case, are somewhat accurately attainable with these tools.

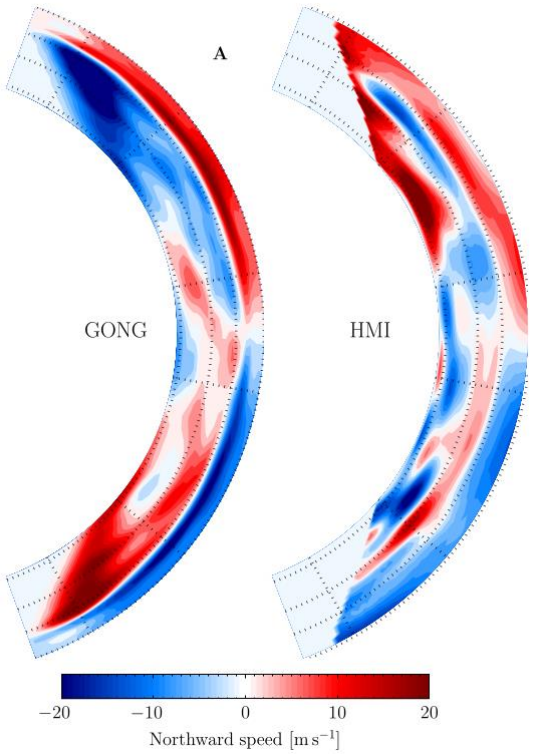

Fig. 23. Cross-sectional views of the meridional flow profiles within latitudes of ±70° and depths above $0.74R_{\odot}$. The dotted lines on each image are plotted at depths $r = (0.76,0.85,0.92,1.0)R_{\odot}$ and at latitudes $\theta = \pm(10°, 40°, 60°)$

The CTL-corrected S − N travel times measured from GONG data and introduced in this section above, were inverted for flows and are shown in Fig. 23. Also provided are the HMI results from (Zhao et al., ApJL, 2013) that were kindly provided by J. Zhao for comparison. GONG and HMI show very good agreement regarding the location of the change of sign from surface poleward flows to equatorward flows at about $r = 0.91R_{\odot}$. The shallow return flow peaks at similar latitudes with amplitude around 5–10 m s^{-1}. Unlike HMI, GONG only shows weak evidence of a second "cell" at low latitudes within 15° of the equator, a feature we suspect is spurious. The equatorward circulation at the bottom of the detection region is consistent with recent predictions from flux-transport models. We do not observe any evidence of multiple cells in latitude at any depths.

The global pattern of the meridional flow are very different, ranging from multiple cells in depth (Zhao et al., ApJL, 2013) and multiple cells in depth and latitude (Schad et al., SolPhys, 2013) to a single-cell picture with a return flow starting in rather shallow layers (Jackiewicz et al., ApJ, 2015; Hathaway, ApJ, 2012, at about 0.9 solar radii) or in deeper regions (Giles et al., Nature, 1997; Braun et al., ApJL, 1998;

Rajaguru at al., ApJ, 2015, below 0.85 solar radii). However, there are several details to keep in mind concerning these inversion results (Jackiewicz et al. ApJ, 2015), e.g., that uncertainties in the results due to systematic effects are likely to be larger than the random errors in the inversion results, that the results were obtained using different instruments, and that they cover different periods in time. Furthermore, the impact of the radial flow component on the travel times was not taken into account in the results obtained by (Zhao et al., ApJ, 2013) and (Jackiewicz et al., ApJ, 2015).

In time–distance helioseismology (Duvall et al., Nature, 1993), flows can be inferred using sensitivity functions (kernels), which are a model for the impact of the flows on travel-time measurements of acoustic waves. Measurements of deep meridional flow have so far been done using the rather classical ray approximation (Kosovichev et al., SolPhys, 1997). In this model, travel times are assumed to be sensitive to flows only along an infinitely thin ray path, which connects the two observation points.

Inversions can be extended to a Born approximation model for the travel-time measurements from Cartesian to spherical geometry. An alternative approach for computing Born kernels was proposed very recently by (Gizon et al., A&A, 2017). These developments permit the use of Born approximation kernels for inferring the deep meridional flow. In the Born approximation (e.g., Birch et al., SolPhys, 2000; Gizon et al., ApJ, 2002), the full wave field in the solar interior is modeled using a damped wave equation, which is stochastically excited by convection. This wave equation is solved in zero-order and in its first-order perturbation, which includes advection in the presence of a flow field. When modeling travel times using the Born approximation, the advection and first-order scattering of the wave field at any location inside the Sun is thereby taken into account.

The ray approximation is expected to be accurate if the underlying flow field does not vary at length scales that are smaller than a wavelength (e.g., Birch et al. 2001). In the case of flows at the bottom of the convection zone, this scale was estimated to be of the order of 200 Mm (Böning et al. ApJ, 2016). If the flow varies on smaller length scales, the Born approximation is thought to be more accurate (e.g., Bogdan, ApJ, 1997; Birch et al., ApJ, 2004; Couvidat et al., ApJ, 2006; Birch et al., AN, 2007).

In addition to modeling the perturbation to the full wave field in the solar interior, an advantage of the Born approximation is that it also provides a model for additional observational quantities, such as disk-averaged cross-covariances and mean power spectra, which is not the case for the ray approximation. The accuracy of the model can therefore easily be validated (Böning et al., ApJ, 2016).

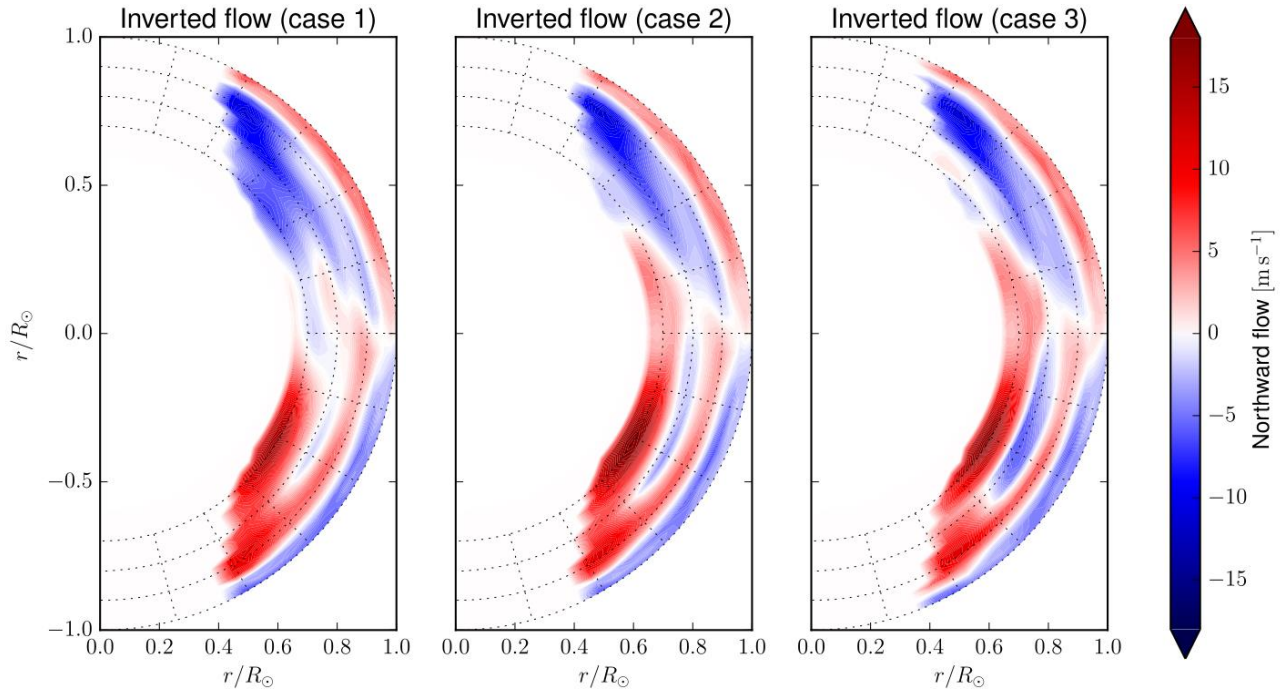

Fig.24. Inverted meridional flow profiles from the refined SOLA inversion using the full covariance matrix and a regularization term for the cross-talk. For the different cases, we used either a medium threshold (case 1) or a low threshold (cases 2 and 3) in the SVD.

In Böning et al., ApJ, 2017 and Böning et al., ApJ, 2017 inversions were made using Born sensitivity kernels. Detail and formalism of validating and performing the real inversion by using full covariance matrix of measured travel-time differences are described accordingly. The main result of this inversion shown the shallow equatorward return flow at depth about $0.9R_\odot$. Single cell structure of meridional flow is in good agreement with other inversion techniqes, while multi-cell structure depend on the threshold used in the singular value decomposition.

CONCLUSIONS

In this work the main scientific results obtained by analyzing more than 30 years of helioseismic observations are presented:

1. Proposed a solution for gap filling problem based on the autocorrelation function of observed solar oscillations of low degree. This particular method utilizes the autocorrelation function of the observed oscillations to efficiently generate long term time series. Developed approach is particularly effective when working with ground-based solar un-resolved full disk observations, where data gaps are common.

2. We provide tables of solar oscillation frequencies of low degree measured in the frame of the IRIS project. In addition to the frequencies, you have also generated

parameters such as linewidths, mode amplitudes, splitting coefficients, and their temporal variations across the solar activity cycle. Studied parameters provide important information about the properties and characteristics of the solar oscillations.

3. We have shown significant variations on correlation amplitudes of wave packets with solar cycle. The maximum perturbation attributable to solar activity is known to be localized in a narrow layer immediately beneath the photosphere. It follows from our results that the maximum perturbation arises at a depth of $(0.83 - 0.85)R_{\odot}$.

4. First helioseismic image of the sunspot beneath the solar surface is reconstructed using time-distance relation properties of solar acoustic waves. It has been revealed that the sunspot's root can reach depths of up to 40 Mm, indicating its significant presence within the solar interior.

5. We have confirmed an acoustic travel time anomalies due to the emergence of active regions from the deep solar convective zone. These acoustic travel time anomalies provide a clear map of upcoming active regions at depths ranging from 40-75 Mm within the Sun. Importantly, this map becomes visible a few days earlier than the active regions appear on the solar surface. This suggests that the acoustic signals can provide advance warning or predictions of the formation and emergence of active regions.

6. We have measured the acoustic radius of the sun and its temporal variations. Measurements derived from ground based GONG and space based MDI observations and both sets show consistency, indicating that the acoustic signals propagate through the solar core in a similar manner. The exceptional precision of the measurement technique employed allows for the determination of temporal variations in the acoustic radius of the Sun within fractions of a second.

7. Obtained detailed measurements of poleward meridional flow as a function of latitude and depth. Our measurements include temporal variations during two phases of solar activity as well. We found evidence to suggest that the apparent second-cell structure reported by some members of the solar physics community at high latitudes is not associated with the surface component of the meridional flow. Instead, it is likely a manifestation of artefacts caused by the solar tilt-angle.

8. By implementing a systematic effect removal, from our meridional travel-time measurements caused by line formation height changes across the solar disk, we were able to recover the equatorward return flow predicted by solar dynamo models which was waiting the its discovery for more than two decades.

“TIQXMMI” MILLIY TADQIQOT UNIVERSITETI HUZURIDAGI FUNDAMENTAL VA AMALIY TADQIQOTLAR INSTITUTI HUZURIDAGI ILMIY DARAJALAR BERUVCHI DSc.03/31.03.2022 T/FM.10.04 RAQAMLI ILMIY KENGASH

FUNDAMENTAL VA AMALIY TADQIQOTLAR INSTITUTI

XOLIKOV SHUKIRJON SODIKOVICH

QUYOSH ICHKI QATLAMLARI XUSUSIYATLARINI FAZO-VAQT GELIOSEYSMIK USULLAR ORQALI TEKSHIRISH

01.03.01 – Astronomiya
((fizika-matematika fanlari))

E’LON QILINGAN ILMIY ISHLAR BO‘YICHA DISSERTATSIYASIZ FIZIKA-MATEMATIKA FANLARI BO‘YICHA FAN DOKTORI (DSc) ILMIY DARAJASINI OLISH UCHUN TAQDIMNOMA

Toshkent – 2023

Fizika-matematika fanlari bo‘yicha fan doktori (DSc) dissertatsiyasi mavzusi O‘zbekiston Respublikasi Vazirlar Mahkamasi huzuridagi Oliy attestatsiya komissiyasida B2022.3.DSc/FM202 raqami bilan ro‘yxatga olingan.

Taqdimnoma “TIQXMMI” Milliy tadqiqot universiteti huzuridagi Fundamental va amaliy tadqiqotlar institutida bajarilgan.

Tadqiqot ishlari natijalari Nice universiteti (Fransiya), Tsing-Hua universiteti (Tayvan), Milliy Quyosh Observatoriyasi (AQSh) va “TIQXMMI” Milliy tadqiqot universiteti huzuridagi fundamental va amaliy tadqiqotlar institutida olib borildi.

Taqdimnoma uch tilda (o‘zbek, ingliz va rus (rezyume)) Ilmiy kengashning internet sahifasida (www.ifar.uz) va “Ziyonet” axborot-ta’lim portalida (www.ziyonet.uz) joylashtirilgan.

Taqdimnoma “TIQXMMI” Milliy tadqiqot universiteti huzuridagi fundamental va amaliy tadqiqotlar instituti huzuridagi DSc.03/31.03.2022 T/FM.10.04 raqamli Ilmiy kengashning 2023-yil “_01_” _avgust_ soat _16^{00}_ dagi majlisida bo‘lib o‘tadi. (Manzil: 100000, Toshkent shahri, Qori Niyoziy ko‘chasi 39-uy, Fundamental va amaliy tadqiqotlar instituti, 108-katta majlislar zali; tel.: 71 237-09-61.; e-mail: info@ifar.uz

Taqdimnoma bilan “TIQXMMI” Milliy tadqiqot universiteti huzuridagi Fundamental va amaliy tadqiqotlar instituti Axborot-resurs markazida tanishish mumkin (____ raqami bilan ro‘yxatga olingan). (Manzil: 100000, Toshkent shahri, Qori Niyoziy ko‘chasi, 39-uy, Fundamental va amaliy tadqiqotlar instituti, 205-kutubxona; tel.: 71 237-09-61

Taqdimnoma 2023-yil “___” _____ kuni tarqatildi.

(2023-yil “___”_____dagi ___ raqamli reestr bayonnomasi)

B.J. Ahmedov
Ilmiy darajalar beruvchi ilmiy
kengash raisi f.-m.f.d., professor

E. X. Karimbayev
Ilmiy darajalar beruvchi ilmiy
kengash ilmiy kotibi f.-m.f. bo‘yicha PhD

KIRISH (Fan doktori (DSc) taqdimnoma annotatsiyasi)

Mavzuning dolzarbligi va zarurati. Gelioseysmologiya quyoshning ichki tuzilishi va dinamikasi haqida batafsil tushunchalar beradi. Olimlar Quyosh yuzasida akustik to'lqinlarning tarqalishini o'rganish orqali Quyosh ichki qismi ichidagi turli qatlamlarning harorati, zichligi va tarkibi haqida ma'lumot berishlari mumkin. Ushbu bilim Quyoshning tuzilishi vaqt o'tishi bilan qanday rivojlanganini tushunishimizga yordam beradi va umuman yulduz evolyutsiyani tushunishimizga hissa qo'shadi. Gelioseysmik tadqiqotlar Quyosh ichida sodir bo‘layotgan turli jismoniy jarayonlarni o'rganish imkonini beradi. Masalan, tadqiqotchilar Quyosh yuzasining tebranishlarini tahlil qilish orqali tashqi qatlamlardagi konveksiya jarayonlarini, turli chuqurliklarda aylanish ko'rsatkichlarini, quyosh dog'lari va quyosh chaqnashlari bilan bog'liq magnit faolligini tekshirishlari mumkin. Ushbu tadqiqotlar quyosh faolligi va energiya uzatilishi mexanizmlari haqida qimmatli ma'lumotlarni taqdim etadi. Quyosh magnit faolligi, shu jumladan quyosh chaqnashlarii va koronal massa chiqarib tashlashlari (CME) kosmik ob-havoga ijobiy ta’sir ko'rsatishi mumkin. Gelioseysmik tekshiruvlar ushbu quyosh portlashlarini yo'lga qo'yayotgan asosiy mexanizm va jarayonlarni tushunishda yordam beradi. Quyosh ichki qismidagi o'zgarishlarni gelioseysmik usullar orqali kuzatib boradigan bo'lsak, quyosh chaqnashlari yoki CMElar sodir bo‘lishi ehtimolligini ko'rsatishi mumkin bo'lgan prekursor sharoitlari va namunalarini aniqlashlari mumkin, shu tariqa kosmik ob-havo prognozi va bashoratida yordam beradi. Gelioseysmik ma'lumotlar quyosh modellari va nazariyalarini sinovdan o'tkazish va rivojlantirish uchun muhim mezon bo'lib xizmat qiladi. Kuzatish natijalarini nazariy bashoratlar bilan taqqoslash orqali olimlar yulduzlar evolyutsiya, energiya uzatilishii va magnit maydonni ishlab chiqarish modellarini tasdiqlashlari, yoki o'zgartirishlari mumkin. Gelioseysmologiya yulduzlar ichida sodir bo'layotgan fundamental jarayonlarni tushunishimizni sinab ko'rish va yaxshilashning o‘ziga xos usulini taqdim etadi.Gelioseysmik tekshiruvlar quyosh va kosmik tadqiqotlar uchun kengroq ahamiyatga ega. Gelioseysmologiyadan olingan bilimlar boshqa yulduzlarni, ularning evolyutsiyasi va ichki dinamikasini tushunishimizga hissa qo‘shadi. Bundan tashqari, Quyosh magnit faolligi va kosmik obhavosini o‘rganish quyosh bo'ronlarining Yerning sun’iy yo‘ldosh aloqasi, elektr tarmoqlari, kosmonavtlar xavfsizligi kabi texnologik infratuzilmasiga ta'sirini yaxshiroq tayyorlash va yengillashtirishga yordam beradi. Gelioseysmologiyada vaqt-masofa gelioseysmologiya va halqa-diagramma tahlili kabi ilg‘or usullar Quyoshning ichki qatlamii haqidagi tushunchamizni yaxshilashda davom etmoqda. Bu usullar Quyosh yuzasida seysmik to'lqinlarning tarqalishini o'rganishva ichki tuzilmalar haqida ma'lumot berishdan iborat. Seysmik

tomografiya usullarining yana bir yutuqlari quyosh yadrosini yuqori o'lcham va aniqlik bilan tasvirlash qobiliyatini ta'minlashi mumkin. Yakunlashtirib aytgandai, gelioseysmik tekshiruvlar Quyosh, uning ichki jarayonlari va kosmik ob-havoga ta'siri haqidagi tushunchamizni ilgari surish uchun dolzarb va zarurdir. Quyosh tuzilishi, dinamikasi va magnit faolligi haqida tushunchalar berish orqali gelioseysmologiya dolzarb astrofizika, quyosh modellarini yaxshilash, kosmik obhavo ta'sirini bashorat qilish va yumshatish qobiliyatimizni oshirishda juda muhim rol o‘ynaydi.

Tadqiqotning xalqaro konteksti. Gelioseysmologiya - bu turli mamlakatlardan kelgan olimlar Quyosh ichki qatlamlari haqidagi tushunchamizni ilgari surish uchun birgalikda harakat qilishni o'z ichiga olgan yuqori hamkorlikdagi tadqiqot sohasi. Xalqaro hamkorlik ma'lumotlar, tajriba va resurslarni baham ko'rish imkonini beradi, bu esa tadqiqotchilarga murakkab muammolarni bartaraf etish va yanada mukammal natijalarga erishish imkonini beradi. Gelioseysmik kuzatuvlari quyosh tebranishlarining yuqori o'lchamli ma'lumotlarini qo'lga kiritish uchun zamonaviy asboblar va qulayliklarni talab qiladi. Bir nechta xalqaro observatoriyalar va kosmosga asoslangan missiyalar, masalan, NASA tomonidan Quyosh dinamikasi observatoriyasi (SDO), NASA va ESA tomonidan Quyosh va Heliosferik observatoriyasi (SOHO) gelioseysmik tadqiqotlarga hissa qo'shadi. Ushbu missiyalar quyosh tadqiqotlari bo'yicha xalqaro hamkorlikni ta'kidlab, ko‘p mamlakatlardan kelgan olimlar va muhandislarning ishtirokini o'z ichiga oladi. Xalqaro hamkorlik gelioseysmik modellar va usullarni tasdiqlash uchun juda muhimdir. Bir nechta tadqiqot guruhlari mustaqil ravishda ma'lumotlarni tahlil qiladilar va ularning natijalarini taqqoslaydilar, topilmalarning barqarorligi va ishonchliligini ta'minlaydilar. Ushbu jarayon potentsial tarafkashlik, noaniqlik yoki cheklovlarni aniqlashga yordam beradi, bu esa modellar va usullarni takomillashtirishga olib keladi. Gelioseysmik tadqiqotlarning xalqaro kontseptsiyasi butun dunyo bo‘ylab tadqiqotchilar o‘rtasida Quyosh ichki qtlamlari haqidagi tushunchamizni ilgari surishga bo‘lgan umumiy qiziqishnii ko‘rsatmoqda. Hamkorlikn, ma'lumotlarni bo‘lishish, bilim va resurslar almashinuvi ushbu global ilmiy faoliyatning muhim tarkibiy qismlari hisoblanadi.

Mavzu bo'yicha tadqiqotning hozirgi holati. Vaqt-masofa gelioseysmologiya - quyoshning ichki qisminiuning yuzasida akustik to'lqinlar tarqalishini tahlil qilish orqali tadqiqotlarda qo'llaniladigan usul. Quyosh ichki qismining tuzilishi va dinamikasi, shu jumladan konveksiya zonasi, radiatsion zona, yadro haqida qimmatli tushunchalar beradi. Quyoshning aylanish profilini xaritalashda vaqt-masofal gelioseysmologiya muhim ahamiyatga ega bo'ldi. Tadqiqotchilar quyosh yuzasi bo'ylab akustik to'lqinlarning tarqalish vaqtlarini o'lchash orqali aylanish darajasini turli

chuqurlikda aniqlashlari mumkin. Bu esa differensial aylanishning kashf etilishiga olib keldi, bu yerda Quyosh ekvatori o'z qutblariga nisbatan tezroq aylanadi. Shuningdek, quyosh dog‘lari va quyosh chaqnashlari kabi yuzaosti oqimlar va quyosh faoliyati o'rtasidagi munosabatlarni o'rganish uchun vaqt-masofa gelioseysmologiya qo'llanilgan. Tadqiqotchilarning aniqlashicha, bu hodisalar ko'pincha yuza-osti oqimi shakllarida lokalizatsiya qilingan tebranishlar bilan bog'liq. Bu usulda Quyoshning p-modda deb ataladigan akustik tebranishlari haqida batafsil kuzatuvlar berilgan. Bu tebranishlar Quyoshning ichki tuzilishi haqida harorat, zichlik, tovush tezligi o‘zgarishi kabi ma'lumotlarni ochib beradi. Vaqt-masofal gelioseysmologiya ushbu parametrlarni yuqori aniqlik bilan o'lchash imkonini berdi. Tadqiqotchilar quyosh ichki qismidagi global meridional aylanma oqimni o‘rganish uchun vaqt masofasidagi gelioseysmologiyadan foydalanganlar. Akustik to‘lqinlarning harakatlarini muntazam kuzatish orqali olimlar ushbu oqimning dinamikasi va o‘zgaruvchanligini o'rganishga muvaffaq bo‘ldilar. Quyoshning umumiy dinamo jarayonida yangi magnit maydonlarining paydo bo'lishi juda muhim rol o‘ynaydi. Olimlar yangi paydo bo'lgan faol maydonlarni o'rganish orqali magnit maydonlarining quyosh ichki qismidan yuzaga qanday suzib chiqishi va olib o‘tilishi haqida tushunchaga ega bo'lishlari mumkin. Bu bilimlar Quyosh magnit siklini tushunishga yordam beradi va taxminan 11 yillik davrga ega bo‘lib, vaqt o‘tishi bilan Quyosh faolligiga ta’sir ko‘rsatishi mumkin.

Tadqiqot mavzusini ish bajarilgan muassasaning ilmiy-tadqiqot faoliyati bilan bog'liqligi. DSc tadqiqotlari bo'yicha kuzatuv ma'lumotlari uchta yer usti bazasi va bitta fazoga asoslangan xalqaro loyihaviy tarmoqlar: Quyoshning ichki qismi bo'yicha xalqaro tadqiqotlar (IRIS), Tayvan tebranishlar tarmog'i (TON), Global tebranish tarmog'i guruhi (GONG) va Michelson Doppler Imager (MDI, SOHO/NASA) doirasida olingan. Hisoblash va tadqiqotlar Fransiya, Germaniya, Buyuk Britaniya, Ispaniya, Tayvan, AQSH universitet va observatoriyalari markazlarida bajarilgan.

Tadqiqotning maqsadi yer va kosmosdan olingan gelioseysmik kuzatuvlarni tahlil qilish; Quyoshning ichki tuzilishini o'rganish, xususan: yuza-osti oqim tuzilishi va uning vaqt evolyutsiyasini; faol maydonlar va ularning quyosh akustik tebranishlari bilan o'zaro ta'sirini; Quyosh meridional aylanishining kengligi va chuqurlik profilini aniqlashdan iborat.

Tadqiqotning vazifalari quyidagilardan iborat:

juda katta miqdordagi gelioseysmik ma’lumotlar tahlilni amalga oshirish uchun statistik jihatdan mustahkam va o'zaro o'lchovli ma'lumotlarni tahlil qilish tarmoqlarni ishlab chiqish;

Past darajadagi quyosh tebranishlari parametrlarining aniq me'zonlari, ilmiy natijalarni chiqarish va olingan natijalarni talqin qilish;

Yuqori aniqlikdagi detektorlar yordamida amalga oshiriladigan quyosh tebranishi kuzatuvlarining vaqt-masofa usullari orqali o'rganish;

Quyosh konvektiv zonasida faol maydonlar paydo bo'lish mexanizmini o'lchash va baholashning asoslarini ta'minlash;

Yuqori o'lchamli doplergrammalarni chastotaviy filtrlashning yangi usullarini ishlab chiqish va ularni gelioseysmik ma'lumotlarni tahlil qilish vositalarining muntazam dasturlariga joriy etish;

Barcha mavjud ma'lumotlar to'plamlari yordamida quyosh meridional oqim o'lchovlarini amalga oshirish, oqimni kenglik va chuqurlik profilini qurish.

Tadqiqotning ob'yekti xalqaro loyihalar doirasida olingan gelioseysmik kuzatuv ma'lumotlari; quyoshni yerdan va kosmosdan olingan yulduz sifatida (oddiy nuqta) va yuqori o'lchamli quyosh dopplergramlari.

Tadqiqot predmeti quyosh tebranishlarining o'lchangan xususiyatlari va xossalari, chastotasi va boshqa parametr jadvallari, Quyosh ichki tuzilishining ishlab chiqilgan modellari hisoblanadi.

Tadqiqot usullari: zamonaviy hisoblash inshootlarida oldindan ishlov berish va ulardan ilmiy natijalar chiqarib olish tartib-taomillarini ishlab chiqish. Kuzatuvlarda keraksiz manba'larni filtrlash orqali quyosh akustik signallarni kuchaytirish. Akustik to'lqin parametrlarini o'lchash orqali Quyoshdagi mahalliy va global miqyosdagi strukturalarni o'lchash. Biz quyosh tasvirini qayta tiklash usulini aniq o'lchovlar uchun filtrlangan yoki sozlangan sferik uyg'unlik koeffitsientlari yordamida amalga oshiramiz. Bunday teskari garmonik dekompozitsiya sferik koordinatalarda olib boradi. Quyosh ichki qismining chuqur qatlamlarini bilish uchun juda muhim bo'lgan akustik tarqalish vaqti o'lchashni xam, faqat sferik geometriya yordamida hosil qilamiz.

Tadqiqotning ilmiy yangiligi:

Quyosh fizikasi jamoasiga past darajadagi quyosh tebranishlarining chastota jadvallarining birlamchi o'lchovlari taqdim etiladi;

birinchi marta Quyosh ichki aylanish tezligi IRIS chastota bo'linish koeffitsientlari yordamida olingan;

birinchi marta Quyosh yuzasi ostidagi quyosh dog'ining tasviri akustik to'lqinlarning xossalaridan foydalangan xolda qurildi;

Quyosh konvektiv zonasining qa'rida paydo bo'lgan faol maydon tasviri yuzasiga suzib chiqmasidan 1-2 kun oldin 40-75 Mm chuqurlikda aniqlanadi;

Quyosh akustik radiusini tengi yo‘q aniqlikda o'lchash imkonini beruvchi yangi usul yaratildi;

Quyosh fizikasi xamjamiyatining ba’zi a’zolari tomonidan yuqori kengliklarda yuz berishi aytilgan ikkilamchi aylanmalar strukturasi global meridional oqimning sirt komponenti bilan bog'liq emasligini ko'rsatuvchi dalillar topildi;

Yerdan olingan GONG kuzatuvlardan foydalanib qutblardan ekvatorga yo‘nalgan qaytuvchi meridional oqim komponentasi tiklandi.

Tadqiqotning amaliy natijalari. Past darajadagi quyosh akustik tebranish aniq chastota o'lchovlari amalga oshiriladi. Quyosh akustik radiusini o‘ta baland aniqlik bilan o'lchashni gelioseysmik usullar bilan amalga oshirish mumkinligi ko'rsatildi. Bundan tashqari, yerdan olingan turli kuzatuvlar bir xil darajadagi aniqlikni ta'minlaydi. Past darajali gelioseysmik usullar astroseizmologiya kuzatuvlariga qo'llaniladi. Faol maydonlarni yuzada paydo bo'lishidan oldin aniqlash kosmik ob-havoni prognoz qilish uchun juda muxim vositadir. Qutblarga yo‘nalgan va qaytish meridional oqimining o'lchovlari Quyosh dinamo simulatsiyalari uchun va Quyoshfaolligi faollik siklini tushunish uchun qimmatli vositadir.

Tadqiqot natijalarining ishonchliligi to'rtta mustaqil asbobni kuzatuvlarini tahlil qilish orqali namoyon bo'lmoqda. Atmosfera sharoitlarining geografik joylashuvi va farqi, Quyosh atmosferasining xar xil balandligida o'lchash barcha kuzatuvlarda umumiy signalga ega bo'lish orqali quyosh akustik tebranish parametrlarining tabiiy kalibrlash imkoniyatlarini taqdim etdi. Olingan ilmiy natijalarning aksariyati kamida ikkita mustaqil loyiha ma’lumotidan hosil bo'ladi. Qayta tiklangan ichki struktura xususiyatlarining aksariyati ikkala, kosmosda va yerga olingan ma’lumotlarga asoslangan.

Tadqiqot natijalarining ilmiy va amaliy ahamiyati. Bu erda taqdim etilgan natijalarning aksariyati ilgari boshqa olimlar yoki tadqiqot guruhlari tomonidan e’lon qilinmagan. Misol tariqasida, ushbu asarning muallifi tomonidan quyosh sirt tebranishlarining teskari sferik garmonik yoyilmasi ishlab chiqilgan va qo'llanilgan. Yuza osti faol maydonlar tasvirlari va meridional qaytish oqimi o'lchovlari o'z kashfiyotini ko‘p yillardan beri kutayotgan edi.

Tadqiqot natijalarini joriy qilinishi. Ushbu tadqiqotda amalga oshirilgan o‘lchovlar quyosh fizikasi bilan bog‘liq ko‘plab tekshiruvlarda asosiy tarkibiy qism sifatida qo‘llanilgan. Nazariy quyosh dinamo simulyatsiyalari o‘z modellarida kapalak sxemasini hosil qilish maqsadida qaytish meridional oqim profilidan foydalangan. Bizning o'lchovlarimizdan qutblarga yo’nalgan meridional aylanish tezligi qutb mintaqalariga plazma oqimi mexanizmiga asoslangan modellarining eng muhim

tarkibiy qismi bo'lib, u quyosh faolligi davrini prognoz qilish uchun muhim ahamiyat kasb etadi.

Tadqiqot natijalarining aprobatsiyasi. Ushbu taqdimnoma natijalari 10 ta xalqaro va respublika ilmiy-amaliy anjumanlarda muhokamadan o'tgan.

Tadqiqot natijalarining e'lon qilinganligi. Taqdimnoma mavzusi bo'yicha jami 21 ta ilmiy ish nashr qilingan, shulardan O'zbekiston Respublikasi Oliy attestatsiya komissiyasining doktorlik dissertatsiyalarining asosiy ilmiy natijalarini chop etish uchun tavsiya etilgan ilmiy nashrlarda 18 ta (Web of Science ilmiy ma'lumotlar bazasida ko'rsatilgan jurnallarda) maqolalar chop etilgan.

Taqdimnomaning tuzulishi va hajmi. Taqdimnoma kirish, beshta bob va xulosadan iborat 116 betni tashkil qiladi.

ISHNING ASOSIY MAZMUNI

Taqdimnomaning kirish qismi: olingan natijalar nomzod va uning hammualliflari tomonidan 18 ta maqolada chop etilgan. Olingan tadqiqot kuzatuvlari xalqaro loyihalar doirasida olinadi: Quyoshning ichki qismi bo'yicha xalqaro tadqiqotlar (IRIS), Tayvan tebranish tarmog'i (TON), Global Oscillation Network Group (GONG), Michelson Doppler Imager (MDI, NASA/SOHO). Barcha maqolalar xalqaro jurnallarda chop etilgan va ko'plab tegishli xalqaro konferentsiyalarda taqdim etilgan. Nashrlarning mavzulari so'nggi 25 yil davomida to'liq disk va yuqori aniqlikdagi gelioseysmik ma'lumotlar tahlilini qamrab oladi. Ushbu maqolalardagi natijalarning aksariyati quyosh qatlamlarida qamalib yotgan quyosh akustik to'lqinlarining vaqt-masofa bog‘lanishlaridan foydalanish orqali olinadi. Gelioseysmologiya so‘nggi o‘ttiz yil mobaynida Quyoshning ichki tuzilishi va dinamikasini o‘rganishning eng muhim vositalaridan biri sifatida paydo bo‘ldi. U Quyosh tebranishlarini o'rganishdan foydalanib, Quyosh qa'rini tekshiradi va uning fizik xossalari haqida qimmatli tushunchalar beradi. Bu erda nomzodning ushbu sohaga qo'shgan bir nechta hissalari taqdim etiladi.

1-bob. Quyoshni yulduz sifatida kuzatuvlari foydalanilgan global gelioseysmologiya qaralgan. Ushbu bo'limda IRIS loyihasidan olingan ilmiy natijalar keltirilgan. IRIS uskunalaridan biri Chimyon tog'i (O'zbekiston) yaqinida joylashgan Qumbel balandligida o'rnatildi. Ushbu qo'lyozma muallifi barcha bosqichlarda ishtirok etib, stansiyani qurdi, iris loyihasi doirasida natijalarni kuzatish, ma'lumotlarni tahlil qilish va ilmiy talqinlarni amalga oshirdi. Birinchi ish (Fossat et al., A&A, 1999) bu yerdan olingan astronomik kuzatuvlarning amaliy muammosiga, vaqt seriyasidagi

bo‘shliqlarga bag‘ishlangan. Bo'shliqning sababi atmosfera sharoitlari, uskunalarning ishlamay qolishi va boshqalar bo'lishi mumkin. Ammo doim yuz tutiladigani, bu quyosh kuzatuvlaridagi asosiy bo‘shliq tungi vaqtdir. Xususan, gelioseysmologiya juda uzoq muddatli, oydan yillargacha uzluksiz o'lchovlarni talab qiladi. Ushbu ish p-moda tebranishlarining to'liq disk o'lchovlarining o'ziga xos va cheklangan holatini ko'rib chiqadi, lekin bu tasvirli gelioseysmologiya masalasiga umumiylashi xam mumkun. Birinchidan, bo'shliqlardagi signalni xar bir moda alohida (yoki aksincha modalar juftligi) interpolyatsiyasi usuli sinovdan o'tkaziladi va ikki kungacha bo'shliqlar uchun samarali ekanligi ko'rsatiladi, lekin signalni shovqinga nisbati signal yaxshi bo'lgan chastota oralig'iga tadqiq qilindi. So'ngra qayd etildiki, to'liq disk signalining avtokorrelatsiya funksiyasi, 20 yoki 30 daqiqada tezda nolga tushgandan so'ng, Fourier spektridagi eng yuqori taqsimotning kvazi-davriyligi tufayli (1 rasmda birinchi 0,5 soat) ikkilamchi kvazi davriy autokorrelyatsiya ko'rsatadi. Ushbu autokorrelyatsiyaning birinchisi, 4 soat masofada, 70 foizdan yuqori bo'lib, cheklangan chastota oralig'ida qariyb 90 foizga ko'tariladi (taxminan 4 va 8 soat lardagi kuchayush). Bu shuni ko'rsatadiki, oson bo'shliqni to'ldirish usulini ishlab chiqish mumkin, agar bo'shliq 8 soatdan oshmasa, barcha chastota oralig'i bo'yicha 90 foizga yaqin ishonch hosil qiladi, ikkala chetida ham kamida 4 soat ma'lumotlar mavjud. Hatto bir yoki ikki davrning qisqa bo'shlig'i mahalliy interpolyatsiyadan ko'ra 4 soat oldin yoki keyinroq olingan ma'lumotlar bilan yaxshiroq to'ldiriladi. Bu holat uchun kuzatuvlarning davomiyligi talabini to'liq disk p-moda gelioseysmologiya uchun sezilarli darajada yengillashtiradi.

IRIS ma'lumotlarining 7 yiliga qo'llaniladigan ushbu usul golf (past chastotali global tebranishlar, NASA / SOHO) uskunasi ma'lumotlarining 2 yilligida allaqachon ko'rilgan barcha past chastotali p-modalarni aniqlashga imkon beradi va ularning chastotalarini aniqlik bilan o'lchash imkonini beradi. So'nggi yigirma yil mobaynida barcha helioseizmologik instrumental dasturlar eng yaxshi vaqtinchalik qamrovni, kuniga 24 soat va yiliga 365 kunni olishga qaratilgan. Bu asosan Fourier spektrida "sidelobes" mavjudligidan qochish uchun. Ushbu sideloblar temporal oyna funksiyasining Fourier almashtiruvlari tomonidan haqiqiy signalning Fourier transformatsiyasining konversiyasi natijasida hosil bo'ladi, bu odatda kuzatuvlar yerdan amalga oshirilganda kamida bir kunlik davriylikni o'z ichiga oladi. Fourier sohasida quyosh tebranishining har bir cho'qqisi va ikkilamchi cho'qqilar yoki sideloblar bilan kuzatuv-oynasi funksiyasining Fourier transformatsiyasi ustiga tarqaladi, bu esa, muqarrar ravishda boshqa haqiqiy cho'qqilarga xalaqit beradi va shu bilan aniq p-moda parametrlarini o'lchashni qiyinlashtiradi (Fassat va boshq., A&A, 1999).

Kuzatuv-oyna effekti Fourier bo'shlig'idagi konvolyatsiya bo'lib, buning uchun dekonvolvatsiya aniq imkonsiz: Fourier transformatsiyasi bo'yicha konvolyutsiya ko'paytmaga aylanadi va biz allaqachon bilamizki, vaqt sohasida bizda haqiqiy signalning 1 yoki 0 dan tayyorlangan oyna funksiyasi bo'yicha ko'payishi mavjud. Fourier bo'shlig'idagi dekonvolutsiya vaqt sohasidagi bo'linish bo'lib, buni nollar bilan amalga oshirish mumkin emas. Keyin taxminan dekonvolulatsiya qilishning bir nechta usullari, vaqt sohasidagi haqiqiy signalning yaqinlashuviga kirmasdan, tuzatilgan energiya spektrini ta'minlashga harakat qilindi. Masalan, (Loudagh S., 1995, Tezis, Universit de Nice) va (Pantel A., 1996, Tezis, Universit de Nice) dissertatsiyalarini ko'ring. Ushbu usullar ma'lum darajada ishlaydi, sidelobe amplitudalarini kamaytiradi va cho'qqilar ichida atrofga tarqalgan quvvatning bir qismini orqaga tortadi. Biroq, ular boj aylanishining kamayishi bilan kamroq va kamroq samarali bo'lib, ular allaqachon 50 foiz atrofida yomon ishlaydi. Muhim nuqta shundaki, ular quyosh tebranish signalining aniq xususiyatlarini butunlay e'tiborsiz qoldiradilar, shunda ular bizning muammo uchun aniq optimallashtirilmaydi. Boshqa usul quyosh signali haqida bilgan narsalarimizni hisobga olish va kuzatilmagan signalni qanchalik ishonchli tasavvur qilishga harakat qilishimiz mumkinligini ko'rishdir. Bir necha davr davomiyligidagi bo'shliqlarni samarali to'ldirish mumkin, agar signal-shovqin nisbati etarlicha yuqori bo'lsa va kuzatuvlarning kuzatishlar soni 50 foizdan kam bo'lmasa. Afsuski, quyosh tebranishlarining odatiy davrlari qisqa (bir necha daqiqa), shunda ko'plab bo'shliqlar, masalan, 15-20 daqiqadan ko'ra, to'ldirilmagan yoki yomon to'ldirilgan bo'lib qoladi. Shovqin nisbatiga signal, ehtimol, spektral oralig'ining ikkala chetida ham past bo'lib qoladi, bu erda eng yaxshi kuzatishlar soni juda muhim bo'lib qoladi.

Biroq, biz har bir shaxsiy tebranish chastota oralig'ining pastki qismida bir necha kun, hatto uzoqroq bir-biriga mos keladi. Shunday qilib, agar biz bitta tebranish spektrini ajratib olsak, u oyna funksiyasi bilan o'ralgan bitta cho'qqidan yasalgan bo'lardi. Shundan so'ng teskari Fourier transformatsiyasi ushbu yagona rejimdagi tebranishni ta'minlaydi, oyna funksiyasi bilan ko'payadi, ya'ni bo'shliqlar bilan. Amplituda va faza sekin o'zgarib bormoqda, xotirani bir necha kundan keyingina yo'qotmoqda. Ushbu ideal holatda, bo'shliqlardagi signal bir-biriga mos vaqtning yarmi, bir necha kunning yaxshi qismi bo'lgan muddatgacha oqilona o'zaro bog'lanishi mumkin. Shundan so'ng qisqa bo'shliqlarni (bir necha davr) samarali to'ldirish mumkinligini ko'rdik, chunki tezlik signali bir necha davr davom etadigan xotiraga ega, bu autokorratsiya funksiyasi tomonidan ko'rsatilgan. Endi ko'rsatilganidek (Gabriel et al., A&A, 1998), bu autocorrelation funksiyasiga birinchi yarim soatdan biroz ko'proq qarash juda qiziq. 1-rasmda IRIS avtokorrelyatsiya funksiyasining dastlabki 10 soati

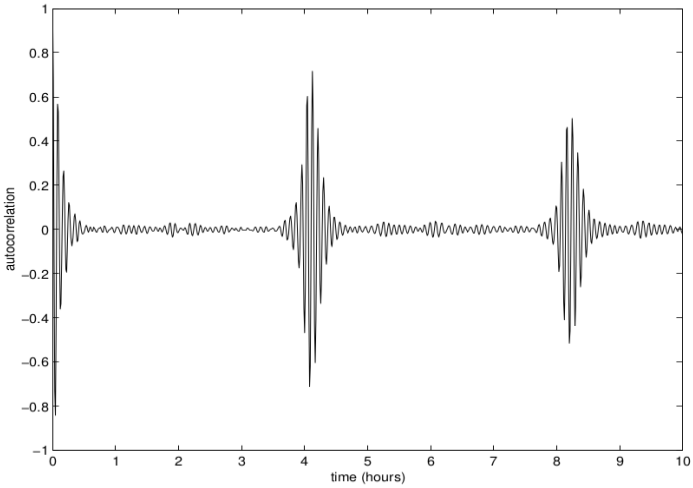

1-rasm. IRIS ma'lumotlar avtokorratsiyasining dastlabki o'n soati (p-mode oraliqda da filtrlangan, 1,5 dan 5 mHz gacha) shuni ko'rsatadiki, boshida tez tushishdan tashqari, 4 va 8 soat atrofida ikkilamchi to'qnashuvlar mavjud. Ular Fourier spektridagi cho'qqilarning kvazi-davriyligi bilan bog'liq. Muhim nuqta shundaki, ikkinchi qobiq 70 foizni koʻpni tashkil etadi va 4 soatdan keyin olingan signal 5 daqiqadan so'ng olingan signaldan ko'ra ko'proq korrelyatsiyalanganligini ko'rsatadi. Bo'shliqni to'ldirishning oson va juda samarali usuli ushbu oddiy faktdan kelib chiqish mumkin.

ko'rsatilgan (Gabriel et al., GOLF signali uchun bir xil ko'rsatish). Biz signalni p rejimidagi chastota oralig'ida (1,5 dan 5 mHz gacha) filtrladik. Ko'rinib turibdiki, signal 4 soatdan ko'proq vaqt o'tgach, juda yuqori darajada bir-biriga mos keladi. U 70 foizdan yuqori bo'lib, bu 5 daqiqadan so'ng uning bir-biriga mosligidan sezilarli darajada katta. Bu Fourier sohasidagi deyarli teng bo'sh chastotali cho'qqilarning natijasi sifatida Gabriel va boshqalar tomonidan shunday talqin qilingan. Ammo bu erda qayd etilishi kerak bo'lgan qo'shimcha oqibatga ega: bu juda ko'p musiqiy qo'shiqlarda, ya'ni preludes yoki sontes va boshqalarda bo'lgani kabi asl signal ham deyarli vaqti-vaqti bilan, kvazi davriyligi 4 soatdan ko'proq bo'lganligini anglatadi. Aniq ijobiy tomoni shundaki, 4 soat oldin yoki 4 soatdan so'ng to'plangan signal bo'yicha bo'shliqni almashtirish 70 foizdan ko'proq ishonch bilan bo'shliqni to'ldirish usulini ta'minlaydi. Ajablanarlisi shundaki, hatto 5 daqiqagacha bo'shliqni to'ldirish ham yaqin atrofdagi ma'lumotlarni bo'shliqdan oldin va keyin o'zaro bog'lab qo'ygandan ko'ra 4 soat oldin olingan (agar shunday bo'lsa) ma'lumotlar orqali yaxshiroq amalga oshiriladi. 2-rasmda (yuqori) ushbu ma'lumotlar to'plamining to'g'ridan-to'g'ri quvvat spektrini ko'rsatadi. Bu o'rtacha 4 individual spektr, 0,085 μHz farqlash qobiliyati bilan o'rta panelda Richardson (Richardson W.H., 1972, JOSA 62) va Lucy (Lucy L.B., 1974, AJ 79) algoritmining ma’no tomonidan oyna funksiyasining dekonvolyutsiyasidan so'ng olingan bir xil ma'lumotlarning kuch spektri ko'rsatilgan.

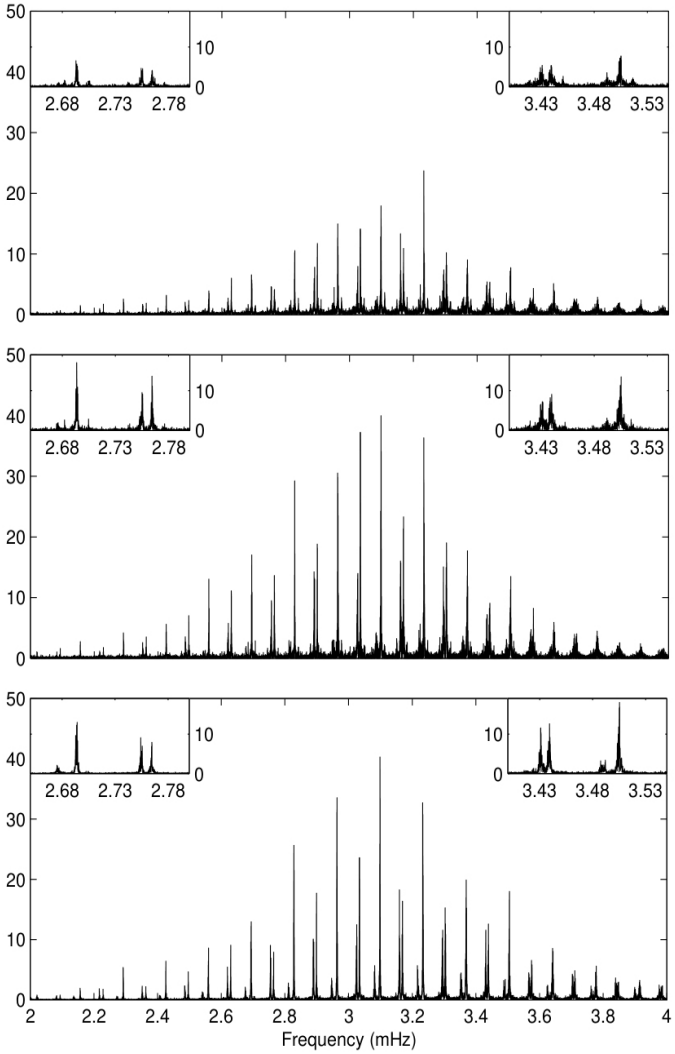

2-rasm. Yuqori qismi IRIS tarmoq ma'lumotlarining 4 yozgi mavsumining to'g'ridan-to'g'ri (o'rtacha) quvvat spektri, 1989-1992 yillarda. Har bir faylning davomiyligi 136,5 kun, shuning uchun chastota o'lchami 0,085 μHz ga teng. Bu quvvat spektrining deraza funksiyasi bo'yicha perturbatsiyasi kattalashtirilgan kichik namunalarda aniq ko'rinadi. O'rta qismi bir xil quvvat spektri Richardson-Lucy deconvolution tomonidan olingan. Har bir cho'qqisi taxminan burch siklining teskarisi bilan ko'payadi, ya'ni atrofdagi shovqinning katta qismi faqat deraza funksiyasi tufayli bo'lgan va cho'qqining ichida orqaga tortib olingan. Biroq, optimallashtirilmaydi va sidelobe tuzilishi, qisqartirilgan bo'lsa-da, hali ham ko'rinadi. Pastki qismda juft modda bo'shlig'i to'ldirish bo'yicha pairof-moddadan keyin hozir olingan bir xil kuch spektri ko'rsatilgan. Fon shovqini sezilarli darajada kamayadi va sidelobes tuzilishi to'liqy yo'q qilinadi. Metodning limitlari haqida batafsil ma'lumot olish uchun matnga qarang.

.

Pastki panelda yuqorida qisqacha tasvirlangan bo'shliqni to'ldirish usuli taqdim etilgandan so'ng olingan bir xil ma'lumotlarning quvvat spektri keltirilgan. Yaxshilash rostdan xam ajoyib. Individual p rejimdagi profillar ancha toza va sideloblarning aksariyati yo'q bo'lib ketadi va eng yuqori mos keladigan protsedura profil

parametrlarining yanada mustahkam va barqaror o'lchovlarini ta'minlaydi. Biroq, kelajakdagi yondashuvimiz doirasida metodni to'ldiruvchi ushbu muayyan bo'shliqning asosiy ahamiyati quyosh bo'shlig'iga tushib qolgan akustik to'lqinlarning vaqt masofasidagi aloqalaridir. Global gelioseysmologiya davrida (IRIS, GOLG, BizSON kabi loyihalar) vaqt masofasi aloqalari hali o'rnatilmagan va hech kim signalni avtokorrelatsiya funksiyalarida 4 soat ichida talqin qilmagan, chunki xuddi shu signal taxminan 4 quyosh radiusi masofasini bosib o'tgan. Keyingi bo'limlardagi o'lchovlarning aksariyati akustik to'lqinlarning vaqtlar-aro aloqasidan foydalanishga asoslangan bo'ladi.

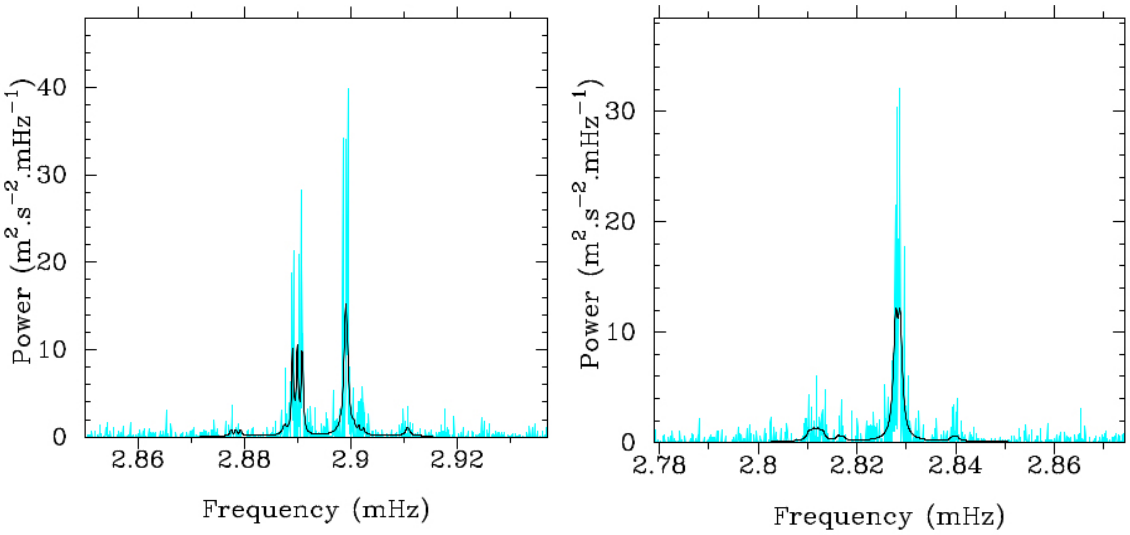

3-rasm. $l = 2$ va $l = 0$ uchun va modaning $n = 20$ quvvat spektri $l = 1$ va $l = 3$ rejimlar $n = 19$.

Keyingi ikki maqolada (Gelly et al., A&A, 1997, Serebryanskiy va boshq., NewAstr, 2001) bu erda yerdan olingan kuzatuvlar yordamida quyosh tebranish chastotasi o'lchovlarining to'liq tafsilotlari keltirilgan. Gelioseysmologiya bo'yicha IRIS tarmog'i 1989 yildan beri faoliyat yuritib keladi. (Gelly et al., A &A, 1997) 1989 dan 1992 gacha bo'lgan to'rt yozgi mavsumda olingan kuzatishlar uchun quyosh p-moda chastotalari jadvallari taqdim etadi. Ushbu tahlil maksimal ehtimollik uyg'unligi texnikasi va spektrning ehtimollik zichligi funksiyasi uchun 22 modelini qo'llaydi. Yakka va hatto juft cho'qqilarning birgalikda mos kelishi (eigenmodes) identifikatsiyasini kuchaytiradi va guruhdagi xato barlarini yaxshilaydi $l = 3 - 1$ $l = 2 - 0$. Chastotalar boshqa kuzatuv natijalari bilan va D_0 $\Delta\nu$ asemptotik yaqinlashuvning va parametrlarining nazariy qiymatlari bilan yaxshi mos keladi. 1989 va 1992 ma'lumotlar to'plamlari orasida 0,25 ± 0,12 μHz kamayish kuzatilmoqda. Bu o‘zgarish quyosh faolligining kamayishi bilan bog‘liq bo‘lib, avvalgi tadqiqotlar natijalari bilan solishtiriladi.

Quyosh eigenmodining so’nuvchi bir o'lchamli osillator sifatida oddiy modeli qo'llanilgan. Ushbu model tabiiy Fourier spektridagi cho'qqilar Lorentz profillari tomonidan asemptotik tarzda tasvirlangan deb hisoblashga imkon beradi. 3-rasmda (chapda) va (o'ngda) juftlardan iborat $l = 2 - 0$ lorentzian fit misol tariqasida $l = 3 - 1$ keltiriladi. Shuni ta'kidlash kerakki, asosiy cho'qqilar atrofida 11,57 mkHz atrofida joylashgan sidelobe cho'qqilarini hisobga olish kerak, chunki yerdan olingan kuzatuvlarning ko'pchiligida 24 soatlik davriy bo'shliqlar keng tarqalgan. (Serebryanskiy et al., NewAstr, 2001) qo'shimcha parametr eng yuqori profil asimmetriyalari hisoblash uchun lorentz funksiyasiga kiritilgan. Ta'kidlanishicha, bu asimmetriya akustik quvvatning lokallashtirilgan (chuqur) manbai bilan modaning rezonansli bo'shlig'i o'rtasidagi o'zaro ta'sir natijasi bo'lishi mumkin, shuningdek, rezonans va quyosh shovqini o'rtasidagi bog'liqlik (Nigam et al., ApJ, 1998) va Doppler yoki fotometrik ma'lumotlar uchun sezilarli darajada farq qilar edi. Bundan tashqari, rezonans bo'shlig'ining yuqori chegarasi balandligining chastota bilan o'zgarishi ham chastotaga asimmetriyaning bog'liqligiga olib keladi (Unno, Yulduzlarning noan'anaviy tebranishi, 1989). Keyinchalik chiziq profilini moslashtirishda assimetriyani e'tiborsiz qoldirish, rejim chastotalarini hisoblashda tizimli xatolarni nazarda tutadi.

(Gizon et al., ApJ, 1997) to'rt marta IRIS ma'lumotlar seriyali (4-6 oy) past darajasi aylanma bo'linish chastotalarining yaxshilangan o'lchovlarni olish uchun ishlatilgan $l = 1,2,3$. Quyoshning tashqi qatlamlarida ma'lum deb hisoblash, markaziy mintaqalar uchun IRIS bo'linishlarining ta'sirini o'rganamiz. Quyosh yadrosida bir qobiqli ham, ikki qobiqli aylanish modeli ham ko‘rib chiqilgan. Tashqi radiativ qobiqdan biroz tezroq aylanadigan yadro ma'lumotlarga eng yaxshi mos keladi. Kuzatishlarning ishonchliligi uchun ba'zi dalillar $l = 3$ multipletlarda differensial aylanishning ko'rinishi bilan ko'rsatiladi. Bu birinchi navbatda quyosh yadrosining real kuzatuvlaridan jadal aylanishini tasdiqlash edi!

2-bob. Yuqori aniqlikdagi quyosh kuzatuvlarini mahalliy gelioseysmik tahlil qilish. Kuzatish gelioseysmologiyasida, chastotalar, profil kengliklari va amplitudalar kabi individual tebranish rejimlarining bunday asosiy parametrlari ularning kuch spektrini tahlil qilish orqali aniqlangan (Serebryanskiy et al. NewAstr, 2001; Fossat et al. A&A, 2003). Hozirga kelib bu parametrlarning barchasi yuqori aniqlik bilan o‘lchangani, ularning Quyosh sikli bilan o‘zgarishi o‘rganilgan. Kuzatilayotgan chastotalar o'zlarining nazariy qiymatlari bilan o’zaro kelishilgan holda. Ushbu o'lchovlar asosan gelioseysmik vaqt davri intensivligi yoki Doppler tezlik Fourier kengaytirish asoslangan. (Duvall et al., Tabiat, 1993) tomonidan ishlab chiqilgan

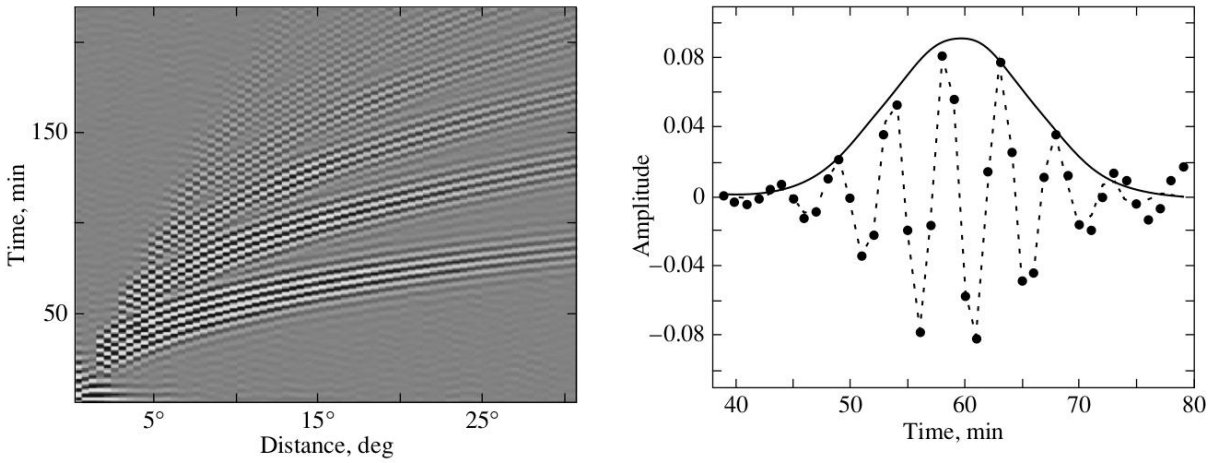

4-rasm. TON bir kunlik seriyasidan kross-korrelyatsiyalilik funksiyasi (chapda). 15° $\Delta \approx$ uchun vertikal kesim (Gabor qobig‘i oson ko‘rish uchun chizilgan).

gelioseysmik ma'lumotlarni (vaqt-masofa tahlili) tahlil qilish uchun yangi usul paydo bo‘lishi bilan, lokal-nobirjinslilik tomonidan ishlab chiqarilgan akustik moda to'lqinli paketlarning tarqalish vaqti bezovtalanishini tahlil qilish orqali Quyosh yuzasi yaqinidagi mahalliy maydonlarning fizik parametrlarini o'rganish mumkin bo'ldi. Bundan tashqari, quyosh ichki qismini mahalliy diagnostika usullari akustik holografiya (Roddier, Comptes Rendus, 1975; Lindsey va Braun, ApJ, 1990; Braun et al., ApJ, 1992), akustik tasvirlash (Chang et al., ApJ, 1997), va boshqa methodlar (Chou et al., ApJ, 2002) vaqt-masofa munosabatlariga asoslangan. Tahlilning standart usullaridan farqli o'laroq, vaqt-masofani tahlil qilishdagi barcha hisob-kitoblar chastotali sohada emas, balki vaqt sohasida amalga oshiriladi. Bu usulning asosiy q‘oya Quyosh ustida akustik to'lqinlarning yo'l vaqtini o'lchashdir. Bu o'z navbatida masalaning xossalari, tovush tezligi, magnit maydoni va oqimlari haqida ma'lumot beradi.

Quyoshda akustik to'lqinlar no-birjinsli, anizotrop va dispersiv muhitda tarqaladi. Manbai mahalliylashtirilgan teran seysmik to'lqinlardan farqli o'laroq, quyosh to'lqinlari stochastik tarzda, konvektiv qobiqning quyi qatlamidagi ko'plab manbalar tomonidan hosil bo'ladi va alohida manbalarni hali kuzatib bo'lmaydi. Quyosh yuzasiga yetib boradigan akustik signal aks etadi va yana Quyosh ichki qismiga tarqaladi, tovush tezligining chuqurlik bilan oshishi tufayli o'z yo'lini egadi va yana yuzaga qaytadi, boshlang'ich nuqtadan ma’lum masofada paydo bo'ladi. Turli to'lqinlar (turli chastotalar va fazoviy kattaliklar bilan) turli yo'ldan yuradi va har xil vaqt oralig'ida va boshlang'ich nuqtadan turli masofalarda yuzaga yetadi. Biroq, bir xil angular faza tezligiga ega bo'lgan to‘lqinlar ω/l (ω bu yerda siklik chastota, va l akustik modaning darajasi) taxminan bir xil nur yo'lidan yuradi (Duvall, Nature, 1982). Bu to‘lqinlar Quyosh

yuzasida nuqtadan nuqtaga tarqaladigan to'lqin paketini hosil qiladi. Tarqalish vaqti va to'lqin paketi bosib o'tgan masofa o'rtasidagi munosabatni o'zaro bog'liqlik funksiyasini qurish orqali olish mumkin (Duvall et al., Nature, 1993). Vaqt-masofa egri chizig'idagi har bir nuqta teng qiymatga ega bo'lgan to'lqin paketiga to'g'ri keladi ω/l. f Koordinatalar bilan va Quyosh yuzasida ikki nuqta uchun r_1 tebranish signallarining o'zaro r_2 bog'liqlik funksiyasi aniqlanadi

$$C(\tau, \Delta) = \int_0^T f(r_1, t+\tau) f(r_2, t) dt$$

bu yerda Δ ikki nuqta orasidagi angular masofa bo'lib, T kuzatishlarning umumiy davomiyligi hisoblanadi. Kechikish τ ikki signal o'rtasidagi vaqt o'zgarishini ko'rsatib beradi. Har qanday doimiy uchun kross-correlatsion funksiyasi quyosh yuzasidagi to'lqin paketlarining koʻrinishidagi masofada Δ to'g'ri keladigan bir nechta maksimalaga ega. Bu maksimala ma'lum bir nur yo'lidan ergashib, yuzaning bir nuqtasidan ikkinchisiga tarqalish uchun belgilangan angular faza tezligiga ega bo'lgan to'lqin paketi uchun zarur bo'lgan vaqtning ma'lum qiymatlarida sodir bo'ladi. Quyosh yuzasida to'lqin paketining ko'rinishi bostirib kirish namunasiga ega bo'lgani uchun, bular «bounce» lar deb ataladi. P-modaning ma'lum bir chastota oralig'ini izolyatsiya qilish uchun p ma'lumotlarga quyidagi Gaussiya chastotasini filtrlash qo'llaniladi:

$$e^{-0.5\left(\frac{\nu-\nu_0}{\omega}\right)^2}$$

ν_0 markaziy chastotasi bu yerda va ω Gaussiya filtrining kengligi; natijada, kross-korrelyatsiya funksiya $C(\tau, \Delta)$ gabor funksiyasi bilan tavsiflanadi

$$G = A cos\left[2\pi\nu\left(t-\tau_{ph}\right)\right] exp\left[\frac{-(t-\tau_{en})^2}{2\sigma^2}\right]$$

Bu erda, A, ν, va σ mos ravishda Gabor funksiyasining amplitudasi, markaziy chastotasi va zarf kengligi; τ_{ph} va τen to'lqin-paket fazasi va «envelpe» ning tarqalish vaqtlari (Duvall et al., Nature, 1993).

Barcha tarqalish masofalarda o'zaro bog'liqlik funksiyasini moslashtirsak, vaqt-masofa egri chizig'ini olamiz (5-rasm). (Δ, τ). Ushbu egri chiziqdagi har bir nuqta bir xil agular faza tezligiga ega bo'lgan va taxminan bir xil nur yo'li bo'ylab ω/l to'lqin paketi tarqaladigan tebranish toʻlqinlariga to'g'ri keladi. Bu yerda τ to'lqin paketining quyosh ichki qismidagi yo'lni agular masofasi bilan ajratilgan yuzadagi ikki nuqta o'rtasida bosib o'tishi uchun kerak bo'lgan vaqtdir Δ. Ushbu ishda biz quyosh maksimal va minimal aktivlik fazasida akustik to'lqinlarning tarqalish vaqtidagi o'zgarishlarni tadqiq qilishga harakat qildik. Bizning natijalarimiz shuni ko'rsatadiki, to'lqin tarqalish vaqtlari o'rtasidagi farq minimal va maksimal darajada $\sim 2s$ boʻlib, bu $0.8R_{\odot}$

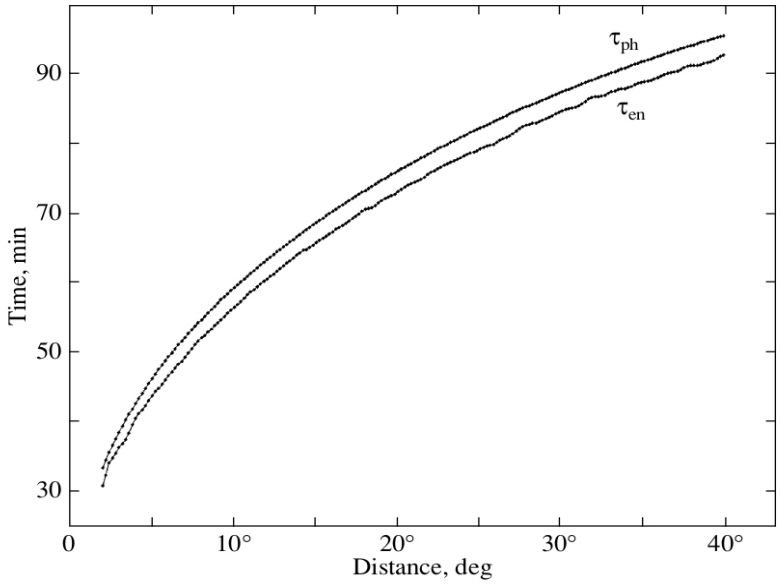

5-rasm. 4-rasmdagi CCFning birinchi zarbasini moslashtirish orqali olingan vaqt masofasi munosabati. Odatda, faza tarqalish vaqti qobiq tarqalish vaqtidan ko’ra silliqroq o’lchanadi.

chuqurlikka tog‘ri keladi; kattaroq chuqurliklarda bu farq kamayadi. Bu, ehtimol, quyosh faolligi namoyon bo'lishiga nisbatan chuqurroq kirib borayotgan akustik to'lqinlar ekanligini ko'rsatmoqda $0.8R_{\odot}$.

Ya'ni faol tuzilmalar konvektiv zonaning yuqori qatlamida lokalizatsiya qilinadi. Amplituda A nur yo'li bo'ylab o'tganidan so'ng boshlang'ich nuqtadan Δ uzoqda yuzaga qaytgan akustik tebranishlarning to'lqin paketining korrelyatsiya darajasini o'lchaydi. Akustik to'lqinlar tarqaladigan qatlamning fizik parametrlari quyosh magnit faolligi davomida o‘zgarishi ma‘lum. Biroq, faol hududlarda muhit parametrlari sezilarli darajada farq qilsa-da, bu o'zgarishlar juda kichik; magnit maydonining o'zgarishlari ayniqsa katta. To'lqin paketi faol maydonlarr bilan o'zaro ta'sirlashgani sababli, u energiyasining bir qismini yo'qotishi kerak (Chou et al., ApJ, 1996); shuning uchun, maksimal quyosh faolligi yillarida, Quyosh ustida faol tuzilmalar soni oshganda, akustik to'lqin paketlarining amplitudalari kamayishi kerak. Bizning o'lchovlar quyosh faoliyati bilan to'lqin paketlari korrelyatsiya amplitudasi nisbiy o'zgarishlar ko'rsatadi, qachon biz to'lqin paketlari korrelyatsiya amplitudasini minimal dan maksimal quyosh faoliyati uchun $10-20\%$ kamayishini ko'rish mumkin. (Burtseva et al., SolPhys, 2009) quyosh faolligi tsikli bilan sokin va faol Quyoshda yuqori quyosh p tebranishlarining l yashash davri o'zgarishi tekshiriladi. Daraja oralig'i $l = 300-600$ va $\nu = 2.5-4.5$ mHz yashash davri SOHO/MDI ma'lumotlaridan faol maydonlarr va sokin Quyosh vaqt-masofa texnikasidan foydalangan holda hisoblandi. Biz o'z tahlilimizni quyosh faolligining to'rt xil fazasida ma'lumotlarga qo'lladik: 1996 (minimal darajada), 1998

(ko'tarilish fazasi), 2000 (maksimal darajada), 2003 (kamayib borayotgan faza). Faol maydonlar bilan hududdan olingan natijalar koʻrsatdiki, faollik ortishi bilan yashash davri kamaydi. Maksimal yashash davri o'zgarishlar 1996 yilda Quyosh minimumi bilan 2000 yilda maksimal o'rtasida; nisbiy o'zgarish barcha l qiymatlari va chastotalar ustidan o'rtacha 13% ga kamayadi. 1996-ga nisbatan yashash davri kamaytiriluvchi ns 1998-yilda 7% ga yaqin, 2003-yilda esa 10% ga yaqin. Sokin mintaqada hisoblangan yashash davri quyosh faoliyati bilan hali ham kamayadi, garchi kamayish kichikroq. Oʻrtacha 1996 yilga nisbatan yashash davri pasayish 1998 yilda 4%ga yaqin, 2000 yilda 10%, 2003 yilda 8% ni tashkil etadi. Shunday qilib, yuqori magnit faolligining mintaqalari qochilganda o'lchangan yashash davri ko'payadi. Bundan tashqari, tinch maydonlarda hisoblangan yashash davri ham faollik davrining o'zgarishini ko'rsatadi.

(Patron et al., ApJ, 1997) quyosh tebranishlari uch o'lchovli quvvat spektr yangi moslashtirish (fitting) usuli tasvirlangan va an'anaviy yondashuvlar bilan solishtirilgan. Yangi usul Lorentsian profillarining parametrlariga uch o'lchamli azimutaldan oʻrtachalash orqali ikki oʻlchamli $k-\omega$ koʻrinishga keltirilgan. Shundan so'ng gorizontal tezlanishlar ushbu parametrlarni to'g'ri saqlashi aniqlanadi, bu esa hisoblash vaqtini ancha kamaytiradi. Ikkala usul ham quyosh disk markazi atrofidagi $(n = 3{,}4)$ taxminan 15^o kvadrat maydonda uchun olingan uch o'lchamli quvvat spektrining ikkita radial buyurtmasi uchun solishtirilgan. Ushbu ishda ishlatiladigan tasvirlar Tayvan tebranishlar tarmogʻi (TON) uskunasi bilan Observatorio del Teide-da olingan [1080x1080] piksel intensivligi tasvirlarining 3 kunlik to'plamiga toʻgʻri keladi. Moslashtirish natijalari ikki usul uchun hisoblangan xatolar ichida moslikga ega. Yangi usul bilan olingan hisoblash vaqtining qisqarishi halqa sxemasi tahliliga qulaylik yaratadi.

Halqa diagramma texnikasining vaqt-masofa usuli bilan birgalikda yana bir muvaffaqiyatli qo'llanilishi Quyosh yuzasi yaqinidagi quyosh dog'i strukturasining oʻzgacha natijalarini koʻrsatgandi (Kosovichev et al., JphCS, 2011). Ushbu maqolada faol maydon NOAA 9787 uchun ringdiagramma tahlili va vaqt-masofa gelioseysmologiyasini taqqoslashning yangi natijalari, buning uchun avvalgi taqqoslash yuza-osti tovush tezligi strukturasida sezilarli farqlarni ko'rsatgani va o'lchovlar va inversiyalarning tizimli noaniqliklari muhokama qilindi. Yangi natijalar shuni ko'rsatadiki, halqa-sxema ham, vaqt-masofasidagi technikalar ham sifat jihatdan o'xshash natijalar beradi, bu esa boshqa faol maydonlar uchun natijalarga mos keladigan xarakterli ikki qatlamli seysmik tovush tezligi strukturasini ochib beradi. Biroq, inversiya natijalarini miqdoriy taqqoslash to'g'ridan-toʻgʻri emas. Bu sezgirlik, farqlash qobiliyati kattaligi va oʻrtachalash kernellari farqlarni hisobga oladi. Xususan,

akustik quvvat kamayishi tufayli, quyosh dog‘i seysmik tuzilishi halqa-diagramma signal hissa sezilarli kamayishi mumkin. Shuni ko'rsatadiki, bu ta'sirni hisobga olish ushbu usullar bilan ko'rsatilgan manfiy va salbiy tovush tezligi o‘zgarishlari o‘rtasidagi o‘tish chuqurligidagi farqni kamaytiradi. Ikkala usul ham quyosh dog'larining seismikrofon tuzilishi ancha chuqur ekanligini ko'rsatishi va yuzadan kamida 20 Mm pastga cho'zilishini ko'rsatishi muhim bo'lib ko‘rinadi, bu esa quyosh dog‘larining nazariy modellariga cheklovlar qo'yadi.

3-bob. Quyosh ichki qismining turli qatlamlarini ajratish. Vaqt-masofa gelioseysmologiyasi Quyosh yuzasidan pastdagi kichik tuzilmalarning sxususiyatlarinii o‘rganish uchun kuchli vositadir. Ushbu texnikaning muvaffaqiyatli dasturlaridan biri Duvall tomonidan Janubiy qutb ma’lumotlaridan foydalangan holda ishlab chiqilgan. GONG ma'lumotlaridan foydalanib, biz quyosh dog‘larida tarqalish vaqti o'zgarishini o'rganamiz. Signal-shovqin nisbatini oshirish uchun vaqt seriyasiga faza tezligi filtrini qo'lladik. Signal-shovqin nisbatini oshirish va to‘lqinlarni ma’lum chuqurliklarga tarqaluvchilarini ajratish uchun bir xil nur yo‘li bo'ylab ma‘lum (Duvall et al., Nature, 1993) sferik garmonik SH koeffitsientlariga faza tezligi filtrini qo'llaymiz va tasvirlarni yana kenglik bo‘ylama sohasidaa (inverse dekompozitsiya) qayta tiklaymiz.

Vaqt-masofa tahlilida akustik signal faol maydonlar ichida yoki tashqarisida alohida qo'llanilishi mumkinligi sababli, bu bizga akustik to‘lqin xususiyatlarini o'lchash va faol va juda ko‘p maydonlarni solishtirish imkonini beradi. (Kholikov, SOHO-14, 2004) da biz quyosh dog'lari ichida akustik to'lqin tarqalish vaqti oshishi muammosini o‘rgandik. Vaqt-masofa gelioseysmologiyaning asosiy usuli Quyosh yuzasidagi ikki nuqta o'rtasidagi o'zaro bog‘liqliklarni hisoblashdir. Bu muayyan holatda biz markaz-aylana korrelyatsiyalaridan foydalandik: belgilangan maqsadli nuqtadagi temporal signali berilgan burchakli masofaga ega bo'lgan aylana atrofida ifodalash orqali yaratilgan signal bilan bog'liq. Tarqalish vaqti parametrlari o'zaro bog'liqliklardan foydalanib, (Kosovichev et al., ApJ, SCORe, 1996) tomonidan tasvirlangan Gabor funksiyasi yordamida olinadi. Markaziy nuqta va aylana o'rtasidagi ajralishni o‘zgartirish orqali biz turli nur yo‘llarini tanlab, Quyosh ichki qismining turli chuqurliklarini tekshirishimiz mumkin. Salbiy vaqt markazdan chiquvchi to'lqinlarning tarqalish vaqtiga to'g'ri keladi. Negativ vaqt ortda qolishi aylanadan markaziy nuqtagacha bo'lgan qo'zg'alish to‘lqinlarining tarqalish vaqti sifatida talqin qilinadi. Agar markaziy nuqta faol mintaqada yoki quyosh dog'ida joylashgan bo‘lsa, unda tebranishlar faqat ijobiy tarqalish vaqtlari ko‘rsatadi.

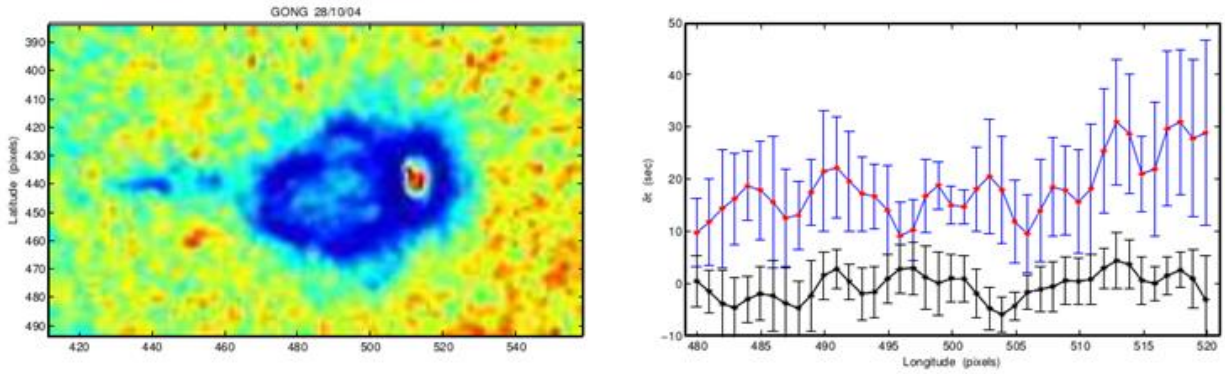

6-rasm. Akustik quvvat xaritasi (chapda panel) va 2003 yil 28 oktyabrdagi katta faol mintaqa uchun chiquvchi va kiruvchi to'lqinlar (o‘ngdagi panel) o'rtasidagi tarqalish vaqti farqlari. Tarqalish vaqti rejasida pastki egri chiziq bir xil o'lchamdagi sokin mintaqadan xisoblanadi. Faza tezligi filtri L = 250 va = 3 mHz ga markazlashtirilgan. O‘ng paneldagi horiizontal o'qi piksellarda quyosh dog'ining uzunligi.

Janubiy qutb, GONG klassik uskunasi va MDI ma'lumotlari yordamida faol maydonlarda tarqalish vaqtining bir daqiqalik kamayishi aniqlangan. Ushbu tahlillarning muhim natijasi shunda ediki, tashariga yo‘nalgan to‘lqinlarining tarqalish vaqtlari ichkariga yo‘nalgan to‘lqinlariga qaraganda taxminan 1 daqiqaga kichikroq bo'lib, faol maydonlardan ketayotgan aniq oqimlarning mavjudligini ko'rsatmoqda. Ushbu tadqiqotda biz o'zgarishlar tezligi filtrlangan SH koeffitsientlaridan qayta ishlangan tasvirlardan foydalanamiz, bu signal-shovqin nisbatini sezilarli darajada yaxshilaydi. Markaziy nuqta va aylana oralig'idagi 1,8 dan 4,5 darajagacha bo'lgan ajratish masofalaridan foydalanib, quyosh dog'lari ichidagi fazo tarqalish vaqti umuman taxminan 20-40 soniyaga kamayishini aniqladik.

(Hsiang-Kuang Chang et al., Nature, 1997) biz Quyosh chuqur qatlamlarida quyosh dog'ini tasvirini qurish uchun shunga o'xshash yondashuvni qo'lladik. Gelioseysmik singayotgan akustik tasvirlashda biz 'hisoblash akustik linzasini' hosil qilamiz. Quyosh yuzasidagi har bir nuqta unga to'sqinlik qilayotgan akustik to'lqinlar tufayli yuzaga kelgan tezlik va intensivlik o'zgarishiga ega. Biz quyosh dog‘lari kosmik arizasidan akustik fazoviy arra elementlari sifatida foydalanishimiz mumkin. Yuzadagi nishon nuqtasidan paydo bo'lgan akustik to'lqin trassasi ichkariga akustik bo'shliq tubiga va yana nishon nuqtasidan uzoqroqda yuzaga tarqaladi. Turli P-rejimlar turli yo'llarga ega bo'lib, mo'ljal nuqtasidan turli vaqtlarda va turli masofalarda yuzaga keladi. Quyoshdagi akustik to'lqinlar bosib o'tgan tarqalish vaqti va masofa o'rtasidagi bog'liqlikka asoslanib, akustik signallarning intensivligini Quyoshning maqsadli nuqtasidan bir-biriga mos ravishda aniqlash uchun sirt ustidagi signallarda tebranish vaqt seriyasini bosqichma-bosqich o'zgartirishimiz mumkin. Garchi yig'ish

maydonining har bir nuqtasidagi P rejimi signali Quyoshning boshqa barcha nuqtalaridan to'lqinlarni o'z ichiga olgan bo'lsa-da, ularning bosqichlari turli farqlash qobiliyatining bir-biriga mosligi bo'lgani uchun bu signallar bekor bo'lishini kutish mumkun. Boshqa mahalliy gelioseysmik usullar bilvosita o'lchanganni teskari qilib, quyi tuzilmani aniqlaydi, ambient akustik tasvir bevosita uch o'lchovli nobirjinslilik yuzaosti tasvirini vaqt kechikish orqali aniqlaydi.

Biz 7 kunlik gelioseysmik vaqt seriyasidan foydalandik, yuzadagi quyosh akustik tasvirni qayta tiklash uchun umumiy davomiyligi 90 soatlik kuzatuvlar, TON bilan olingan. Kuzatuv chiziqning intensivligi $Ca_{II}K$ chiziqda, tasvirlari 1996 yil 21-27 iyun oralig'ida olingan va sinov nishoni sifatida quyosh dog'i maydonii NOAA 7973 tanlangan. Ma'lumotlarni qayta ishlash tartibi quyidagicha. (1) Har bir kuzatilgan K - line to'liq disk tasvir quyosh aylanish o'qi $sin\theta$ ϕ bo'ylab θ tekislangan ϕ bir sferik koordinata tizimida mos ravishda kengligi va bo'ylama bu yerda u koordinatalar ichiga transform etiladi. 2) Quyosh yuzasining differensial aylanishi olib tashlanadi. (3) Tebranish amplitudasi har bir fazoviy nuqtada intensivlik vaqti seriyasidan 15 freymli yugurma o'rtachasini chiqarib tashlash orqali hisoblanadi. (4) Signalni 2,7-6,5 mHz oralig'ida izolyatsiya qilish uchun gauss filtri qo'llaniladi. (5) vaqtdagi maqsadli nuqtadan kelib chiqqan signal t, signallarni tinch Quyoshdan olingan bir martalik vaqt-masofaga bog'liqlik asosida tegishli vaqt kechikishlarida o'lchanadigan maqsadli nuqtadan turli shakldagi masofalarda yig'ish orqali o'zgarishlariga mos keladi. Signallar aylana perimetri bo'ylab yig'iladi, 2-26º maqsadli nuqtadan, 31-80 daqiqadan so'ng tarqalish vaqtlariga mos $t$keladi. (6) vaqt seriyasidagi har bir t uchun bosqichli yig'indi takrorlanadi, so'ngra turli vaqtlarda to'rtburchakli amplitudalar qo'shilib, maqsad nuqtasidan qilingan akustik intensivlik olinadi. 7) Protsedura ikki o'lchovli akustik tasvirni hosil qilish uchun mo'ljal maydonidai barcha nuqtalar uchun takrorlanadi. Biz sokin va magnit maydonlarga sokin Quyoshning vaqt-masofa aloqasini qo'lladik. Faol mintaqada magnit maydonining mavjudligi P-rejimlar davridan (taxminan 5 daqiqa) ancha kichik bo'lgan umumiy tarqalish vaqtining kichik P o'zgarishini taqdim etadi. Bundan tashqari, shuni ta'kidlash kerakki, vaqt-masofa egri chizig'idagi ikki qo'shni nuqtaning tarqalish vaqtidagi farq bo'lgan differentsial tarqalish vaqti bizning umumiy tarqalish vaqti o'rniga bizning fazaga mos keladigan texnikamizga kiradi. Magnit maydoni tufayli differentsial tarqalish vaqtining o‘zgarishi umumiy yo‘l vaqtining o‘zgarishidan ancha kichik bo‘lishi kutiladi. Shuning uchun magnit maydonining mavjudligi natijamizga hech qanday ta'sir ko'rsatmasligini kutamiz.

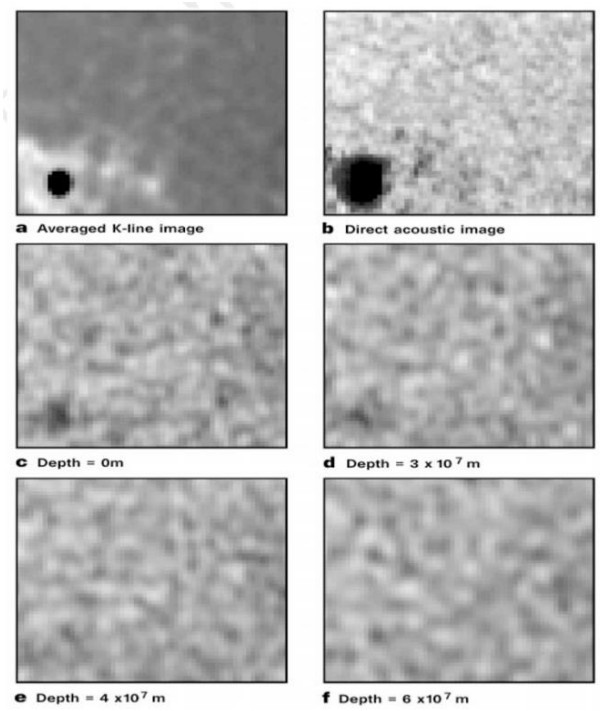

7-rasm. K-chiziqli tasvir (a), to'g'ridan-to'g'ri akustik tasvir (b), turli chuqurliklarda (c-f) qayta ishlangan akustik tasvirlar. K-chiziq tasviri o'rtacha 7 kunlik kuzatuvlar davomida olingan. Quyosh dog'i hududida akustik intensivlikni susaytirish, sirt yuzasida aniq va chuqurlik bilan kamayadi.

7-rasmda juda muhim kuzatish hodisalarini ko'rsatadi. Bu yuza ostidagi quyosh dog'ining birinchi akustik tasviri keltirilgan. Bundan tashqari, bu Quyosh konvektiv zonasida quyosh dog'i ildizlarining chuqur tabiatini kuzatuvli tasdiqlashdir. Vaqt masofa texnikasini Quyosh ichki qismining chuqur qatlamlariga qo'llash Quyosh yuzasiga chiqishidan oldin paydo bo'lgan faol maydonni xaritaga tushirishga bag'ishlangan (Kholikov, SolPhys, 2013). Quyosh yuzasi faolligi Quyoshning ichki qismidan paydo bo'lgan magnit oqim mahsuli hisoblanadi. Yangi paydo bo'lgan kuchli magnit maydonlari turli konfiguratsiyalarning faol mmaydonlarni tashkil etadi. Aktiv maydonlarning fizik xossalari, shuningdek ba'zi jihatlari evolyutsiyasi turli kuzatish va nazariy usullar bilan yaxshi o'rganilgan (Fan, ApJ, 2008; Birch et al., ApJ, 2013). Biroq, uning yuzaga kelishidan oldin magnit oqimni aniqlashushbu sohadagi mos t muhim fanlardan biri bo'lib qolmoqda. Xususan, kosmik ob-havo va quyosh aktivlik tsikli bashoratlari ushbu tekshiruv natijasiga bog'liq. (Ilonidis et al., Science, 2011) bir chuqur-yo'naltirilgan vaqt-masofa texnikasini qo'llash tarqalish-vaqti g‘alayonlanish anomaliyasini tekshirdilar. Ular 40-75 Mm chuqurlikda katta tarqalish vaqtidagi siljishlarni topdilar. Biroq, (Braun, Science, 2012) akustik holografiya texnik birxil faol mintaqalarning tarqalish vaqtlarini o'lchash hech qanday tarqalish vaqti anomaliyalarini ko'rsatmaganligini ma'lum qildi. Nazariy simulyatsiyalarga ko'ra, chuqur qatlamlarda

paydo bo'lgan Ω-sortmoq tufayli yuzaga kelgan ommaviy oqim tufayli kutilayotgan tarqalish vaqtidagi o'zgarishlar magnitudasi bir necha soniyadan oshmasligi kerak (Fan, ApJ, 2008). Modellashtirish buoyant magnit oqimi, (Birch et al., ApJ, 2010) shuningdek, tarqalish vaqti perturbatsiyalari 30 Mm chuqurlikda 40 m s^{-1} oqim tezligi uchun taxminan bir soniya ekanligini ta'kidladi. Pastki burilish nuqtalarida tarqalish vaqtlarining sezgirligi gorizontal oqimlar uchun yuqori bo'lgani uchun, (Ilonidis, et al, Science, 2011) tomonidan kuzatilgan katta vaqt-o'zgarishlar va boshq kuchli magnit maydonidagi o'zgarishlar bilan bog'liq emas. Bundan tashqari, bunday katta tarqalish-vaqtlariga faqat magnit maydon perturbations mas'ul bo'lmasligi mumkin. (Chou et al., ApJ, 2002), konvektiv zonaning bazasida taxminan 0,015 soniya tarqalish vaqti (≈ 200 mm) taxminan 10 5 G gacha bo'lgan magnit maydon kuchiga (4 - 7) × 10^5 G ga teng. Bizning maqsadimiz NASA SOHO/MDI kosmik missiyasi tomonidan olingan ma'lumotlardan foydalangan holda GONG gelioseysmologiya tarmog'idan (yerga asoslangan) mustaqil ishlab chiqilgan texnika va qo'shimcha o'lchovlarni qo'llash orqali (Ilonidis et al., 2011) natijalarini takrorlashga qaratilgan edi. Biz uchta faol mintaqa (AR) uchun MDI va GONG Doppler tezligi tasvirlarini ishlatganmiz: NOAA 10488, 8164 va 10132. Ular 1996-2003 yillar oralig‘ida turli davrlarda kuzatilgan. Har bir AR uchun biz 2 - 3 kun davomida ularning paydo bo'lishidan kelib chiqqan holda ma'lumotlarni tahlil qildik. Garchi biz ishlatgan ishlov berish bosqichlari (Ilonidis et al., Science, 2011) tomonidan ishlatilganlardan farq qilsa-da, asosiy natija bir xil bo'lib qoldi.

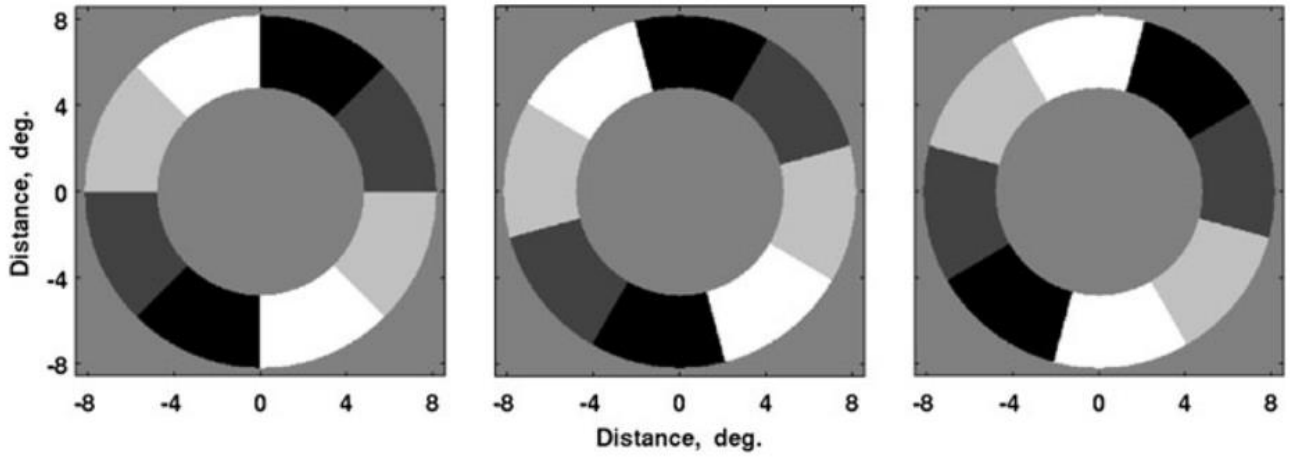

8-rasm Diqqatni jamlovchi o'zaro bog'liqlik o'lchovlari uchun 45 o'qning konfiguratsiyalari. Har bir o'q markaziy nuqtaga nisbatan 22 yoy masofaga bo'linadi. Quyosh tebranish signallarining o'zaro bog'liqligi o'rtacha diametrli qarama-qarshi nuqta-yoy lokationlari o'rtasida xisoblanadi.

Standart vaqt-masofa tahlilida ma'lumot kubini Fourier sohasiga aylantirib, ma'lum faza tezligi parametrlari (faza tezligi va temporal) bilan akustik to'lqinlarni

tanlash uchun filtrni qo'llash va vaqt-masofa sohaga qaytish orqali filtrlanadi. Ma'lumot kublarining hajmi odatda 30 × 30 daraja kenglik va uzunlik bo'lib, davomiyligi qariyb 8 soatni tashkil etadi. Muayyan parametrlarga ega bo'lgan faza tezligini filtrlash akustik to'lqinlarni taxminan bir xil nur-yo‘li va pastki burilish nuqtasini tanlangan chuqurlik oralig'ida ajratib turadi. Signal-shovqin nisbatini oshirish uchun (Ilonidis et al., Science, 2011) o'zgartirilgan faza tezligi filtrini ishlatib, Gaussian shakl filtrini Π-shape filtri bilan almashtirdi, u markazda tekis va chetlarida Gaussian; ikkala tadqiqotda bir xil faza tezligi filtri ishlatilgan. Filtrning yassi qismi 21 – 29 km s^{-1} faza tezligi oralig'iga to'g'ri keladi . Filtrlash jarayonining asosiy bosqichlari quyidagilar:

–Diskning markaziy 120 × 120 daraja kengligi va bo'ylama qismi yordamida sferik garmonika (SH) koeffitsientlariga individual Doppler tezligi tasvirlarini aylantiriladi.

– Faza tezligi filtrini (l, m) kuzatilgan vaqt seriyasining barcha alohida SH koeffitsientlariga qo'llaniladi.

– Filtrlangan koeffitsientlardan foydalangan holda tebranish tasvirlari qayta tiklanadi; ularni ushbu bog'lanish yordamida qayta tiklash mumkin

$$V(\theta, \phi) = \sum_{l=0}^{l_{max}} \sum_{m=0}^{l} C_l^m P_l^m(\theta) e^{im\phi + \delta\phi}$$

Bu yerda C_l^m SH koeffitsientlari, P_l^m tartibi l bilan bog'liq Legendre polinom bo'lib m θ, mos ravishda kenglik va bo'ylama bo'ladi. ϕ sirtning $\delta\phi$ differensial aylanishini olib tashlash uchun differensial aylanish profili (Libbrecht et al., Quyosh ichki va atmosfera, 1991), kenglik va vaqtning funksiyasi (ma'lumot kubining o'rtasiga nisbatan). Tanlangan faza tezligi parametrlari l oralig'i $l = 70 - 200$. SH koeffitsientlarining juda yuqori darajalarini ishlatishning hojati yo'qligini anglatadi, shuning uchun $l_{max} = 300$ barcha ehtiyojlarimizni qoplaydi.

– Qayta ishlangan tasvirlarni kuzatish yuqoridagi tenglamaning o'ng tomonidagi murakkab eksponent argumentiga yuza differensial aylanish profili burchak tezligini kiritish orqali amalga oshiriladi.

Ushbu qayta ishlangan ma'lumotlarning chuqur e'tiborli o'zaro bog'liqlik hisob-kitoblari muhokama qilingan sxemadan foydalangan holda ishlab chiqariladi (Ilonidis, Science, 2011). 21 – 29 km s^{-1} gacha bo'lgan faza tezligi uchun kross-korrelyatsiya funksiyasining maksimal cho'qqisi ajralish masofasiga to'g'ri keladi $\Delta = 12–13^0$. Har qanday berilgan markaziy maqsadli mintaqa pozitsiyasi uchun, bu hisob-kitoblarda ishlatiladigan aylana diametrlari $D1 = 9.6^0$, . $D2 = 16.32^0$ Aylana teng sonli yoylarga bo'linadi. Ushbu tahlil uchun biz 60°, 45°, 36°, 30°, 25,71°, 22,5°, 20° ark o'lchamlaridan foydalanamiz. Har bir holatda, biz diametriy qarama-qarshi juftliklar orasidagi signalni

o'zaro bog'lashga o'tish uchun bir necha o'q bor. Har bir ark konfiguratsiyasi 1/3 uzunligi bo'yicha chapga va o'ngga buriladi va bu 21 mustaqil konfiguratsiyani amalga oshiradi. 8-rasm 45° yoyning uchta konfiguratsiyasidan iborat diagramni namoyish etadi. Aylana kengligi markaziy mavqega nisbatan 22 ta ekvidistant ost-aylanalarga bo'linadi. Xoch korrelyatsiyalari har bir o'q konfiguratsiyasi uchun qarama-qarshi ost-aylana o'rtasida xisoblanadi. Individual o'zaro bog'liqliklarni Gabor to'lqiniga moslashtirish qiyin, shuning uchun har bir xoch korrelyatsiyasini moslashtirish o'rniga, biz turli tarqalish masofalari uchun o'zaro bog'liqliklarni birlashtirdik. Ushbu 22 ta o'zaro bog'liqlikni o'rtacha ko'zdan kechirishdan oldin, biz ularnibutun maqsadli mintaqada o'rtacha o'lchovlar orqali olinadigan o'rtacha vaqt-masofa aloqasi yordamida markaziy tarqalish masofasi joylariga bir joyga aylantirdik. Ushbu operatsiya interpolyatsiya orqali amalga oshirilishi mumkin. Interpolyatsion noaniqliklardan saqlanish uchun Fourier shift teoremasidan foydalandik:

$$\psi(t-\tau_{\Delta}) = F^{-1}\{e^{-i\omega\tau_{\Delta}}\Psi(\omega)\}$$

Barcha tarqalish masofalari bo'yicha o'zaro bog'liqliklar hisoblanib, o'rtacha hisoblanib bo'lgach, tanlangan maqsadli hududlar uchun tarqalish vaqti xaritalari standart Gabor to'lqinlarini moslashtirish tartibi bilan quriladi (Duvall et al., Nature, 1997). O'lchamdagi tipik faol mintaqani qamrab olish uchun 13°×13°, tarqalish vaqti xaritalari paydo bo'lishi kutilayotgan AR joylarida markazlashgan. O'lchovlar AR paydo bo'lishidan oldin 2 - 3 kunlik vaqt davomida quyosh yuzasiga o'tkazilgan.

9-rasmda paydo bo'lish vaqtidan oldin ketma-ket to'qqizta tarqalish vaqti xaritasi keltiriladi; har bir xarita har bir panelda ko'rsatilgan vaqtlarda 8 soatlik ma'lumot kubi yordamida hosil qilinadi. Ushbu xaritalardagi tarqalish vaqtidagi tebranishlar 0 (ko'k) dan −15 (qizil) soniyagacha bo'ladi. Bir nechta kichik xususiyatlarga qaramay, eng kuchli tebranishlar ikki joyda sodir bo'ladi va 7 soat qoladi. Shuni ham aytib o'tish kerakki, birinchi xarita AR yuzada paydo bo'la boshlagan vaqtdan 11 soat uzoqlikda joylashgan. MDI magnetogram va tegishli AR joylarining davomli tasvirlari pastki qatorning so'nggi uchta panelida ko'rsatilgan. Tarqalish vaqtlari hisoblangan vaqt mobaynida sezilarli sirt magnit maydoni yo'q. 27 Oktober ustida 15:30 UT ning magnitogrammasida AR yuzada aniq ko'rinib turadi va shakllana boshlaydi. Ikki kundan so'ng olingan davomiylik tasvirida AR ning ikkita alohida komponenti ko'rsatiladi. Bizning ishimiz shuni ko'rsatadiki, chuqur fokuslash vaqti-masofali gelioseysmologiya o'lchovlari haqiqatan ham ba'zi paydo bo'lgan AR larning dalillarini taqdim etadi, vaqt o'zgarishi magnitudalari simulyatsiyalardan taxmin qilingan bashoratlardan ancha katta (Fan, ApJ, 2008). (Xoliqov et al., SolPhys, 2008) mahalliy

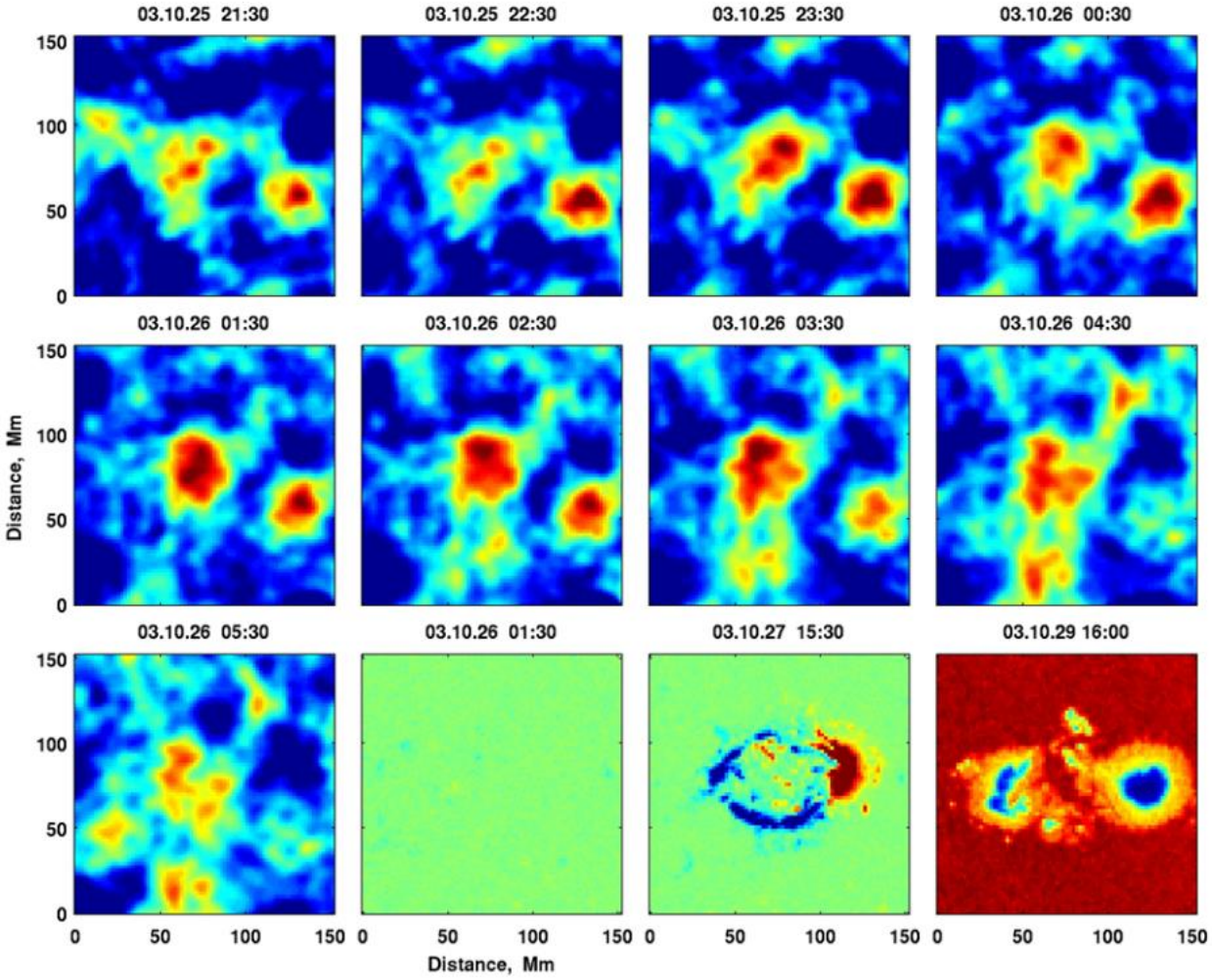

9-rasm. Aktiv maydon 10488 ning tarqalish vaqti xaritalarini chuqur jamlash (pastki qatorda ikkita qator va chap rasm). Ushbu o'lchovlar uchun fokus chuqurligi 40 – 70 Mm ni o'z ichiga oladi. Har bir xarita paydo bo'lgan faol mintaqa joylashuvida markazlashgan 8 soat vaqtli MDI ma'lumotlar kublari yordamida yaratiladi (sana va vaqt yuqorida ko'rsatiladi). Paydo bo'lishidan oldin va keyin magnit maydonlaripastki qatorning so'nggi uchta panelida nd a keyingi vaqt davom etadigan tasvir taqdim etiladi. Faol mintaqa joylashuvi 25-26 oktyabrda paydo bo'lishidan oldin yuzadan pastda va 29 oktyabrda yuzaga kelganidan keyin ikki marta tarqalish vaqtining sezilarli darajada ikki marta strukturasini tezlashtirilishini ko'rsatadi.

gelioseysmologiya texnikasini quyoshning global tebranishlari muammolariga muvaffaqiyatli tatbiq etishdir. So‘nggi o‘n yil mobaynida Quyosh sikli bo‘yicha quyosh radiusi o‘zgarishlari turli usullar bilan o‘rganib chiqildi. Biroq, natijalar tez-tez munozarali edi (Laclare et al., SolPhys, 1996; Noël, A&A, 2004; Kuhn et al., ApJ, 2004). Aksincha, f-moda chastotalariga asoslangan gelioseysmik metodlari (Schou et al., ApJ, 1997) tomonidan taqdim etilgan akustik-radiusli o'lchovlar juda mos keladi. (Antia, A&A, 1998; Dziembowski at al., ApJ, 2005). Global quyosh tebranishlarining autokorrelatsiya funksiyasining (ACF) xossalari bir nechta mualliflar tomonidan tahlil

qilingan. P rejimidagi yashash vaqti o‘lchovlari 70 kunlik GOLF ma'lumotlarining ACF-dan olingan (Grec et al., Sounding Solar and Stellar Interiors, 1997). 500 kunlik kuzatuvlarning uzoq ketma-ketligi batafsil o'rganildi (Gabriel et al., A&A, 1998). Ular ACF cho'qqilarining kechikishining variatsiyalari so‘nish vaqti bilan bog'liq emasligini, balki katta chastota ajratish deb ataladigan, $\Delta\nu = \nu(n+1,l) - \nu(n,l)$, chastota bu yerda ν , l sferik garmonik daraja, n esa radial tartib rejimning radial tartibining natijasi ekanligini aniqladilar. Katta va kichik chastotali ajratmalarni o'lchash [kichik chastotali ajratish ACF $\delta\Delta\nu_l = \nu(n,l) - \nu(n-1,l+2)$ va uning modulyatsiyasi tomonidan taklif qilingan (Kholikov et al., Yulduzli tuzilma va habitable planetani topish, 2004). Yulduzli tebranishlar uchun diagnostika vositasi sifatida ACF-dan foydalanish (Roxburg et al., MNRAS, 2006), shuningdek, yulduzli yadroda AKF modulyatsiyasidan akustik-to'lqinli refraksiyonun kuchini o'lchash usulini ishlab chiqdi (Roxburg et al., MNRAS, 2007).

Buning chun GONG va MDI oylik sferik-garmonik (SH) koeffitsientli vaqt seriyasidan foydalanganmiz $l = 0–3$. Ushbu vaqt seriyalari sferik-garmonik funksiyalarga individual to'liq diskli Doppler tezligi tasvirlarini proyeksiyalash orqali hisoblanadi. Har daqiqada olingan tasvirning parchalanishi SH ning nisbiy kuchlarini ifodalaydigan raqamlar to'plamini o'sha (l,m) tasvir uchun turli qiymatlar bilan ta'minlaydi. Sferik-garmonik koeffitsientlar deb ataluvchi bu sonlar keyin har biri uchun vaqt seriyasi to'plamini tuzish uchun qayta tartiblanadi (l,m). Odatda SH vaqt qator uzunliklar GONG uchun 36 kun va MDI uchun 72 kun. Bizning ma'lumotlar to‘plami 1995 dan 2007 gacha bo'lgan vaqt davri. Vaqt seriyali gaussiya filtri bilan filtrlangan FWHM = 2.0 mHz markaz chastotasi $\nu = 3.3$. Filtrlash SH vaqt seriyasiga Fourier transformatsiyasini qo'llash, filtrni chastota sohasida qo'llash va keyin ACF berish uchun filtrlangan quvvat spektrini yana vaqt sohasiga aylantirish orqali amalga oshirildi. ACF har bir l va m uchun alohida hisoblandi. 10-rasmda $l = 0$ 36 kunlik muddatning vaqt seriyasi uchun ACF misoli ko'rsatilgan. Eng dominant cho'qqisi, taxminan to'rt soatlik lag, $\Delta\nu \approx 135$μHz ning quyosh qiymatidan kelib chiqadi. Bu qiymat quyosh yuzasidan markazga va orqaga tovushning o'zgargan tarqalish vaqtidir. Akustik to'lqin Quyosh yuzasidan ko'p qayta tarqalgani sababli, cho'qqisi to'rt, sakkiz, ... kechikishlarda paydo bo'ladi. ACF cho'qqisining joylashuvi Quyoshning akustik (T) radiusi kuzatuv nuqtasidan uzoq tomonga va orqa tomonga quyosh orqali to'lqinning tarqalib ketishi tufayli to'rttaga ko'payib, to'rtta radii masofani bosib o'tganligi taxminidir. Tovush yo'l T vaqti sifatida ifodalanganidek, birliklari sekundlar. Cho'qqining joylashuvini olish uchun biz vaqtdan boshlab texnikani qo'llaymiz - masofadagi gelioseysmologiya, bu erda to'lqinlarning korrelyatsiyalari taxminan Gabor

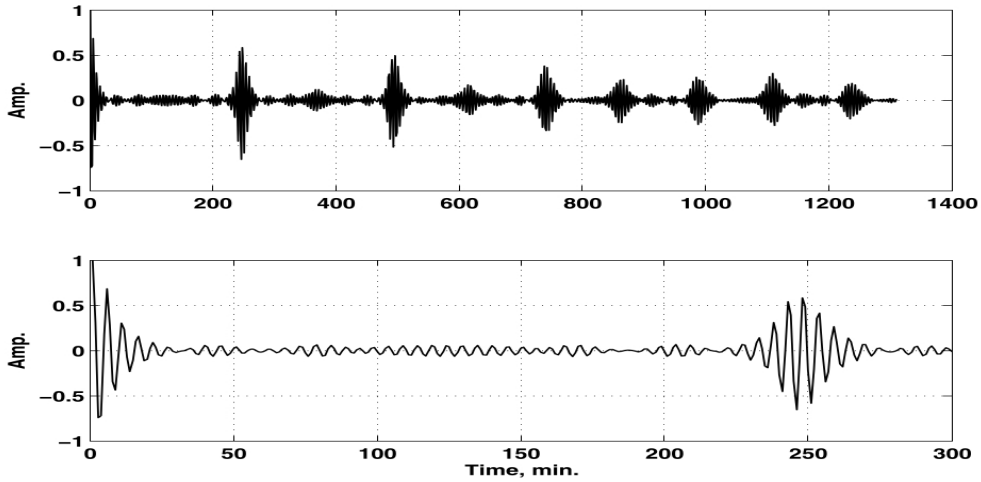

10-rasm. Autocorrelation funksiyasi GONG 36 kunlik vaqt seriyasidan xisoblanadi $l = 0$. Dominant cho'qqisi katta chastotali ayirmaga to'g'ri keladi $(\Delta\nu)$

funksiyasi shaklida ko'rsatilishi mumkinligi ko'rsatilgan. Shunday qilib, uning maksimal atrofidagi cho'qqini Gabor to'lqiniga moslashtiramiz. Oldingi qismda aytib o'tilganidek, fazo tarqalish vaqti zarf tarqalish vaqtiga qaraganda aniqroq o'lchanishi mumkin. 11-rasmda $l = 0$ $l = 3$ besh kunlik seriyalar to‘plami uchun vaqt seriyasidan olingan bosqich tarqalish vaqtlari ko‘rsatilgan.

O'lchovlar Savitzky - Golay usuli yordamida 1,5 yillik siljiydigan oyna bilan silliqlanadi. ACFdan olingan katta ajralmalar juda kichik xato barlarga ega. 11-rasmda odatiy xato barlari taxminan 0,1 soniya. Ushbu xatolar Gabor moslash protsedurasining norasmiy hisob-kitoblaridan emas, balki besh kunlik vaqt seriyasidan hisoblangan o'rtacha o'lchovlarning tarangligidan baholanadi. GONG va MDI natijalari orasidagi akustik radiusdagi bir sekundlik farqning kelib chiqishi noma'lum. Shuningdek, biz GONG va BiSON chastota jadvallaridan o'lchovlarni $\Delta\nu$ tahlil qildik. O'rnatilgan T chastotalardan olingan vaqt seriyasi eng yuqori mos keladigan tahlil natijasida yuzaga kelgan ancha katta xatolar tufayli quyosh faolligi aylanishi bilan hech qanday o'zgarishlarni ko'rsatmaydi. Eng yuqori mos keladigan chastota farqlaridagi odatiy xatolar odatda taxminan 0,5 μHz bo'lib, T taxminan 0.25 soniyadagi xatoga mos keladi. Rasmning eng muhim xususiyatlari. 11 yillik quyosh faolligi sikli bilan antikor bog'liq bo'lgan akustik radiusning aniq ko'rinadigan variantlari. Barcha past darajadagi rejimlar uchun minimum va maksimal faollik fazalari $l = 0-3$ orasidagi o'zgarishning magnitudasi bir sekunddan kam bo'ladi. Bu kichik o‘zgarishlarni alohida chastota ajralishidan ko‘rib bo‘lmaydi, unda qat’iyatning aniqligi 100 martadan ko‘proq bo‘ladi. Quyosh akustik radiusidagi o'zgarishlar zichlik shkalasi balandligining o'zgarishidan kelib chiqadi, bu esa yuqori aks ettirish nuqtasining chuqurligiga ta'sir

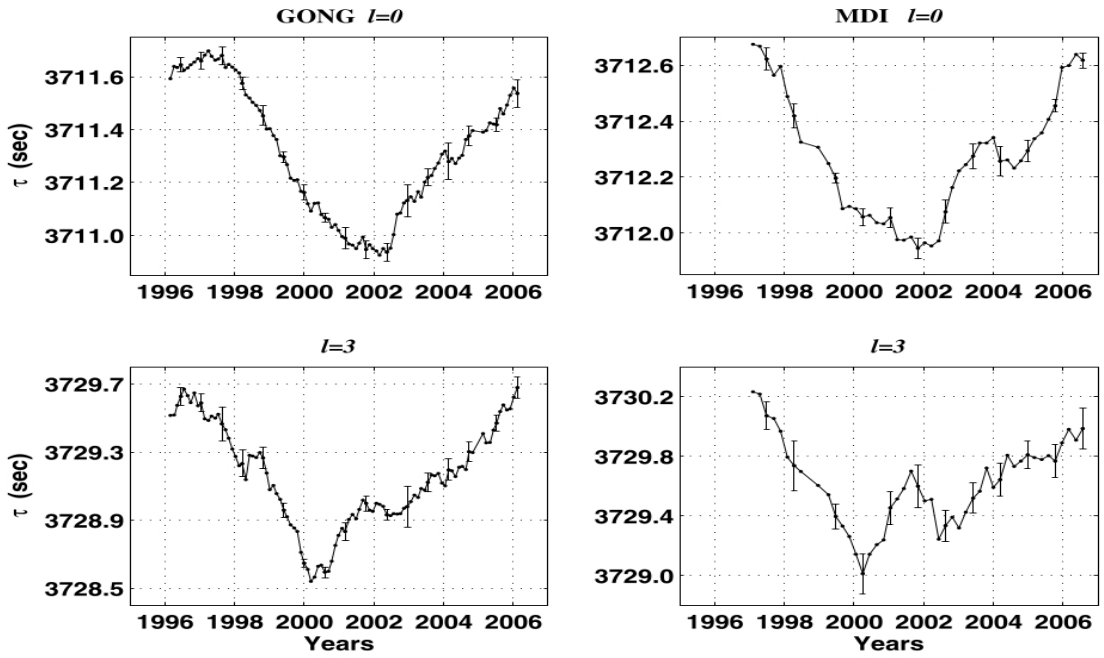

11-rasm. Quyoshning AKustik radiusi GONG (chapda) va MDI (o'ngda) dan vaqt funksiyasi sifatida. Individual avtokorrelatsiya funksiyalari besh kunlik vaqt seriyasidan olingan. O'lchovlar 1,5 yillik yugurish oynasi bilan tekislanadi. Quyosh faolligi darajasi bilan sezilarli antikorelyatsiyani aniq ko'rish mumkin.

qiladi yoki ichki tovush tezligining o'zgarishidan kelib chiqadi. Bizning o'lchovlarimizdan biz radius o'zgarishlarining chuqurligiga bog'liqligini aniqlay olmaymiz, ammo aniqki, quyosh faolligi bilann teskari korelyatsiyasi aniq.

4-bob. Quyosh meridional oqim o'lchagichlari. Quyosh fizikasining muhim maqsadlaridan biri kvazi-davriy Quyosh faolligining kelib chiqishi va uning Quyosh dinamosi bilan aloqasini tushunishdir. Quyoshdagi ichki dinamikaning asosiy jarayoni meridional aylanish bo'lib, u dinamo modellarida juda muhim tarkibiy qism hisoblanadi. Bu katta hajmli aylanish klassik shakl taxminan 10-20 m s^{-1} har yarimsharda yuza-yaqin poleward (qutblarga yo’nalgan) oqimi, va amplitudasi bir nechar marta kichik konveksiya zonasining pastki qismida "qaytish" ekvatorward (ekvatorga yo’nalgan) oqimi bo'lib, magnit tartibi zaif [Giles, PhD tezis, Stanford, 2000]. Ushbu bo'limda biz 1995 yildan buyon faoliyatdagi GONG va MDI kuzatuv ma’lumotlaridan meridional oqim o'lchovlariga qilgan izlanish va qo’shgan hissamizni tasvirlaymiz. Magnit-bo’lakchalarni kuzatish yordamida dastlabki tadqiqotlar (Komm et al., SolPhys, 1993; Snodgrass et al., SolPhys, 1996) va sirt Doppler o'lchashlar (Hathaway, ApJ, 1996; Nesme-Ribes et al., A&A, 1997) quyosh yuzasida poleward meridional oqimi va quyosh aylanishi bilan oqim o'zgarishlarini topdi. Oqimlarning

chuqurlik profilini aniqlab beradigan gelioseysmik kuzatuvlar bunday oqim mavjudligini ilk bor ko’rsatdi (Giles et al., Nature, 1997). 10 - 20 m s^{-1} konvektsiya zonasi yuzasi va yuqori qatlamlari o'rtacha poleward oqim mantiqiy bo'lib ko‘rinadi. (Giles, Doktorlik dissertatsiyasi, Stenford, 2000) meridional oqimning vaqt evolyutsiyasini o'rganish uchun birinchi bo'lib mahalliy gelioseysmologiya texnikasi, vaqt - masofa (Duvall et al., Nature, 1993) dan foydalangan. Natijalar 23-faollik davr mobaynida Quyosh maksimaliga nisbatan kamaygan oqimning amplitudasining o'zgarishini ko'rsatdi. (Chou et al., ApJ, 2001) natijalarni uzaytirdi, shuningdek, avvalgi tsikl davomida olingan ma'lumotlar yordamida quyosh minimumiga nisbatan amplitudaning oshishini topdi. Michaelson Doppler Imager (MDI) ma'lumotlarini halqa-diagramma tahlili (Haber et al., ApJ, 2002; Basu at al., ApJ, 2003), tsikl 23 ko'tarilish bosqichida, va Global Oscillation Network Group (GONG) ma'lumotlar (González Hernández et al., ApJ, 2006; Zaatri et al., SolPhys, 2006), xuddi shu tsiklning kamayib borayotgan bosqichida, quyosh tsikli bilan meridional oqimning umumiy o'zgarishini tasdiqladi, quyosh minimaliga nisbatan katta amplitudaga ega. (Ulrich et al., ApJ, 2005) yuzadagi nuqtalarni izlaydigan usul yordamida deyarli ikkita quyosh aylanishi uchun meridional oqimning vaqtinchalik o'zgarishini ko'rsatadi. Shuningdek, ular meridional oqimning amplitudasi bilan Quyosh sikli o‘rtasida antikorelyatsiyani topishdi. Magnit faolligi konsentratsiyasi kengligi atrofidagi meridional oqimning muayyan xatti-harakati ushbu mualliflarning aksariyati tomonidan qayd etilgan. Ekvator atrofidagi oqimning faollik kengliklariga nisbatan keskin gradienti, bu kuzatuvlarda yuza magnit faolligining ko'payishi bilan ko'payadi. (Gizon, PhD tezisi, Stanford, 2003) yuqori magnit faolligi sohalaridan qo'shgan hissasini yo'q qiluvchi ikkita Karrington aylanishini faqat faollik kengliklaridagi sokin joylarini tahlil qildi va meridional oqimdan sezilarli farqni topdi. Ushbu natija shuni ko'rsatdiki, katta faol mintaqa komplekslari (Zhao et al., ApJ, 2001; Haber va boshq., SolPhys, 2004; Komm et al., ApJ, 2004; Braun et al., Helio- va Asteroseismology: Oltin kelajakka tomon, 2004) faol kengliklarga yig'iladigan meridional oqimning ushbu kuzatilgan tarkibiy qismi uchun javobgar bo'lgan. (Zhao et al., ApJ, 2004) faol komplekslarni o'rab turgan oqimlardan tashqari faol kamarlarda qo'shimcha komponent bo'lishi mumkinligini ta'kidladi, chunki ular faollik bilan bog'liq oqimlarning maksimal chuqurligidan past qoldiq oqimlarni topdilar. Ushbu bo'limdagi birinchi ish (González Hernández et al., SolPhys, 2008) halqa-diagramma yondashuvi yordamida olingan meridional oqim o'lchovlarini tasvirlaydi. Gong (http://gong.nso.edu/data) dan olti yillik yuqori aniqlikdagi kuzatuvlar quyosh aylanishining pasayishi 23-faollik davri, bizga mahalliy gelioseysmologiya yordamida meridional oqimni davomiylik bilan o'rganish uchun

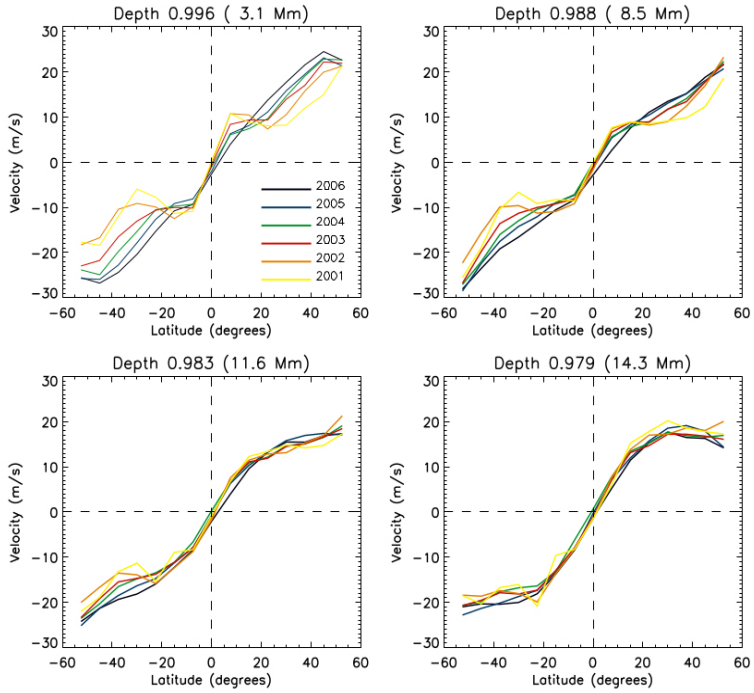

12-rasm. To'rt xil chuqurlikda GONG uzluksiz ma'lumotlar majmuini halqa-diagramma tahlil qilish orqali olingan meridional oqimning yillik o'rtacha ko'rsatkichlari. Yuzaki qatlamlarda aniq kuzatilgan quyosh aylanishining o'zgarishi chuqurroq qatlamlarda kamroq namoyon bo'ladi.

misli ko'rilmagan imkoniyat berdi. Bundan tashqari, yuza faolligining statistik ahamiyatga ega bo'lgan ko'rsatiladigan oqimga ta'sirini o'rganishni imkoni boʻldi. 12-shakl GONG yuqori aniqlikdagi ma'lumotlarning doimiy to'plamiga standart halqa-diagramma tahlilini (Haber et al., ApJ, 2002) qo'llash orqali olingan yillik o'rtacha meridional oqimni ko'rsatadi. Faol kamarlar atrofidagi to'lmalar yoki oqimlar raqamlarda aniq ko'rinadi. Ushbu ishda biz o'rtacha barcha mavjud ma'lumotlarni o'rtacha meridional oqim o'lchashlari bilan yuza magnit faolligining ko'rsatiladigan oqimlarga qanday ta'sir qilishini tekshirish uchun faqat sokin Quyosh hududlaridan foydalanish orqali olinganlar o'rtasida o'xshashlik koʻramiz.

Biz quyosh yuzasidan meridional oqimni 23 tsiklining kamayib borayotgan fazasi uchun taxminan 16 Mm chuqurlikka oqimni xosil qilish uchun 2001 yil iyul oyidan 2006 yil dekabr oyigacha GONG yuqori farqlash qobiliyatli Dopplergramning standart halqa-diagramma tahlilini (Hill, ApJ, 1988) qo'llaymiz. Halqa-sxema usuli o'sha muayyan soha uchun o'rtacha gorizontal tezlik vektorini olish uchun mahalliylashtirilgan hududlarda tarqalayotgan yuqori darajadagi to'lqinlarni o'rganadi. Ushbu toʻrtburchak disklar mozaikasini tahlil qilish orqali to'lqinlar tarqaladigan chuqurlik oralig'ida uch o'lchovli tezlik xaritasini ishlab chiqish mumkin. Odatda ring-diagramma tahlili diskning markazida pikselga taxminan 1,5 Mm o'lchamdagi 1664

daqiqali to'liq diskli Dopplergramlar seriyasidan foydalanadi. 15^0-diametrli maydonlarga apodizatsiya qilingan 16^0 kvadratdan iborat disklar sirt aylanish tezligida birxillashtirilgan. Uch o'lchovli FFT birxillashtirilgan maydonchalarga qo'llaniladi va tegishli quvvat spektri gorizontal-tezlik oqimi tufayli chastota o'zgarishi muddatini o'z ichiga olgan Lorentzial-profil modeli yordamida o'rnatiladi (Haber et al., ApJ, 2002). Nihoyat, o'rnatilgan tezliklar tezlik oqimlarining chuqurlikdagi bog'liqligini tiklash uchun eng kam kvadratli usul yordamida teskari masalani echish orqali qo‘lga kiritiladi. Gong halqa-diagramma dasturlar to‘plami bu yerda taqdim etilgan ishlar uchun ishlatilgan. Dasturlar tafsilotlarini (Corbard et al., SOHO 12 / GONG+ 2002, 2003) da topish mumkun. Bitta maydonchani tahlil qilish natijasida bir necha chuqurlikda bitta hor (v_x, v_y)izontal-tezlik vektori olinadi.

Meridional aylanishni o'rganish uchun v_y hisoblangan oqimlarning tarkibiy qismiga e'tibor qaratamiz. Yuqori kengliklarda mahalliy-gelioseysmology yordamida olingan oqimlariga quyosh burchak davriy o'zgarish ta'sir ko'rsatadi B_0(González Hernández et al., SolPhys, 2006; Zaatri et al., SolPhys, 2006). Ta’siri haqida hozircha to‘liq tushunchaga ega emasmiz. (Beckers, Astronomische Nachrichten, 2007) muammoni tahlil qildi va boshqa tuzatish natijasida ancha boshqacha natijalarga olib kelishi mumkinligini ko'rsatdi. Shunday qilib, biz oqimlarni to'g'rilamaslikka qaror qildik. B_0-burchak effekti barcha hisoblangan oqimlarning yillik o'rtacha ko'rsatkichlariga teng ta'sir ko'rsatishi sababli, bizni qiziqtirgan vaqtinchalik o'zgarishlar hali ham o’zgarmas bo'lishi kerak. GONG uskunasi tomonidan taqdim etilgan ma'lumotlarning uzluksiz oqimi tufayli biz 5,5 yil davomida uzluksiz tezlik oqimlarini oldik. Har yili o'rtacha to'rtta chuqurlikda meridional oqimni 12-rasmda ko'rish mumkin. Yuzaga yaqin, taxminan 3 Mm chuqurlikda Quyosh aylanishi minimal darajada ilgarilab borishi bilan oqimlarning amplitudasining sezilarli darajada oshishini ko'rish mumkin, bu avvalgi natijalarni tasdiqlaydi. Faol kamarlar atrofidagi zarbalar bu chuqurlikda juda aniq va amplituda kamayib borayotgan magnitetik faollik bilan kamayadi. Standart halqa sxemasi tahlilidan foydalangan holda cheklangan rezolyutsiyaga yetkazilgan bo'lib, yuqori kenglikdagi oqimlarning o'zgarishi faol mintaqalar atrofidagi tashkil etilgan oqimlarning hissasi tufayli ta'sir sifatida ham talqin qilinishi mumkin. Standart halqa-sxema tahlillari yordamida Quyosh meridional aylanishinini qiymatlaridan faol kengliklar ta’sirini ajratib tashlash ancha murakkab masala, ayniqsa quyosh faolligi yuqori yillar davrida. Biroq to’la ma'lumotlar to'plamining 2003-2004 yillardagi davrijuda past faollikning katta sohalari bilan bir qatorda yuqori faollik sohalarini taqdim etadi, bu esa barcha hududlar bo'yicha o'rtacha ko'rsatkichga

ega bo'lgan meridional oqimlar bilan faqat sokin mintaqalardan

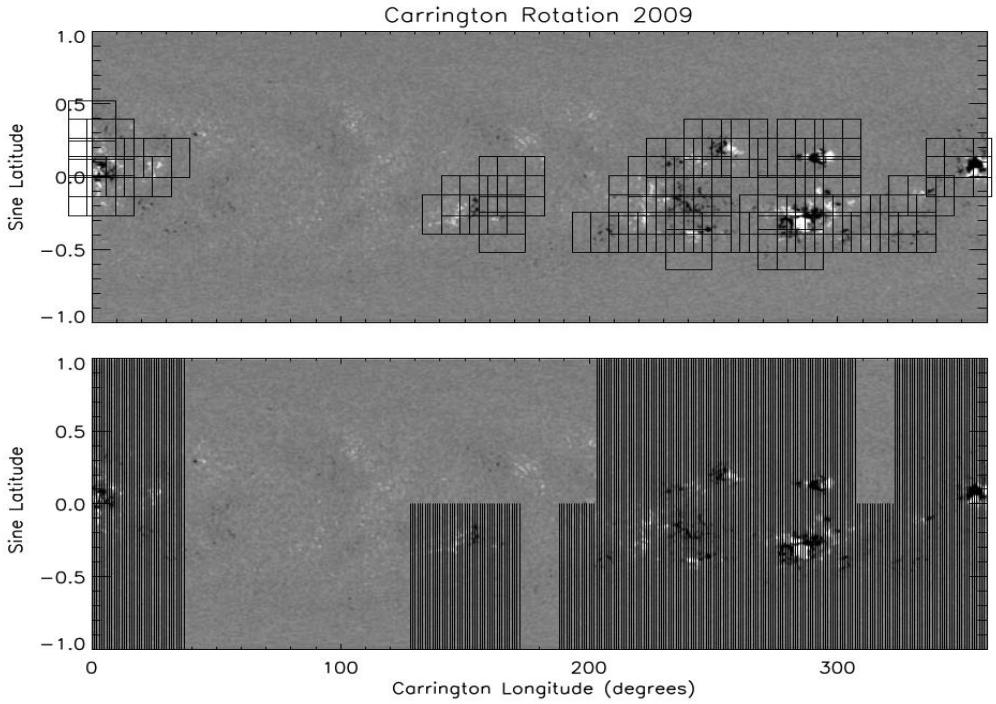

13-rasm. Carrington aylanishi 2009 uchun qo'llaniladigan yuza magnit faoliyati bilan bog'liq ma'lumotlarni yo'qotish uchun ikki xil yondashuv. Yuqori panelli shows maska 1: faqat yuza magnit faoliyati bilan bog'liq bo'lgan patnislar yo'q qilinadi. Pastki panelda niqob 2 ko'rsatilgan: bir yarim shardagi barcha patnislar va sirt magnit faolligiga ega bo'lgan muayyan patnis bilan bir xil uzunlikda yo'q qilinadi.

olinganlar o'rtasida statistik jihatdan sezilarli solishtirish imkonini beradi. Sokin hududlarni faollardan ajratib olgan birinchi urinish bu ma'lum bir ko'rsatkichdan yuqori o'rtacha magnit maydon kuchiga ega bo'lgan diskchalarning barchasini olib tashlashga asoslangan edi (1-niqob). Bizning maqsadlarimiz uchun yuza faolligining ko'p qismini o'n Gauss tashkil etgandek tuyuldi. 13-rasmning yuqori panelida ushbu yondashuv yordamida olib tashlangan hududlar ko'rsatilgan. Kvadrat hududlar halqa-sxema standart sohalariga to'g'ri keladi. Ushbu yamalar olib tashlangandan so'ng, qoldiq meridional oqim deyarli barcha sohalarni o'z ichiga olgan holda olingan oqim bilan bir xil bo‘ldi (14-rasm).

Ikkinchi urinish sirt faoliyati bilan bog'liq ma'lumotlarni yanada agressiv ravishda olib tashladi. U o'n Gaussdan yuqori o'rtacha magnit maydon kuchiga ega bo'lgan hududlarni (niqob 2) va shu hudud joylashgan yarimshar o‘lchashlari olib tashlanishidan iborat (12-rasmning pastki paneliga qarang). Bunda uzoq masofalarga cho'zilgan yuza faolligi bilan bog'liq oqimlar butunlay olib tashlanadi. Biz bu yerda muayyan faol mintaqa atrofida oqimlarini tashkil etish Ekvatorni kesib o‘tmaydi, degan taxminni qildik. Bu faoliyat Ekvatorga juda yaqin bo'lganda to'liq to'g'ri emas, ammo

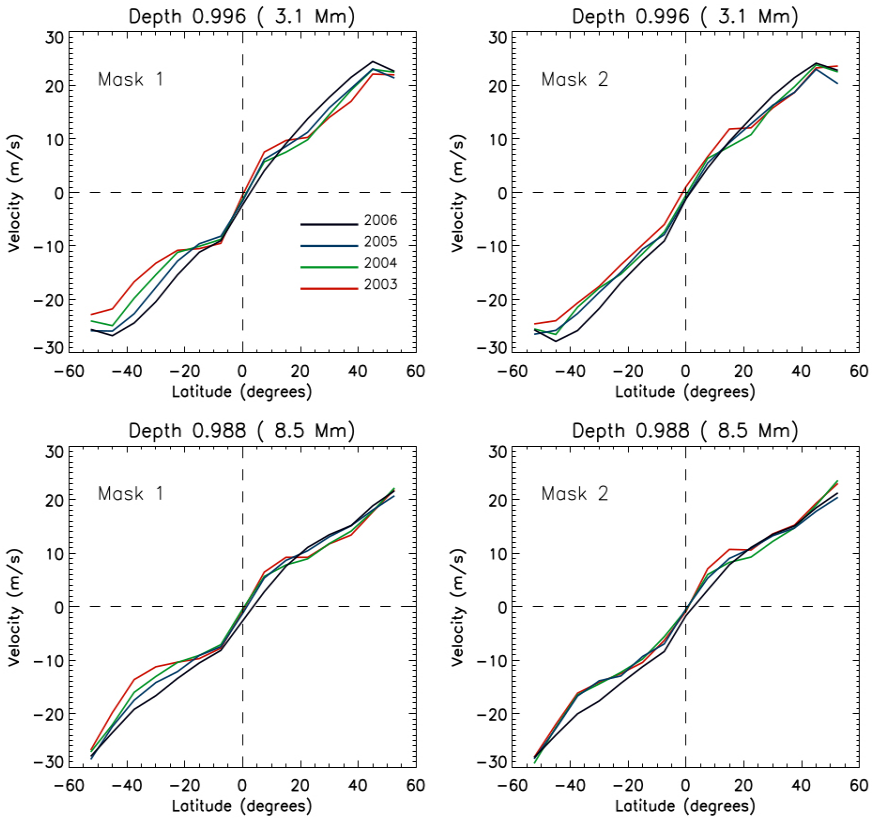

14-rasm. Niqob 1 (chapda) va niqob 2 (o'ngda) qo'llashdan so'ng ikki xil chuqurlikda GONG uzluksiz ma'lumotlar majmuini halqa-diagramma tahlil qilish orqali olingan meridional oqimlarning yillik o'rtacha ko'rsatkichlari. Quyosh aylanishining o'zgarishiyanada agressiv maskalash tartibini qo'llagandan so'ng kuchayadi.

statistik jihatdan biz ekvatorni har ikki yo'nalishda kesib o'tayotgan oqimlar bekor bo'lishini kutamiz. Olib tashlangan joylar 2009 yil Carrington aylanishi uchun 12-rasm ning pastki panelida qayta quyuq rangli. Ikkala holatda ham muayyan soha uchun o'rtacha magnit maydoni MDI magnitogrammalari yordamida hisoblab chiqilgan.

Faoliyatning sirt maydonlarini olib tashlashdan oldin va keyin ikkita muayyan chuqurlikda 2003-2006 yillar davomida olingan meridional oqim 14-shaklga taqdim etiladi. Oqimning umumiy tendentsiyasi, faollik pasayishi bilan ko'payishi o'zgarmaydi. Shunga qaramay, niqobni qo'llagandan so'ng trend kamroq ko'zga tashlanadi. Biroq,h atto eng agressiv maskalash usulini qo'llanilsada, ayniqsa, 6,0 mm atrofida chuqurlikda qo'shimcha aylanish butunlay ketmaydi.

Mavjud ma'lumotlarning barchasini, shu jumladan sirt magnit faolligining sohalarini o'rtacha ko'rayotganda, temporal o'zgarish kenglamaga bog'liq bo'lib, quyosh minimal va quyosh maksimal faolligi farqi 40 gradus kenglamada 10 m/s larga yaqin. Quyoshning ichki qismiga nisbatan variatsiya kamroq namoyon bo'ladi, maksimal farqi 10 Mm chuqurlikda taxminan 5 m s^{-1} bo'ladi. O‘zgarishlar janubiy yarimsharda katta

bo'lib, yuza faolligiga to'g'ri keladi. Yuza faolligining barchasini olib tashlagandan keyin ham (niqob 2), oqimning quyosh minimaliga nisbatan o'zgarishi davom etadi, ammo tezlanish kichikroq bo'ladi. Biz boshqa mualliflar tomonidan ilgari ma'lum qilingan faol kamarlardagi qo'shimcha aylanma borligini tasdiqlaymiz. (Spruit, SolPhys, 2003) faol hududlarda pastki harorat tufayli torsional tebranishni geostrofik oqim sifatida tushuntiradigan modelni taqdim etdi. Ushbu model chetlaridan magnit faolligining asosiy kengligi markazi tomon oqimlarning chetdan kelishini bashorat qiladi. Bu torsional tebranishning meridional versiyasi bo'lib, yuzada uning maksimal amplitudasi taxminan ≈ 6 ga teng . Model, shuningdek, chuqurlik bilan bu tebranishlar tez pasayishini bashorat qiladi, bu 30 Mm dan pastga yo'q bo'lib ketadi. Biroq, bizning natijalarimiz faol kamardagi oqimlarning tezroq pasayishini ko'rsatmoqda, ular 10 - 14 Mm atrofida yo'q bo'lib ketadi.

Faol kengliklarda kuzatilgan qo'shimcha aylanish Quyosh aylanishi bilan farq qiladi, quyosh minimaliga qarab pasayadi. Faollik markaziga yo'naltirilgan bu oqimlar yuza faolligining hissasi olib tashlanganda yo'q bo'lib ketmaydi, garchi oqimlarni hisoblash uchun faqat sokin Quyoshdan olingan ma'lumotlar ishlatilganda amplituda kamayadi. Faqat sokin Quyoshdan foydalanganda faol kengliklarda olingan meridional oqim ikkita Carrington aylanishini vaqtida olingan, dastlabki o'rganishda (González Hernández et al., JphCS, 2008) barcha mavjud ma'lumotlar yordamida hisoblab chiqilganidan farq qiladi. Bu topilma (Gizon, PhD tezisi, Stenford, 2003) natijalarini tasdiqlaydi. Ushbu cheklangan tadqiqotlar shuni ko'rsatdiki, qo'shimcha aylanish atrofdagi katta faol komplekslar mavjud (Zhao et al., SolPhys, 2001; Haber et al., SolPhys, 2004; Komm et al., SolPhys, 2004; Braun et al., Helio- va Asteroseismology: Oltin kelajakka yo'naltirilgan, 2004). Biroq, biz bu erda taqdim etayotgan tizimli tadqiqot shuni ko'rsatadiki, ushbu qo'shimcha aylanishni faqatyuza faoliyati bilan bog'langan mahalliylashtirilgan oqimlar hisobga olib bo'lmaydi, chunki u faqat sokin Quyoshdan olingan ma'lumotlardan foydalanganda ham davom etmoqda.

Ushbu bo'limning ikkinchi ishi 1995-2001 vaqt davri uchun GONG ma'lumotlaridan foydalangan holda meridional tarqalish vaqtidagi farqlarni olish va tahlil qilishga bag'ishlangan (Kholikov et al., SolPhys, 2014). Biz global gelioseysmologiya ga mo'ljallangan original past o'lchamli GONG "Classic" (May 1995 - avgust 2001) bilan olingan butun Global Tebranish Tarmoq Guruhi (GONG) ma'lumotlar to'plamidan va Yaqinda, GONG+ mahalliy-gelioseysmology ma'lumotlar olish system (avgust 2001 - dekabr 2010) shimol va janubga qarab akustik to'lqinlar tarqalish vaqtlarini olish uchun foydalanganmiz. Vaqt-masofa gelioseysmologiyasidagi asosiy g'oya quyosh diskidagi ikki joy Δ orasidagi signallarining tarqalish vaqtlarini

hisoblashdir, ular har bir joyda tezlik o'zaro bog'liqligi yordamida (Duvall et al., Nature, 1993) topiladi. Bir xil faza tezligiga ega to'lqinlar to'lqin paketini hosil qiladi va quyosh ichki qismidagi bir xil nur yo'li bo'ylab bir xil chuqurlikka kirib boradigan paketni tashkil qiladi. Faza-tezlik filtrini qo'llash o'zaro bog'liqlik o'lchovlarida signal-shovqin nisbatini oshiradi.

Faza tezligini filtrlashning standart tartibi oddiy. Bir qator tezlik tasvirlarini qayta tiklash va kuzatishdan so'ng, ma'lumot kubi Fourier sohasiga aylantiriladi va ma'lum bir faza tezligiga ega bo'lgan faza tezligi (ω/k_h) filtri qo'llaniladi va yana vaqt sohasiga aylantiriladi. Shunday qilib, filtrlangan tasvirlarda faqat faza tezligining ma'lum bir diapazoniga to'g'ri keladigan to'lqinlar mavjud. Yuqoridagi protsedurada gorizontal Fourier transformatsiyasini ishlab chiqarganimiz sababli, to'lqinlar tekis parallel deb hisoblashimiz kerak. Ushbu taxmin faqat yuqori darajadagi rejimlar uchun to'g'ri keladi, chunki chuqurroq kirib boradigan to'lqinlar endi tekis parallel emas. Bu shuni anglatadiki, chuqur qatlamlar uchun o'lchovlarni sferik geometriyada faza tezligini filtrlash bilan tahlil qilish kerak. Shuning uchun, har qanday chuqurlikka kirib boradigan to'lqinlarni ajratib olish uchun biz sferik garmonikaning (SH) vaqt seriyasidan foydalanamiz. Bu holda biz (kenglik, uzunlik) o'rniga faza-tezlik filtrini ω/L ω/k_h $L \approx \sqrt{l/(l+1)}$ ga qo'llashimiz mumkin. So'ngra filtrlangan SH koeffitsientlari yordamida biz vaqt sohasidagi tezlik tasvirlarini qayta tiklaymiz.

Meridional oqimni aniqlash uchun to'lqin yo'l vaqtini doimiy uzunlikda ikki joy o'rtasida yotadigan bir xil nur yo'li bo'ylab qarama-qarshi yo'nalishlarda o'lchash zarur. Bu holda, ikki yo'nalish o'rtasidagi tarqalish-vaqt farqi, asosan, oqimning meridional (shimoliy-janubiy) komponentiga sezgir (Kosovichev et al., SolPhys, 1997). Yuqoridagi rekonstruktsiya jarayonida bunga erishish uchun biz faqat yaqin zonal rejimlardan foydalanishimiz mumkin $m \ll l$. Birinchi o'lchovlarimizda biz faqat $m = 0$ koeffitsientlardan (to'g'ri shimoliy-janubiy yo'nalishda) foydalanardik. Keyinchalik amin bo'ldikkii, qo'shimcha kichik m koeffitsientlardan foydalanish o'zaro bog'liqliklarda signal-shovqin nisbatini yaxshilaydi. Ushbu muayyan tahlilda biz pastki m koeffitsientlarning 30% dan foydalandik.

Tarqalish vaqti farqlarni olish uchun qadamlar:

- Barcha chuqurliklarni qoplash uchun sakkiz xil l oralig'i tanlandi 0.97 - 0.67 $R_\odot$. Har bir l oralig'iga mos keladigan faza tezligi filtri parametrlari aniqlandi.
- Tezlik tasvirlari 142 GONG-oy (36 kunlik) vaqt seriyasi uchun faqat past-m koeffitsientlari yordamida qayta tiklandi.
- O'zarobo g'liqlik funksiyalari (CCF) hisoblandi.
- Xoch-korrelyatsiyalar bo'ylama $-30^0 \leq \varphi \leq 30^0$ oralig‘i uchun o‘rtachalandi.

- Shimolga va janubga tarqalish vaqtlari Gabor to'lqiniga o'zaro bog'liqlikning salbiy va manfiy kechikishlarini moslashtirish orqali topildi.
- Qarama-qarshi yo'naltirilgan ikkita yo'l vaqti o'rtasidagi farq har bir faza-tezlik filtriga to'g'ri keladigan yo'l masofalari Δ uchun xisoblanadi. 15 yil ichida tarqalish vaqtidagi farqlarning o'rtacha ko'lanishi natijasida noaniqlik darajasi juda past bo'ldi.

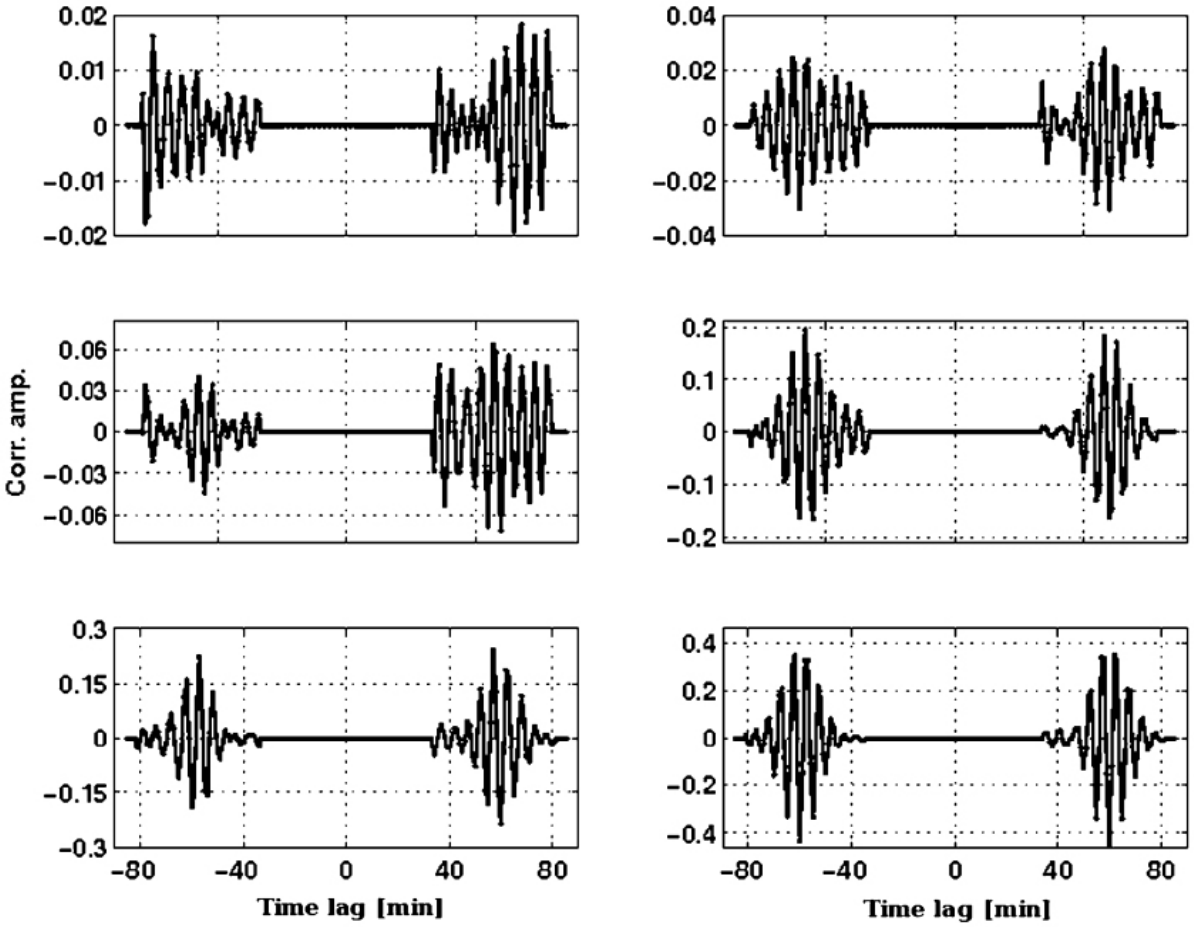

15-rasm. Xoch-korrelyatsiyalash fasonlari ikki kenglikda uch xil filtrlash bilan bilan sug'orildi: $\theta = 60^0$ (chap ustun) va $\theta = 0^0$ (o'ng ustun). Yuqori: hech qanday filtrlashsiz, o'rta: o'zgarishlarni surish filtri, pastki: o'zgarishlarni filtri ziyod yuqori m filtri. O'zaro bog'liqliklarning mustahkamligi sezil darajada oshgani ko'rinib qo'yildi.

15-frasm m-filtrlash kross-korrelyatsiya funksiyalarining signal-shovqin nisbatini qanday yaxshilanganini koʻrsatadi. Ayniqsa, 65º gacha bo'lgan yuqori kengliklarda Gabor to'lqinlari tomonidan Gauss qobigʻiga mos kelishi muhimdir. Yaxshi signal-to-shovqin nisbati tufayli, yuqori m filtrlangan CCFs har ikki o'zgarishlar-tezlik yoki xom faqat CCF ko'ra ancha muvaffaqiyatli armatings beradi. Bu filtrlash holda, CCF fit 50 dan yuqori kengliklarda xam olinishi mumkin.

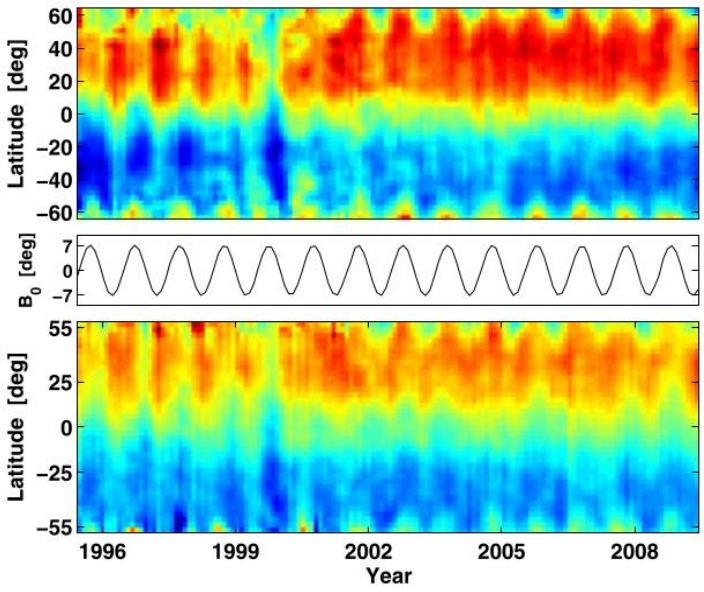

16-rasm. Faza-tezlik filtri hamda ajratish masofasi $\Delta = 7^0$ (yuqori) va $\Delta = 15^0$ (pastki) uchun yuqori m filtr bilan tarqalish vaqtidagi farqlar. Xar kuni alohida sayohat vaqtidagi farqlar 36 kunlik intervalda o'rtacha ko'rsatkichga ega bo'ldi. O'rta panelda quyosh B_0-burchak va aynish o'zgarishlari ko‘rsatilgan. 1-yil davriylik GONG Klassik vaqt davrida ancha kuchli bo'ladi.

Oldinga va teskari hisoblashlar tarqalish farqi moda bo'shlig'i ustidan o'rtacha oqim tezligiga taxminan chiziqli proportsional ekanligini ko'rsatdi: bir soniyaning vaqt farqi taxminan 10 - 20 m s^{-1} oqim tezligiga to'g'ri keladi (Giles et al., SOHO 6/GONG 98, 1998). 16-rasmdagi GONG SH vaqt seriyasidan olingan ikkita alohida ajratish masofalari uchun shimoliy-janubiy t ravel-time farqlari keltirilgan. Ko'k va qizil rang janubga va shimolga qarab tarqalayotgan oqimga mos keladi. Ikkala yarimsharda B_0 burchak bir yillik kvazi-davriy signal (teskari fazasi) yillik o'zgarishning ta'sirini ko'rsatadi. Yuqori kengliklarda vaqt farqining ishora o'zgarishi haddan tashqari egiluvchan burchakli davrlarda sodir bo'ladi, bu esa soxta bo'lishi mumkin bo'lgan ikkinchi hujayrali tuzilishga sabab bo'ladi. Bizning o'lchovlarimiz 22 va 23 tsikllarining ikkita minimal va bitta maksimal fazasini qamrab oladi. Vaqt farqlaridagi temporal o'zgarishlarni talqin qilish quyosh burchagi B_0 bilan bog'liq bo'lishi mumkin bo'lgan ashyolar tufayli qiyin. 16-rasmda yuqori kengliklarda bir yillik davriylik aniq ko'rsatilgan. Bu davriylik burchak bilan mustahkam bog'liq B_0. Bundan tashqari, bu davriylik barcha kengliklarda mavjud va hatto ekvator atrofida ham ko'rinadi. Ushbu ashyoning sababi GONG-Klassik vaqt davridagi burilish burchagi (burilishning kattaligi oshgani) ekanligiga dalillar, bu esa kuchli proyeksiya ta'sirini keltirib chiqaradigan past farqlash qobiliyati bilan tasvirlar olinganiga bog‘liq. Vaqtinchalik o'zgarishning umumiy naqshini ko'rish uchun biz kichik masofani ajratish masofalari

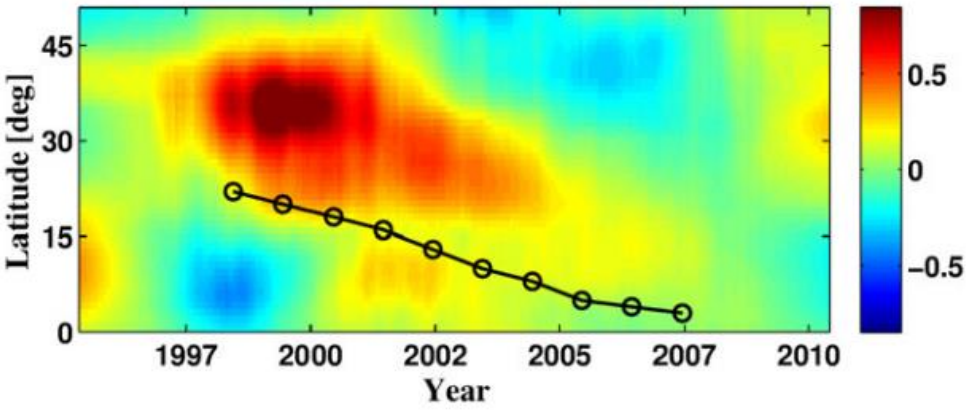

17-rasm Vaqt farqlarining $\Delta = 6 - 9^o$ masofalari uchun o'zgarishi, taxminan $0.92R_\odot$ pastroq burilish nuqtasiga mos keladi. Xarita ikkala yarimshar uchun ham o‘rtacha ko‘rsatkichdir. Vaqt farqlari ikki o'lchamli Gaussian yugurish oynasi 3º kenglik va 1,8 yil vaqti bo‘yicha silliqlashdi. Magnit-faollik kamarining tahminiy joylashuvi qora doiralarda chiziladi.

uchun vaqtni farq qiladigan o'lchovlarni (3º kenglikda va 1,8 yil o'z vaqtida) qattiq silliqladik (17-rasm).

2007-2010 yillarning vaqt oralig'i farqi chiqarib tashlandi va ikkala yarimshar ham o'rtacha (ishora o'zgarishi bilan) bo'ldi. O'zgarishlarning kapalak-shaklga o'xshash tuzilishi quyosh aylanishining kengligi bilan bog'liq bo'lib, faollik kamariga nisbatan tizimli ravishda o'zgaradi. Ushbu o'zgarishlar, ehtimol, faol mintaqalarning oqimi bilan bog'liq va faollik aylanishi bilan meridion oqim tezligining global o'zgarishi emas. Ushbu maqolada ishlatiladigan eng kichik tarqalish masofalari odatiy quyosh dog'i hajmidan kattaroq; shuning uchun faol hududlarda oqimlar bizning o'lchovlarimizga sezilarli ta'sir ko'rsatmaydi. Ushbu tadqiqotning asosiy e'tibori vaqt farqlarining chuqur profilini qurish edi. 15 yil davomida o'rtacha o'lchovlar sezilarli darajada tizimli va anglash shovqin kamayadi, ayniqsa burchak tufayli yillik davriyligi B_0. 18-rasmda 1995-2010 yillarda 3658 kunlik o'lchovlar uchun o'rtacha vaqt farqlari kenglik and ajratish masofasi (chap panel) funksiyasi sifatida keltirilgan. Kenglik tarmog'i shimoliy-janubiy yo'nalishdagi ikkita joyni bog'laydigan nur yo'lining o'rta nuqtalariga to'g'ri keladi. Kichik ajratish masofalarida o'lchashlar 63º gacha bo'lgan kengliklar uchun amalga oshirilishi mumkin. Katta ajratish masofalari uchun, yakuniy nuqtalardan biri 70º kengligidan yuqori bo'lib, Gabor-to'lqinli moslashtirish tartibi uchun etarli signal-shovqin nisbatini ta'minlay olmaydi. 60º atrofidagi kichik masofalar uchun vaqt farqining magnitudasining pasayishi ikkala yarim sharda ham ko'rinadi, lekin u ishorani o'zgartirmaydi, bu kichik ajratish o'lchovlarida ham shunday bo'ladi. Yuqori kengliklarga nisbatan vaqt farqlarining kamayib borayotganiga dalillar bor, ammo biz qarshi cell-larning hech qanday alomatlarini ko‘rmayapmiz.

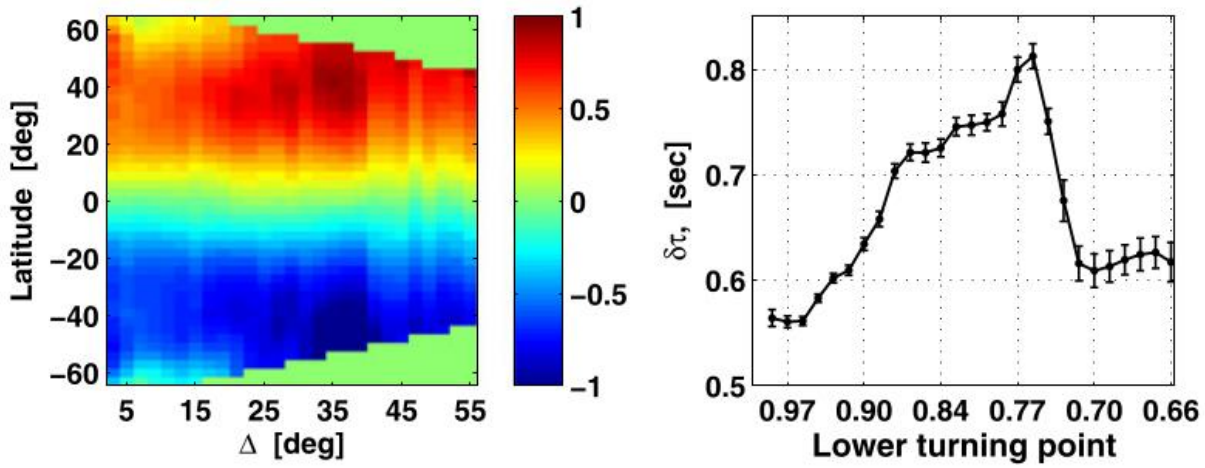

Fig. 18 Sayohat vaqtidagi farqlar kenglik va ajratish masofasi funksiyasi sifatida (chap panel). Colormap sekundlarda sayohat vaqti o'lchovlari oralig'ini ko'rsatadi. O'ng paneli: atrofida kengliklarga mos simmetrik gorizontal kesma 35º- 40º. abscissa chap panelda ishlatiladigan ayirish masofalarining pastki burilish nuqtalarini ko'rsatadi. Taxminan keskin pasayish $0.76R_{\odot}$ aniq.

Ushbu o'rtacha xaritaning asosiy xatti-harakati chuqurlik bilan vaqt farqining ortishi. 18-rasm (o'ng pane l) pastki burilish nuqtasining funksiyasi sifatida 35 º– 40º kenglik oralig'iuchun o'rtacha vaqt farqini ko'rsatadi. Monotonik ko'payishdan $0.76R_{\odot}$ keyin chuqurroq chuqurlikda keskin kamayadi. Bu tomonidan muhokama qilingan yorug'lik tezligi muammosi bilan bog'liq bo'lgan ashyo bo'lishi mumkin(Duvall et al., GONG 2008 / SOHO 21, 2009) yoki proyeksiyaga asoslangan boshqa muammolar bo‘lishi xam mumkun. Boshqa tomondan, bu nima uchun bu muayyan chuqurlikka tushishini tushuntira olmaydi: ashyolar katta masofalar uchun yanada kuchliroq bo'lishi kerak. Mumkin bo'lgan sabablardan biri quyida teskari oqim (ekvatorga) mavjudligi bo'lishi mumkin $0.76R_{\odot}$. $\Delta = 51 - 57^{o}$ yo'l masofalari uchun o'lchovlar $0.68R_{\odot}$ chuqurlikga to'g'ri keladi. Ushbu to'lqinlar asosan yuqori qatlamlarda vertikal ravishda tarqaladi, bu esa ularni poleward oqimlariga kamroq sezgir qiladi. O'zaro bog'liqliklardan olingan vaqt o'zgarishi butun nur yo'li bo'ylab integratsiyalashgan o'lchovlar bo'lgani uchun, yuqori konveksiya zonasida meridional oqimning ba'zi hissalari bunday katta ajralish masofa o'lchovlarida mavjud bo'lishi mumkin.

5-bob. Meridional aylanishning kenglik va chuqurlik profili. Quyosh dinamosi, magnit oqim transporti va Quyosh aylanishi modellarida meridional aylanish juda muhim rol o'ynaydi (Glatzmaier et al., ApJ, 1982; Vang Ilim, et al., ApJ, ApJ, 1989, 1991, 2002; Choudhuri et al., A&A, 1995; Dikpati et al., ApJ, 1999; Nandy et al., Nature, 2011). Meridional oqim yaqin sirt qatlamlarida taxminan 10-20 ms^{-1} amplitudasi bilan har bir yarimsharda poleward bo'lib , o'rta kengliklarda kuchli

cho'qqiga chiqadi (Duvall, SolPhys, 1979; Hathaway, ApJ, 1996; Braun et al., ApJ, 1998; González Hernández et al., ApJ, 1999, 2006; Basu et al., ApJ, 1999; Basu et al., ApJ, 2010; Hathaway et al., Ilm, 2010; Ulrich, ApJ, 2010).

Massa qutblarga to'planmaganligi sababli, ikkala yarimsharda ham qaytish ekvatorga oqib o'tadigan oqim konveksiya zonasida bir joyda, ehtimol uning osti yaqinida ishlayotganiga ishoniladi. Ushbu meridional aylanishni o'nlashtirishga bo'lgan eng istiqbolli va to'liq urinishlardan biri bu (Giles et al., Tabiat, 1997 yil; Giles, PhD tezisi, Stenford, 2000) bo‘lgan. Quyosh va Heliosfera observatoriyasi kosmik kemasining Michelson Doppler Imager gelioseysmik ma'lumotlaridan foydalanib, Giles qutblarga yo’nalgan meridional oqimlari konveksiya zonasining deyarli barcha qatlami bo'ylab davom etganligini va amplitudasi atiga bir necha m s-1 bo’lgan qaytish, ekvatorga oqib o'tishining takotelinasi yaqinida bilvosita dalillari mavjudligini aniqladi. Uning usullari va tahlili ommaviy muhofaza qilish cheklovini qo‘ydi. Shunday qilib, paydo bo'lgan surat ikki yopiq aylanuvchi oqimdan, har yarimsharda bitta hujayradan iborat bo'lib, ular yuzadagi ekvatordan ajralib, chuqur ichki qismidagi ekvator tomon yaqinlashadi. O'shandan beri boshqa gelioseysmologiya tadqiqotlari turli xil uslublar ko'plab turli xil qarashlarni taklif qildi. Masalan, (Chou et al., ApJ, 2001; Bek et al., ApJL, 2002; Chou et al., ApJ, 2005) o'rta kengliklarda meridional aylanishning qo'shimcha "hujayrasini" kuzatishdi, bu turli xil va vaqt o'tishi bilan farq qiladigan hujayra edi. Bundan tashqari, (Zhao et al., ApJ, 2004) va (González Hernández et al., ApJL, 2010) bunday hujayra bir konvergent oqim maydoniga ega ekanligini topishdi (Kameron et al., ApJ, 2010). Darhaqiqat, katta hajmdagi oqim profillari (meridional va zonal yo'nalishlarda) Quyosh aylanishi bilan ancha kuchli farq qilishi aniqlandi va bir nechta tadqiqotlar oqimning amplitudasi tsiklning kuchi bilan (masalan, Komm et al., SolPhys, 1993) anti-bog'liqligini aniqladi; Chou va boshq., ApJL, 2001; Haber et al. ApJ, 2002; Basu et al., ApJ, 2003; González Hernández et al., SolPhys, 2008; Gizon et al., SolPhys, 2008). Sirt poleward oqimining kengligi oldingi ikki tsiklda keng tarqalgan bo'lib, ba'zi gelioseysmik o'lchovlar yuqori kenglikdagi, teskari ekvatoral sirt komponentini ko'rsatadi (Dikpati et al., ApJ, 2012). Murakkablikka qo'shish uchun so'nggi kuzatuvlar konveksiya zonasiga (Xolikov et al., SolPhys, 2011), va (Hathaway, ApJ, 2012) ekvatorga qaytish oqimini 70 Mm chuqurlikda joylashtiradi.

(Zhao et al., ApJL, 2012b) asosiy rol o’ynagan vaqt-masofa o'lchovlarida (Duvall et al., Tabiat, 1993) yangi tizimli markaz-dan-chetga signalini kuzatdi, bu esa o‘z navbatida ishonchli chuqur meridional oqim o'lchovlarini olishda va yuqorida aytib o'tilgan noo'rin natijalar manbalaridan biri bo'lgan, (Zhao et al., 2012b) aylanishni olib tashlangandan so'ng, sharq-g'arbiy o'lchovlarda topilgan tizimli tarqalish-vaqti

almashinuvlari tufayli, meridional (shimoliy-janubiy) o'lchovlardan olib tashlash edi. Bu tuzatish bir necha xil kuzatuvlar yordamida izchil gelioseysmik o'lchov olib keldi. Ushbu signalning manbai butunlay tushunilmasa-da, u quyosh diski bo'ylab chiziq hosil bo'lish balandliklarining o'zgarishi kabi mavjud kuzatuv cheklovlari bilan bog'liq bo'lishi mumkin, bu esa turli joylar o'rtasidagi o'zaro bog'liqlik o'lchovlarida qo'shimcha akustik tarqalish vaqtidagi o'zgarishlarni keltirib chiqaradi. (Baldner et al., ApJL, (2012) tashqi quyosh konveksiya zonasida konvektsiyadan vertikal oqimlarning ta'siri shunga o'xshash tarqalish vaqti o'lchovlariga ta'sir qilishi mumkinligini ko'rsatdi.

Keyinchalik, (Zhao et al., ApJL, 2013) quyosh konvektsiya zonasida ikki meridional aylanish hujayralarini o'lchash uchun ularning mahalliy texnikasini qo'lladi, shu bilan birga (Schad et al., ApJL, 2013) murakkab ko'p hujayrali tezlik tuzilishi dalillarini olib keldi. Kosmosga asoslangan ma'lumotlardan olingan ushbu yangi va hayajonli topilmalar ushbu muhim yirik oqimlarning o'zgartirilishi mumkin bo'lgan tushunchani ni taqdim etdi.

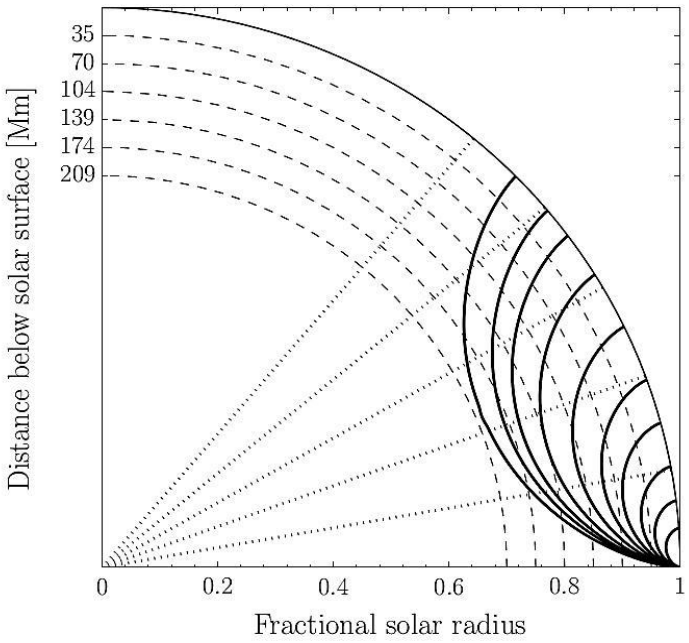

Fig.19. Biz ishlaydigan 10 ta faza tezlikli filtrlar uchun taxminiy nur yo'llarining tasviri. Yo'llarni izlash uchun real quyosh modelidan foydalaniladi. Biz faqat ko'rib chiqilgan markaziy masofa uchun nuqta-to-ark ajratish masofasini uchirib chiqamiz. Nuqtali beshta chiziq 10^o ko'paytmada rejalangan. Nurlarning pastki burilish nuqtasi uchun Mm chuqurligi shkalasi mos yozuvlar uchun y o'qi bo'yicha beriladi.

(Kholikov et al., SolPhys, 2014) da biz (GONG) ma'lumotlarga qo'llaniladigan vaqt-masofali gelioseysmologiya yordamida meridional aylanish oʻrganamiz. Bu erda biz amalga oshiradigan tarqalish vaqti o'lchovchilari protsedurasini batafsil tasvirlaymiz, bu standart bo'lmagan va (Zhao et al., ApJL, 2012a) va (Hartlep et al., ApJ, 2013) usullaridan farq qiladi. Konveksiya zonasiga chuqur tekshirish uchun GONG tasvirlarining 600 dan ortiq kundalik to'plamlaridan foydalanamiz. Gometrik va kuzatish ashyolarini kamaytirish uchun biz 85% dan ortiq toʻldirish sikli va quyosh burilish burchagi bo'lgan vaqt davrlari bo'lgan sanalarni tanladik $B_0 \leq 4^o$. Bu qat'iy

talablar dan foydalanish mumkin bo'lgan ma'lumotlar miqdorini ancha kamaytiradi. Faraz qilamizki, yuqorida aytib o'tilgan markaz-dab-chetga tizimli quyosh diskidagi har qanday yo'nalishda bir xil bo'ladi va biz uni faqat kuzatishlarning ekvatorial mintaqasi yordamida hisoblaymiz. Tarqalish vaqtidagi farqlar shimoliy-janubiy oqimlar uchun hisoblanib, sharq-g'arbiy signalni chiqarib tashlash yo'l bilan tuzatilgan. Ushbu ishda biz GONG Doppler tezligi tasvirlaridan foydalanamiz va 652 ta kunlik, yil davomida 85% dan yuqori to‘ldirilishi bo'lgan 2004-2012 vaqt davri mobaynida kunlik kuzatuvlar to'plamlarini tanladik. Odatda tarqalish vaqti o'lchovlari quyosh sathida ma'lum Δ masofalar bilan ajratilgan ikkita joy o'rtasida o'zaro bog'liqlik funksiyasi tahliliga asoslangan (Duvall et al., Nature, 1993). Ma'lumki, bir xil faza tezligiga ega to'lqinlar to'lqin paketini hosil qiladi va taxminan bir xil nur yo'li bo'ylab tarqaladi. CCF-larning signal-shovqin nisbatini oshirish uchun, faza tezligi filtrlari muayyan to'lqin paketlarini ajratish uchun ushlatildi. Meridional oqim signalini aniqlash uchun biz konstant uzunlikda bir juft nuqta (aniqrog'i, nuqta va yoy) o'rtasida yotadigan bir xil nur yo'li bo'ylab qarama-qarshi yo'nalishlarda tarqalayotgan to'lqinlar uchun to'lqin yo'l vaqtini o'lchaymiz. Bunda ikki qarama-qarshi yo'nalishda tarqalayotgan to'lqinlar uchun tarqalish vaqti farqi faqat oqimning meridional (shimoliy-janubiy) tarkibiy qismiga sezgir bo'ladi. O'n xil faza tezligi filtrlari $0.98– 0.70R_{\odot}$ chuqurliklarin qoplash uchun mo'ljallangan tarzda tanlandi. Faqat 1,8 dan 4,5 mHz gacha bo'lgan vaqt chastotalari ichidagi rejimlar saqlanib qoladi. Bu erda ko'rib chiqilgan filtrlangan to'lqin paketlarining taxminan nur yo'llari 19-rasmda tasvirlangan. Nuqta va signal o'rtasidagi CCF berilgan uzunlik uchun o'rtacha 30^{o} yoy ustida yotadi. To'rtta asosiy yo'nalishdagi arklar ko'rib chiqiladi. Har bir filtrlangan ma'lumotlar to'plami uchun kross korrelyatsiyalari CCF dagi birinchi qavariq maksimali atrofida $0,75^{o}$ ko'payish bilan barcha tarqalish masofalari uchun hisoblangan. Umumiy hisobda 72 ta korrelyatsiya funksiyasi $\Delta = 2,75–47^{o}$ ni qamrab olgan yo'l masofalari uchun xisoblanadi. O'zaro bog'liqlik o'rtacha 250 ga yaqin uzunlikdagi qadam bilan $-45^{o} \leq \phi \leq 45^{o}$ oraliqda o'zgaradi . Bo'ylama bo‘ylab kichikroq oraliqdan foydalanish ko'proq to'g'ri markaz-dan-chetga tuzatish beradi, lekin kross-korrelyatsiya o'lchovlarning signal-shovqin nisbati pasayishiga olib keladi. Torroq oraliq yordamida oddiy solishtirish individual o'lchovlarning o'zgaruvchanligi sezilarli darajada oshganini ko'rsatdi. Biz taxminan 1 soniya tarqalish vaqt farqlariga qiziqqanimiz sababli, biz kengroq uzunlik oralig'idan foydalanishga qaror qildik. Shimoliy va janubga sayohat vaqtlari Gabor to'lqinli funksiyasini xoch korrelyatsiyalarining ham salbiy, ham manfiy kechikishiga (τ) moslashtirish orqali olingan. Ikki qarama-qarshi yo'naltirilgan tarqalish vaqti farqi har bir faza tezligi filtriga mos keladigan tarqalish masofalari Δ uchun hisoblanadi. Biz

"janubiy minus shimoliy" (S-N) tarqalish-vaqt farqlari atamasidan foydalanamiz. Bundan tashqari, "sharq minus g'arb" (E-W) yo'nalishidagi tarqalish vaqtidagi farqlar ham yuqorida ko'rsatilgan ma'lumotlarni qayta ishlash tartibining barcha aniq qadamlari yordamida hisob-kitob qilingan. Ushbu o'lchovlar uchun tarqalish vaqtlari o'rtacha ±20 dan ortiq kenglikda olingan. Ichki quyosh aylanishi tufayli doimiy o'zgarishhar

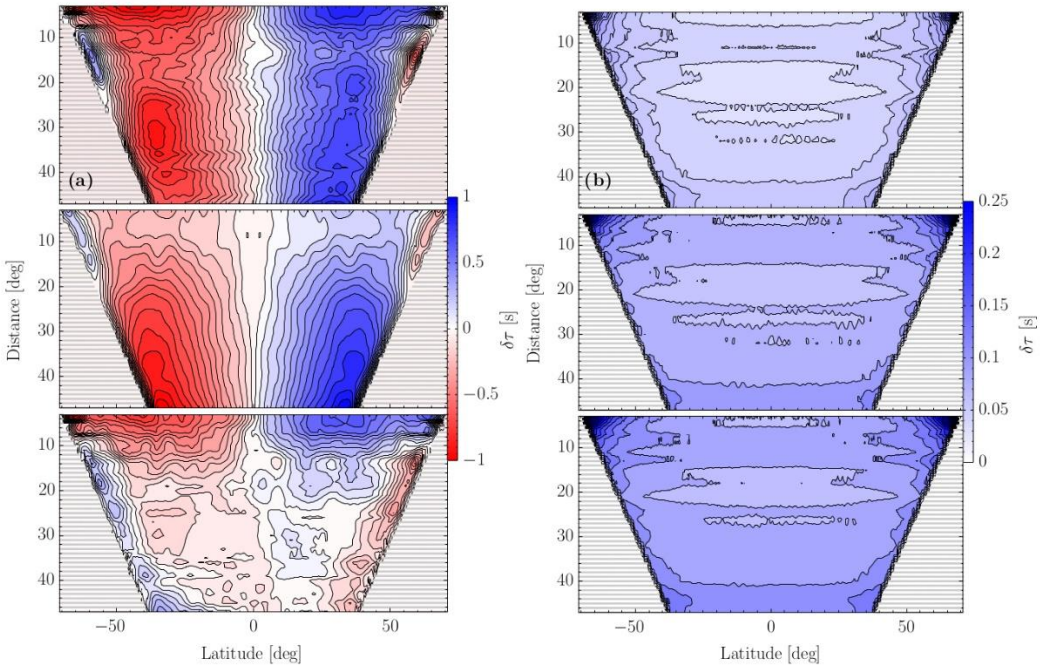

20-rasm. 652 kunlik Doppler tezligi tasvirlari to'plami yordamida olingan tarqalish vaqtidagi farq xaritalari. Ustun (a) mos ravishda yuqoridan pastga S-N, E-W va S-NE-W kontur xaritalarini ko'rsatadi. Ustun b) ustun (a) har bir panel bilan bog'liq tegishli o'lchov noaniqliklarini rejalashtiradi. E'tibor bering, har bir ustundagi o'rta paneldagi x o'qi uzunlik bo'lib, kenglik uchun ko'rsatilgandek bir xil raqamli shkala qiymatlari mavjud (±75^o). To‘rlangan mintaqalarida markaz-dan-chetga cheklovlari tufayli hech qanday o‘lchovlar hisoblanmaganligi ko‘rsatilgan.

bir tarqalish masofasi o'lchovi uchun ayirib, olib tashlanadi. Ushbu o'lchovlar meridional kuzatishlar uchun sistematikani to'g'rilash uchun ishlatiladi. 20-rasmning yuqori chap panelida kenglik va tarqalish masofasining funksiyasi sifatida taqdim etilgan o'rtacha 652 kundan ortiq S-N tarqalish vaqtidagi farqlar ko'rsatilgan. Berilgan yo'l masofasidagi har bir nuqta o'zaro bog'lanish sxemamizdagi nuqta va o'q orasidagi o'rta pozitsiyaga to'g'ri keladi. Xoch korrelyatsiyalarining tugunlari yotgan joyda juda yuqori kenglikdagi ma'lumotlardan saqlanish uchun o'lchovlar masofaning vazifasi sifatida kesiladi. Noaniqliklar ikkinchi ustunda berilgan, har bir uzunlik va har kuni uchun alohida o'lchovlardagi dispersiyadan xisoblanadi. Bular o‘rtachalangan signalning juda kam foizidir. Har bir yarimsharda poleward meridional oqimning imzolari 20(a)-rasmda aniq ko'rinib turadi. Bu ko'rsatkichdagi rang belgilanishi shundayki, ko'k rang shimoliy qutb tomon oqimga mos keladi, janub qutbi tomon qizil oqim. Darhaqiqat, kutilganidek o'rta kenglikdagi cho'qqidan tashqari, chuqurlik (ya'ni

tarqalish masofasi) bilan tarqalish vaqtidagi farqning ko'payishi ham kuzatilmoqda. Bunga bir yoki bir nechta sistematika sabab bo‘lishi kutiladi. Buni yanada chuqurroq o'rganish uchun bir xil ma'lumotlar to'plamidan qo'yilgan E-W tarqalish vaqtlari 20-rasm ning o'rta panelida x o'qidagi uzunlikning vazifasi sifatida ko'rsatilgan. Markaziy meridianga nisbatan E-W xaritasi simmetriklashtirildi, chunki biz ma'lumotlar differentsial aylanishni hisobga olish uchun izlanganidan beri ikkita (sharq / g'arbiy) gem ispherelari o'rtasida sezilarli farqlar bo'lmasligini kutmoqdamiz. Ushbu o'lchovlar S-N xaritasi kabi markaz-dan-chetga o'zgarishning o'xshash namunasini ko'rsatadi.

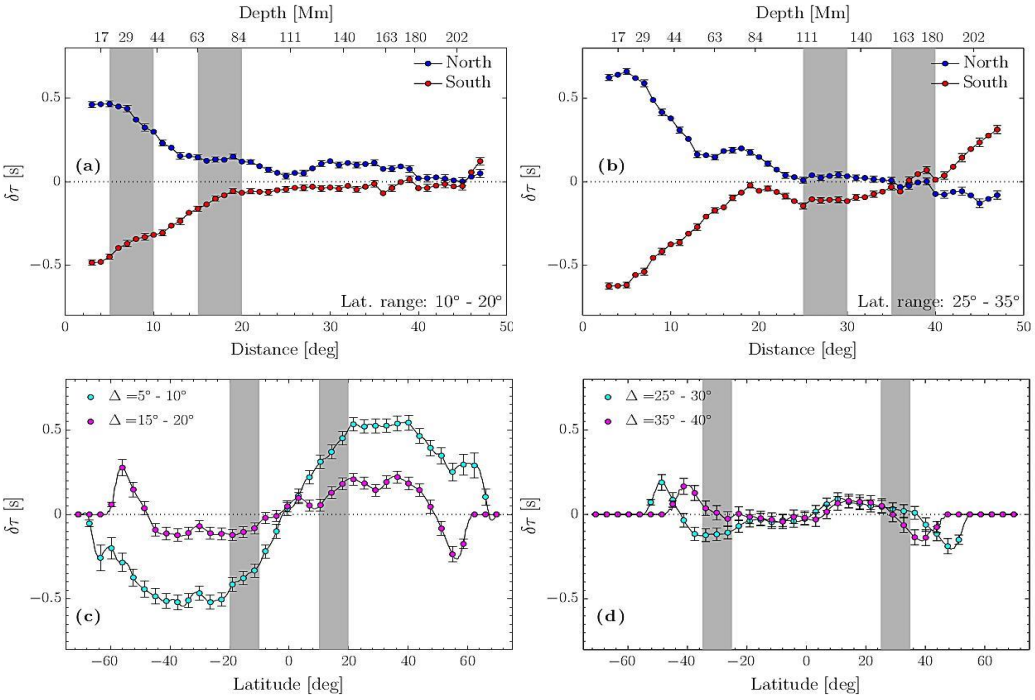

21-rasm. To'g'rilangan S-N tarqalish vaqtidagi farqlarning chuqurligi va kengligi bilan kesishadi. Yuqori qator panellari a) va b) sho'lchov masofasi (*Δ*) bilan bo'lgan sifatida har bir yarim shardagi sayohati bo'lgan farqlarini ko'rsatkichda qayd etilgan 10^o banddan ortiq o'rtacha kenglik oralig'i uchun. Xar bir sayohat masofasi uchun pastki burilish ko'rdi chuqurligi uchun proksi yuqori x-axisda ko'zda. Quyida tegishli uchastkalarda ko’’rtib sayohat masofalari kulrang rangda oydinlik kiritdi. Panellar c) va d) yo'l vaqtlarini 5^o masofalarda interval bo'yicha o'rtacha kenglikdagi birlashuvchisi sifatida ko'rsatish. Panellarda kenglik oralig'i a) va b) panellarning (c) va d) kulrang qutilarida bo'lgan. Noaniqliklar barcha chunin uchun ko'rsatiladi va faqat faqat uchun hayratlanarli ma'lumotlar nuqtalarida shunoslik.

(Zhao et al., ApJ, 2012a) turli kuzatish ma’lumotlaridan tarqalish vaqtining juda batafsil tahlili haqida xabar berdi. Ular Markaz-dat_chetga o'zgarishlarining shakli va magnitudasi Gelioseysmik va Magnit Imager o'lchovlarining Doppler, davomiylik, chiziq asosiy va chiziq chuqurligi uchun juda farq qilishini aniqlaganlari sababli, bu o'zgarishlarga quyosh kelib chiqishining har qanday yirik quyi yuza oqimi sabab bo'lmaydi , degan xulosaga kelish mumkin. Bu erda biz xuddi shu tartibga rioya qilamiz va S-N o'lchovlarini E-W o'lchovlarini olib tashlaymiz, natija 20(a) ning pastki

panelida ko'rsatilgan. Bu tuzatish yo'l vaqtining chuqurlik bilan ko'payish tendentsiyasini olib tashlaydi. Bundan tashqari, ishora o'zgarishlarining ba'zi dalillarini ko'rish mumkin.

21-rasmda tarqalish vaqtidagi farq xaritalari orqali turli kesmalar ko'rsatilgan. Panellar (a) va (c) pastki kengliklarda va qisqaroq yo'l masofalarida kesmalar bo'lsa, panellar (b) va d) o'rta kenglik va kattaroq tarqalish masofalari uchun. Ushbu raqamlar, avvalgi tadqiqotlarda kuzatilganidek, tarqalish vaqtidagi farqlar turli chuqurliklar uchun 30^o atrofida o'rta kengliklarda eng kuchli ekanligini tasdiqlaydi. Ushbu vakillik shimoliy va janubiy yarimsharlar o'rtasida aniq, ammo o'zgacha asimmetriyani ko'rsatadi. Eng asosiysi, biz ikki holat uchun o'lchovlarda ishoraning o'zgarishi sodir bo'lganligini ham kuzatamiz: 1) har bir yarimsharda taxminan 15^o dan katta bo'lgan tarqalish masofalari uchun yuqori kengliklarda va (2) har bir yarimsharda taxminan 20^o dan katta bo'lgan katta masofalar uchun.

Darhaqiqat, agar ushbu signallar uchun katta hajmdagi oqimlar javobgar bo'lsa, 21(a) va (b) oqimning keng kenglik oralig'i uchun 15^o –20^o gacha bo‘lgan masofalarni o'tkazishda ishora o'zgarishiga yaqinlashish tendentsiyasini ko'rsatadi. Kattaroq masofalarda bu signal keyin o'zining ustunli hissini tiriltiradi, oxir-oqibat yana eng chuqur chuqurliklarida orqaga qaytadi. Bu juda keng ko'lamda muhokama qilingan ko'p hujayralilar tuzilishini ko'rsatadi (Zhao et al., ApJ, 2012a, 2013), u qutbli oqimlarni oralig'ida $0.91R_\odot$ ekvatorga oqib $0.82 - 0.91R_\odot$ tushganini va keyin yana buning ostida polewardni topdi. (Schad et al., ApJL, 2013) tomonidan boshqa, global yondashuv yordamida meridional oqimning ko'p hujayrali tuzilishining yana bir o'lchovchisi haqida xabar beradi. Bu yerda ko'rib chiqilgan maksimal kengliklarda (20-rasmda eng yaqqol ko'rinib turibdi) barcha masofalarda ishoraning o'zgarishi B_0, yaqinda (Xolikov et al., SolPhys, 2014) ko'rsatilganidek, quyosh o'zgarishi tufayli yuzaga kelgan tizimli sabab bo'lishi mumkinligi haqida ogohlantiramiz. Biroq, bu yerdagi o‘lchovlarda bunday ashyo biroz hayratlanarli, chunki biz ma’lumotlarni qamrab olishni bu burchak kichik bo‘lganda davrlar bilan cheklab qo‘yganmiz. Yana bir ehtimoliy sabab oddiygina maxsus tuzatish usulidan va uning har qanday tabiiy sistematikasidan foydalanish bo'lishi mumkin. Quyosh diski bo'ylab markaz-dat-chetga variantining haqiqiy kelib chiqishi hozirda yaxshi tushunilmaydi. Ehtimol, bu ta'sir, ehtimol, disk markazidan masofa bilan spektral chiziq hosil qilish balandligining oshishi bilan bog'liq.

(Jackiewicz et al., ApJ, 2015) ishida olingan tarqalish vaqti o'lchovlaridan foydalangan holda meridional oqimlarning inversiya natijalari tasvirlangan (Xolikov et al., ApJ, 2014). Odatda, gelioseysmik o'lchovlar akustik nurlar nazariyasi jihatidan

teskari bo'ladi (masalan, Kosovichev et al., SCORe'96, 1997), bu bilan qarama-qarshi $\delta\tau$ yo'nalishlarda tarqaladigan to'lqinlarning tarqalish vaqtidagi farqlari faqat ma'lum nur yo'li bo'ylab ichki oqimlarning asta-sekin o'zgarishi bilan bog'liq deb hisoblanadi. Quyosh markazdan va kenglikdan uzoq r va θ bo'lgan koordinata tizimida ishlash, yaxshi ma'lum invers muammosini hal qilishni talab qiladi:

$$\delta\tau = \int K(\theta, r) \cdot u(\theta, r) ds$$

bu erda $\delta\tau$ delta va kenglik funksiyasi sifatida o'lchanadigan vaqt farqlari oqim u bo'lib, K sezgirlik yadrolarini ifodalaydi. GONG sayohat vaqtlarini sharhlash uchun biz har bir o'lchov uchun yadrolarni hisoblaymiz, ya'ni Δ=3°-47° oralig'idagi barcha 45° qiymatlar uchun, markaziy chastota qiymati uchun 3300 mHz dan foydalanamiz. Biz yuqoridagi tenglamani tarqalish vaqtidagi farqlarni o'zgarib, o'rtacha mahalliylashtirilgan o'rtacha yoki SOLA (Pijpers et al., A &,1994; Jackiewicz et al., SolPhys, 2012) texnikasi orqali eshamiz. Inversiya jarayonini sinab ko'rish va tasdiqlash uchun biz uni chuqurlik va kenglik funksiyasi sifatida taniqli quyosh differentsial aylanish profilini takrorlash uchun qo'llaymiz.

(Kholikov et al., ApJ, 2014) da muhokama qilingan E- W o'lchovlaridan tashqari, biz aylanish ma'lumotlarini saqlaydigan tekislanmagan ma'lumotlarning tarqalish vaqti o'lchovlarini ham qildik. Geometriya shundayki, berilgan kenglik va ajralish masofasi uchun o'zaro bog'lanishlar nuqtadan yoylarga hisoblanib, unda nuqta doimo markaziy meridianda bo'lib, yoylar o'sha kenglikka markazlashgan yarim sharlardan birida yotadi. G'arbga signal (prograde) sharqqa signaldan (retrograd) chiqariladi, keyinchalik oldinroq tasvirlangan CTL effektidan ozod bo'lgan aylanishning kutilayotgan ta'sirini ortda qoldiradi. Boshqacha qilib aytganda, sof simmetrik CTL effekti har bir yarimsharda ushbu o'lchash geometriyasi bilan bir xil ishoraga ega bo'lgani uchun, olib tashlanishi bekor qilinadi. Ushbu hisob-kitoblar keyinchalik ko'p masofalar va kengliklar uchun, taxminan 360 kunlik ma'lumotlar uchun amalga oshiriladi. Quyosh aylanishi uchun teskari qilish uchun biz quyidagi parametrlarni to'plamidan foydalanamiz: $0.8R_\odot$ maqsadli funksiyaning joylashuvi - $1.0R_\odot$ 60° dan +60° gacha bo'lgan qadamlar bilan 2,5° qadam bilan kengligi $0.01R_\odot$ va kengligi FWHM va $r = 0.04R_\odot$ FWHM$\theta = 5^o$, mos ravishda. Yanada oqilona taqqoslash uchun global gelioseysmik natijalar har bir chuqurlikda ishlatiladigan maqsadli funksiya bilan aylantirish orqali inversiya rezolyutsiyamizga silliqlanadi. Nihoyat, natijalarning ikkala to'plami 0°-20°, 20° -40° va 40° -60° dan uch kenglikdagi qadamlar ustida o'rtacha bo'ladi. Taxminan 1000 kunlik HMI ma'lumotlarining global tahlillaridan vaqt o'rtacha aylanish profili bilan taqqoslash (Howe et al., JphCS, 2011) 22-rasmda ko'rsatilgan.

Mahalliy-gelioseysmik inversiyamizning noaniqliklari ichida natijalar ekvator atrofidagi yaqin yuza mintaqasidan tashqari aksariyat chuqurlik va kengliklar bo'yicha moslikga ega. Umuman olganda, har qanday kelishmovchiliklarga, shu jumladan turli xil uskunalar va bir-biriga qarama-qarshi bo'lmagan vaqt seriyalariga ko'plab mumkin bo'lgan hissalar mavjud. Ba'zi nomuvofiqliklarga qaramay, bu keng miqyosli oqimlar, bu holda kuchli bo'lsa-da, bu vositalar bilan biroz aniqroq bo'lishi mumkin.

GONG ma'lumotlaridan o'lchanadigan va yuqoridagi ushbu bo'limda taqdim etilgan CTL tomonidan tuzatilgan S − N tarqalish vaqtlari oqimlar uchun teskari bo'lib, 23-rasmda ko'rsatilgan. Bundan tashqari, taqqoslash uchun J. Zhao tomonidan taqdim etilgan (Zhao et al., ApJL, 2013) HMI natijalari ham taqdim etilgan. GONG va HMI ishorasining sirt poleward oqimlaridan ekvatorga qarzdorligiga o'zgarish joyi to'g'risida juda yaxshi kelishuvni ko'rsatadilar $r = 0.91R_{\odot}$. 5-10 m s^{-1} atrofida amplitudali shunga o'xshash kengliklarda tubsiz

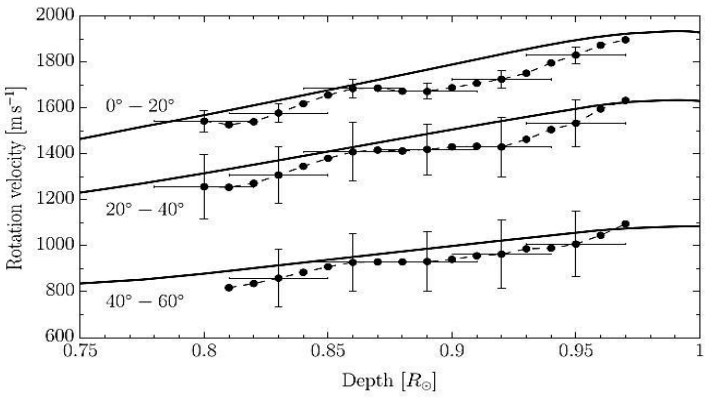

22-rasm. Global helioseismik natijalarga (qattiq chiziqlar) ega bo'lgan sayohati bo'lgan sayohati uchun farqlarni (doiralar bilan chiziqli chiziqlar) teskari chiziqlardan taxmin qilingan quyosh (differentsial) aylanishni yaxshi ko'rayotganlarni farqlash . O'rtacha ko'rsatkichlar egalanganidek uchta kenglik sopol idishlari orqali bo'lgan.

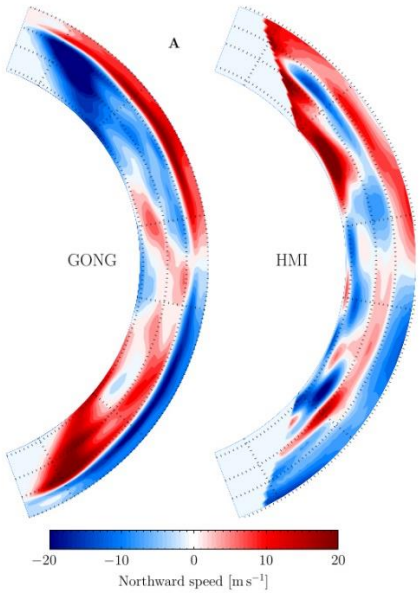

23 rasm. Meridional o'zak profili ±70° kengliklarda va yuqorida chuqurliklarda kesikli ko'rinishi $0.74R_{\odot}$. Xar bir rasmdagi nuqtali chiziqlar chuqurlikda $r = (0.76, 0.85, 0.92, 1.0)R_{\odot}$ va kenglikda $\theta = \pm(10°, 40°, 60°)$ chizilgan

qaytish oqimi cho'qqilari. HMI dan farqli o'laroq, GONG faqat ekvatordan 15° masofada past kengliklarda ikkinchi "hujayra"ning zaif dalillarini ko'rsatadi. Bu xususiyatni biz soxta deb hisoblaymiz. Aniqlash mintaqasining pastki qismidagi ekvator bo'limi aylanmasi oqim-transport modellarining so'nggi bashoratlariga mos keladi. Biz hech qanday chuqurlikda va kenglikda bir nechta hujayralarning hech qanday dalillarini kuzatmaymiz.

Meridional oqimning global namunasi juda boshqacha bo'lib, chuqurligi va kengligi bo'lgan bir nechta hujayralar (Zhao et al., ApJL, 2013) va bir nechta hujayrali hujayralardan (Schad et al., SolPhys, 2013) ancha tubsiz qatlamlardan boshlab qaytish oqimi bilan bir hujayrali rasmgacha (Jackiewicz et al., ApJ, 2015; Hathaway, ApJ, 2012) yoki chuqurroq mintaqalarda (Giles et al., Nature, 1997; Braun et al., ApJL, 1998; Rajaguru at al., ApJ, 2015). Biroq, inversiya natijalari (Jackiewicz et al., ApJ, 2015) haqida bir necha tafsilotlarni yodda tutish kerak, masalan, tizimli ta'sir tufayli natijalardagi noaniqliklar inversiya natijalaridagi tasodifiy xatolardan kattaroq bo'lishi mumkin, natijalar turli asboblar yordamida olingan ma’lumotlar vaqtida turli davrlarni qamrab oladi. Bundan tashqari, radial oqim komponentining sayohat vaqtlariga ta'siri (Zhao et al., ApJ, 2013) va (Jackiewicz et al., ApJ, 2015) tomonidan olingan natijalarda hisobga olinmagan. Vaqt-masofa gelioseysmologiyada (Duvall et al., Nature, 1993) oqimlarni sezgirlik funksiyalari (yadrolar) yordamida ko'rsatish mumkin, bu oqimlarning akustik to'lqinlarning tarqalish vaqtidagi o'lchovlariga ta'siri uchun namunadir. Chuqur meridional oqimning o'lchovlarijuda klassik nurlar yordamida amalga oshirildi (Kosovichev et al., SolPhys, 1997). Ushbu modelda tarqalish vaqtlari faqat cheksiz nozik nur yo'li bo'ylab oqimlarga sezgir deb hisoblanadi, bu esa ikki kuzatuv nuqtasini bog'laydi. Inversiyalar karteziyadan sferik geometriyagacha bo'lgan tarqalish vaqti o'lchovlari uchun Born taxminiy modeliga uzatiladi. Hisoblash uchun muqobil yondashuv Born yadrolari juda yaqinda (Gizon et al., A&A, 2017) tomonidan taklif qilindi. Bu o'zgarishlar chuqur meridional oqimni aniqlash uchun tug'ilgan yaqinlashish yadrolarining qo’llanilishiga ruxsat beradi. Tug'ilganda taxmin (masalan, Birch va boshq., SolPhys, 2000; Gizon et al., ApJ, 2002), Quyosh ichki to'liq to'lqin maydoni, bir so’nuvchi to'lqin tenglamasi yordamida modellashtirilgan, qaysi konveksiya bilan stochastik hayajonlangan. Bu to'lqin tenglamasi nol tartibli va uning birinchi tartibli perturbatsiyasida yechiladi. Bu to'lqinlar oqimi maydonining mavjudligida adveksiyani o'z ichiga oladi. Tug'ilish yaqinlashuvi yordamida tarqalish vaqtlarini modellashtirishda Quyosh ichidagi har qanday joyda to'lqin maydonining paydo bo'linishi va birinchi darajali tarqalish hisobga olinadi. Agar asosiy oqim maydoni bir to'lqin uzunligi (masalan, Birch va boshq. 2001) dan kichik bo'lgan

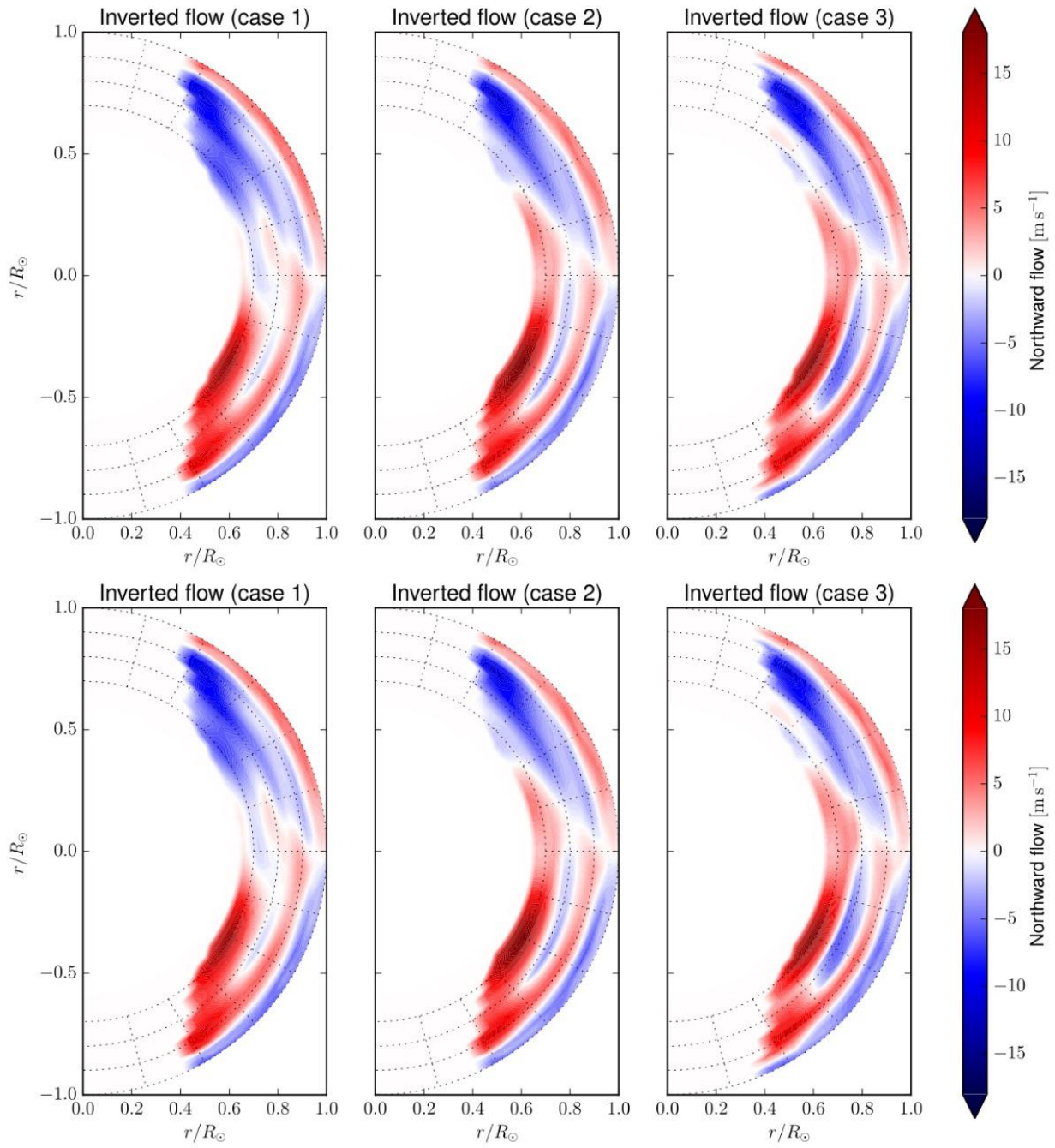

24-rasm. To'liq kovarians matritsasida va kross-talk uchun muntazamlashtirish atamasi yordamida hisoblangan SOLA inversiyasidan meridional oqim profillari. Turli holatlar uchun biz SVD-da o'rta ko'rsatkichni (case 1) yoki past ko'rsatkichni (2 va 3-holatlar) ishlatdik.

uzunlikdagi me‘zonlar farq qilmasa, nur taxminan aniq bo'lishi kutilmoqda.

Konveksiya zonasining pastki qismida oqimlar taqdirda, bu ko'lami 200 Mm tartibda bo'lishi taxmin qilingan (Böning et al., ApJ, 2016). Agar oqim kichikroq uzunlikdagi me’zonlar bo'yicha farq qilsa, Tug'ilgan yaqinlashuv aniqroq deb hisoblanadi (masalan, Bogdan, ApJ, 1997; Birch et al., ApJ, 2004; Couvidat et al., ApJ,

2006; Birch et al., AN, 2007). Quyosh ichki qismidagi to'liq to'lqin maydoniga perturbatsiyani modellashtirishdan tashqari, Born yaqinlashuvining afzalligi shundaki, u disk o'rtacha kross-kovarianslar va o'rtacha quvvat spektri kabi kuzatuv miqdorlarini qo'shish uchun modelni ham taqdim etadi. Bu nurga yaqinlashish uchun bunday emas. Shuning uchun modelning aniqligi osongina tasdiqlanishi mumkin (Böning va boshq., ApJ, 2016). (Böning et al., ApJ, 2017) va (Böning et al., ApJ, 2017) inversiyalari Born sezgirligi yadrolari yordamida amalga oshirildi. O'lchang'ich tarqalish-vaqt farqlarining to'liq kovarians matritsasini qo'llash orqali haqiqiy inversiyani tasdiqlash va bajarishning detali va formalizmi ga muvofiq tavsiflanadi. Ushbu inversiyaning asosiy natijasi chuqurlikda tubsiz ekvatorga qaytish oqimini ko'rsatdi $0.9R_{\odot}$. Meridional oqimning yagona hujayra tuzilishi boshqa inversiya texniklari bilan yaxshi mos bo'lsa, ko'p hujayrali struktura yagona qiymatning parchalanishida ishlatiladigan ko'rsatkichga bog'liq.

XULOSALAR

Bu taqdimnomada 30 yildan ortiq gelioseysmik kuzatishlarni tahlil qilish orqali olingan quyidagi asosiy ilmiy natijalar keltirilgan:

1. Past darajadagi kuzatilayotgan quyosh tebranishlarining avtokorrelatsiya funksiyasi asosida boʻshliqni to'ldirish muammosi uchun yechimni taklif qildik. Ushbu muayyan usul uzoq muddatli seriyalarni samarali ishlab chiqarish uchun kuzatilgan tebranishlarning avtokorrelasyon funksiyasidan foydalanadi. Ishlab chiqilgan yondashuv, ayniqsa, ma’lumotlar boʻshliqlari keng tarqalgan joyga asoslangan quyoshni kuzatishda ajratish qobilyati boʻlmagan toʻliq disk kuzatishlar uchun samarali boʻladi.

2. IRIS loyihasi doirasida oʻlchanadigan past darajadagi quyosh tebranish chastotalari jadvallari taqdim etilgan. Chastotalardan tashqari, chiziq kengliklari, tebranish amplitudasi, boʻlinish koeffitsientlari va quyosh faolligi sikli boʻylab ularning vaqt boʻyicha oʻzgarishi kabi parametrlarni ham keltirilgan. Oʻrganilgan parametrlar Quyosh tebranishlarining xossalari va xususiyatlari haqida muhim ma’lumotlarni beradi.

3. Toʻlqin paketlarining Quyosh faollik davri bilan korrelyatsiya amplitudalarida sezilarli oʻzgarishlar olindi. Quyosh faolligiga bogʻliq maksimal perturbatsiya fotosfera ostida tor qatlamda jamlanganligi koʻrsatildi. Maksimal perturbatsiya $(0.83 - 0.85)R_{\odot}$ chuqurlikda paydo boʻlishi bizning natijamizdan kelib chiqadi.

4. Quyosh yuzasi ostidagi quyosh dogʻining birinchi gelioseysmik tasviri quyosh akustik toʻlqinlarining vaqt-masofa bog’liqlik xossalari yordamida qayta tiklandi.

Ma’lum bo‘lishicha, quyosh dog‘ining ildizlari 40 Mm gacha chuqurlikka yetishi mumkin, bu uning Quyosh qatlamlari ichida sezilarli mavjudligini ko‘rsatadi.

5. Quyoshning chuqur konvektiv zonasidan faol mintaqalarning paydo bo‘lishi tufayli akustik tarqalish vaqti anomaliyalarini tasdiqlandi. Bu akustik tarqalish vaqti anomaliyalari Quyosh ichida 40-75 Mm gacha bo‘lgan chuqurliklarda bo‘lajak faol mintaqalarning aniq xaritasini taqdim etadi. Ta’kidlash joyizki, bu xarita Quyosh yuzasida faol mintaqalar paydo bo‘lgandan bir necha kun oldin ko‘rinadi. Bu akustik signallar faol mintaqalarning paydo bo’lishi va paydo bo’lishi haqida oldindan ogohlantirish ko’rsatkichlarni taqdim etishi mumkinligini ko‘rsatadi.

6. Quyoshning akustik radiusi va uning vaqtga bog‘liq o’zgarishlari o’lchandi. Yerdan (GONG) va kosmosdan (MDI) olingan kuzatuvlar o’lchovlari bir-biriga mosligini ko’rsatadi va bu akustik signallar quyosh yadrosidan o’xshash tarzda tarqaladi. Qo’llanilgan o’lchash texnikasining o’ta aniqligi soniyaning bo’laklari aniqligida Quyoshning akustik radiusidagi vaqtinchalik o’zgarishlarni aniqlashga imkon beradi.

7. Qutbga yo’nalgan meridional oqimning kenglik va chuqurlik funksiyasi sifatidagi batafsil o’lchovlari olindi. Bizning o’lchovlarimiz quyosh faolligining ikki fazasi davomida ham vaqtinchalik o‘zgarishlarni o‘z ichiga oladi. Quyosh fizikasi jamoatchilining ba’zi a’zolari tomonidan yuqori kengliklarda ma’lum qilingan yaqqol namoyon bo’lgan ikkinchi hujayra tuzilishi meridional oqimning yuza komponenti bilan bog‘liq emasligini ko‘rsatuvchi dalillarni topdik. Ehtimol, bu hujayra Quyosh burilish burchagi tufayli yuzaga keladigan artefaktlar evaziga yuzaga kelishi mumkun.

8. Meridional tarqalish vaqti o‘lchovlaridan quyosh diski bo‘ylab chiziq hosil qilish balandligi o‘zgarishi tufayli xosil bo‘lgan tizimli ta’sirni olib tashlandi. Buning natijasida, yigirma yildan ortiq vaqt davomida o‘z kashfiyotini kutayotgan quyosh dinamo modellari tomonidan bashorat qilingan ekvatorga qaytish oqimini tiklashga muvaffaq bo‘lindi.

НАУЧНЫЙ СОВЕТ DSc.03/31.03.2022.T/FM.10.04 ПО ПРИСУЖДЕНИЮ УЧЕНЫХ СТЕПЕНЕЙ ПРИ ИНСТИТУТЕ ФУНДАМЕНТАЛЬНЫХ И ПРИКЛАДНЫХ ИССЛЕДОВАНИЙ, "ТИИИМСХ" НАЦИОНАЛЬНЫЙ ИССЛЕДОВАТЕЛЬСКИЙ УНИВЕРСИТЕТ

ИНСТИТУТ ФУНДАМЕНТАЛЬНЫХ И ПРИКЛАДНЫХ ИССЛЕДОВАНИЙ

ХОЛИКОВ ШУКИРЖОН СОДИКОВИЧ

ЗОНДИРОВАНИЕ ПОДПОВЕРХНОСТНЫХ СВОЙСТВ СОЛНЦА С ПОМОЩЬЮ ПРОСТРАНСТВЕННО-ВРЕМЕННОЙ ГЕЛИОСЕЙСМОЛОГИИ

01.03.01 – Астрономия
(физико-математические науки)

ПРЕДСТАВЛЕНИЕ
по присуждению ученой степени доктора наук (DSc) по астрономии на основе научных публикаций без защиты диссертации

Ташкент – 2023

Тема диссертации доктора наук (DSc) по физико-математическим наукам зарегистрирована в Высшей аттестационной комиссии при Кабинете Мнистров Республики Узбекистан за номером B2022.3.DSc/FM202.

Результаты исследований выполнены в Университете Ниццы (Франция), Университете Цин-Хуа (Тайвань), Национальной солнечной обсерватории (США) и в Институте фундаментальных и прикладных исследований при “ТИИИМСХ” Национальный Исследовательский университет.

Представление научного исследования на трех языках (узбекский, английский и русский (резюме)) размещено на веб-странице Научного совета (www.ifar.uz) и Информационно-образовательном портале “Ziyonet” (www.ziyonet.uz).

Представление научного исследования состоится «**_01_**» **_августа_ 2023 года в _16^{00}_ часов** на заседании Научного Совета **DSc.03/31.03.2022.T/FM.10.04** по защите диссертаций на соискание ученых степеней при Институте фундаментальных и прикладных исследований, “ТИИИМСХ” Национальный Исследовательский университет по адресу: 100000, г. Ташкент, Qori Niyaziy Street 39, Институт фундаментальных и прикладных исследований, Зал 108; Тел.: 71 237-09-61; email: info@ifar.uz.

С представлением научного исследованияможно ознакомиться в Информационно-ресурсном центре при Институте фундаментальных и прикладных исследований, “ТИИИМСХ” Национальный Исследовательский университет (регистрационный номер ____) (Адрес: 100000, г. Ташкент, Qori Niyaziy Street 39, Институт фундаментальных и прикладных исследований, Зал 205; Тел.: 71 237-09-61).

Представление научного исследования разослано «____» _____ 2023 г.
(протокол рассылки № 49 от __ _____ 2023 г.).

Б.Ж. Ахмедов
председатель Научного совета по присуждению
ученых степеней, д.ф.-м.н., профессор

Э.Х. Каримбаев
ученый секретарь Научного совета по присуждению
ученых степеней, PhD ф.-м.н.

ВВЕДЕНИЕ (Аннотация к представлению)

Целью исследования является анализ данных гелиосейсмических наблюдений, полученных с земли и из космоса; изучение внутреннего строения Солнца, в частности: структуры подповерхностного течения и его эволюции во времени; активные области и их взаимодействие с солнечными акустическими колебаниями; широтный и глубинный профиль солнечной меридиональной циркуляции.

Задачами исследования являются:

- разработать статистически надежные и интеркалиброванные процедуры анализа данных для выполнения гелиосейсмического анализа большого объема;
- точные измерения параметров солнечных колебаний низкой степени, извлечение научных результатов и интерпретация полученных данных;
- изучение взаимосвязи между временем и расстоянием наблюдений солнечных колебаний, выполненных с использованием детекторов высокого разрешения;
- измерения и понимание механизма возникновения активных областей в зоне глубокой солнечной конвекции;
- разработать новые методы частотно-пространственной фильтрации доплерограмм высокого разрешения и внедрить их в стандартные программы анализа гелиосейсмических данных;
- провести измерения солнечного меридионального потока, используя весь доступный набор данных, построит широтный и глубинный профиль потока.

Объектом исследования являются гелиосейсмические наблюдения, полученные в рамках международных проектов: Солнце как звезда и солнечные допплерограммы высокого разрешения, полученные как с земли, так и из космоса.

Предметом исследования являются измеренные свойства и характеристики солнечных колебаний, таблицы частот и других параметров, разработанные модели внутреннего строения Солнца.

Методы исследования: разработка процедур предварительной обработки и извлечения научных данных на современных вычислительных средствах. Усиление солнечного акустического сигнала путем фильтрации нежелательных источников сосуществующих компонентов из наблюдаемых. Исследование структур локального и глобального масштаба на Солнце путем измерения параметров акустических волн. Используя метод реконструкции изображения

солнечных колебаний с использованием коэффициентов сферических гармоник, которые были отфильтрованы или настроены для конкретных измерений. Такое обратное сферическое гармоническое разложение осуществляется в сферических координатах. Акустические измерения времени прохождения также производится только с использованием сферической геометрии, которая имеет решающее значение для исследования глубоких слоев недр Солнца.

Научная новизна исследования заключается в следующем:

представлены первые измерения таблиц частот солнечных колебаний низкого порядка обществу физики солнца.

впервые были получены оценки внутреннего вращения Солнца с использованием коэффициентов частотного расщепления IRIS.

впервые построено изображение пятна под поверхностью Солнца с использованием свойств акустических волн.

активная область, всплывающая из основания солнечной конвективной зоны, обнаружена на глубине 40-75 тыс. км ниже поверхности на 1-2 дня раньше появления на поверхности.

разработан новый метод позволяющий измерить акустический радиус Солнца с исключительной точностью.

выявлено доказательства того, что кажущаяся структура второй ячейки, о которой сообщают некоторые члены сообщества физиков Солнца в высоких широтах, не связана с поверхностным компонентом меридионального потока.

используя наземные наблюдения GONG, построена меридиональная составляющая потока, направленная к экватору;

Практические результаты работы. Проведены точные измерения частот акустических колебаний Солнца низкой степени. Было продемонстрировано, что с помощью гелиосейсмических методов возможно измерение акустического радиуса Солнца с превосходной точностью. Более того, наблюдения с Земли могут обеспечивать точность такого же уровня. Для астросейсмологических наблюдений можно применять гелиосейсмические методы низкой степени. Обнаружение активных областей до того, как они появятся на поверхности, является очень потенциальным инструментом для прогнозирования космической погоды. Измерения направленного к полюсу и обратного меридионального потока являются ценными компонентами для моделирования солнечного динамо и понимания цикла солнечной активности.

Достоверность полученных результатов исследования демонстрируется путем анализа данных, полученных четырьмя независимыми приборами.

Географическое положение и различие атмосферных условий, а также измерения на разной высоте солнечной атмосферы обеспечили естественные возможности калибровки параметров акустических колебаний Солнца за счет наличия общего сигнала во всех наблюдениях. Большинство полученных научных результатов получены как минимум из двух независимых проектных данных. Большинство восстановленных свойств внутренней структуры воспроизведены как по наземным данным, так и по данным, полученным из космоса.

Значение результатов исследования. Большая часть представленных здесь результатов не была ранее получена другими учеными или исследовательскими группами. В качестве примера автором работы разработано и применено обратное сферическое гармоническое разложение поверхностных колебаний Солнца. Визуализация активной области под поверхностью и измерения меридионального возвратного потока ждали своего открытия десятилетиями.

Внедрение результатов исследования.

Измерения, выполненные в этом исследовании, использовались в качестве ключевого компонента во многих исследованиях, связанных с физикой Солнца. Теоретическое моделирование солнечного динамо использовало профиль обратного меридионального потока для создания диаграммы бабочки солнечных пятен в своих моделях. Полярная меридиональная скорость циркуляции по нашим измерениям является наиболее важным компонентом в моделях полярных регионов, основанных на механизме переноса потока, которые играют важную роль в прогнозировании цикла солнечной активности.

Публикации результатов исследований.

Результаты, полученные в рамках данной докторской работы, представлены в 18 рецензируемых статьях, опубликованных в престижных научных журналах, рекомендованных Высшей аттестационной комиссией Республики Узбекистан для публикации основных научных результатов докторской диссертации и размещенных в Web of Science. научная база данных.

Структура и объем представление. Представление состоит из введения, пяти глав и заключения. Объем Представление составляет 116 страниц.

ВЫВОДЫ

В данном представлении приведены следующие основные научные результаты, полученные путем анализа более чем 30-летних гелиосейсмических наблюдений:

1. Предложено решение задачи заполнения пробелов на основе автокорреляционной функции наблюдаемых солнечных колебаний низкой степени. Этот конкретный метод использует функцию автокорреляции наблюдаемых колебаний для эффективного создания долгосрочных временных рядов. Разработанный подход особенно эффективен при работе с наземными солнечными неразрешенными наблюдениями полного диска, где пробелы в данных типичны.

2. Приведены таблицы частот солнечных колебаний низкого порядка, измеренных в рамках проекта IRIS. В дополнение к частотам также сгенерированы такие параметры, как ширина линий, амплитуды мод, коэффициенты разделения и их временные вариации в течение цикла солнечной активности. Исследованные параметры дают важную информацию о свойствах и характеристиках солнечных колебаний.

3. Получены значительные вариации амплитуд корреляции волновых пакетов с солнечным циклом. Показано, что максимальное возмущение, связанное с солнечной активностью, локализовано в узком слое непосредственно под фотосферой. Из наших результатов следует, что максимальное возмущение возникает на глубине (0,83-0,85)$R_{\odot}$.

4. Первое гелиосейсмическое изображение солнечного пятна под поверхностью Солнца реконструировано с использованием свойств соотношения времени и расстояния солнечных акустических волн. Обнаружено, что корень пятна может достигать глубины до 40 тыс. км, что указывает на его значительное присутствие в недрах Солнца.

5. Подтверждены акустические аномалии времени пробега из-за появления активных областей из глубокой солнечной конвективной зоны. Эти акустические аномалии времени прохождения дают четкую карту всплывающих активных областей на глубинах от 40 до 75 тыс. км на Солнце. Важно отметить, что эта карта становится видимой на несколько дней раньше, чем активные области появляются на поверхности Солнца. Это говорит о том, что акустические сигналы могут обеспечивать заблаговременное предупреждение или указание (предвестники) на формирование и появление активных областей.

6. Определен акустический радиус Солнца и его временные вариации. Измерения, полученные из наземных наблюдений GONG и космических наблюдений MDI, показывают согласованность, указывая на то, что акустические сигналы распространяются через солнечное ядро аналогичным образом. Исключительная точность используемой методики измерения позволяет

определить временные вариации акустического радиуса Солнца в пределах долей секунды.

7. Получены подробные измерения направленного к полюсу меридионального течения в зависимости от широты и глубины. Наши измерения включают также временные вариации в течение двух фаз солнечной активности. Мы нашли доказательства того, что очевидная структура второй ячейки, о которой сообщают некоторые члены сообщества физиков Солнца в высоких широтах, не связана с поверхностным компонентом меридионального потока. Вместо этого, вероятно, это проявление артефактов, вызванных углом наклона Солнца.

8. Измерен обратный поток, направленный к экватору, предсказанный моделями солнечного динамо, который ждал своего открытия более двух десятилетий. Это стало возможным после удаления систематического эффекта из наших меридиональных измерений времени прохождения, вызванного изменениями высоты формации линий на солнечном диске,

ЭЪЛОН ҚИЛИНГАН ИШЛАР РЎЙХАТИ
LIST OF PUBLISHED WORKS
СПИСОК ОПУБЛИКОВАННЫХ РАБОТ

Бўлим I (part I; часть I)

1. Tripathy, S., Jain, K., Kholikov, S., Hill, F., Rajaguru, S.~P., Cally, P.~S., " A study of acoustic halos in active region NOAA 11330 using multi-height SDO observations", Advances in Space Research, 61, 691, (2018), doi: 10.1016/j.asr.2017.10.033.
2. Boning, V. G., Roth, M., Jackiewicz, J., Kholikov, S., " Inversions for Deep Solar Meridional Flow Using Spherical Born Kernels", ApJ, 845, 2, (2017), doi: 10.3847/1538-4357/aa7af0.
3. Boning, V. G., Roth, M., Jackiewicz, J., Kholikov, S., " Validation of Spherical Born Approximation Sensitivity Functions for Measuring Deep Solar Meridional Flow", ApJ, 838, 53, (2017), doi: 10.3847/1538-4357/aa6333
4. Jackiewicz, J., Serebryanskiy, A., Kholikov, S., " Meridional Flow in the Solar Convection Zone. II. Helioseismic Inversions of GONG Data", ApJ, 805, 133, (2015), doi: 10.1088/0004-637X/805/2/133.
5. Keys, D., Kholikov, S., Pevtsov, A., "Application of Mutual Information Methods in Time-Distance Helioseismology", Solar Physics, 290, 659, (2015), doi: 10.1007/s11207-015-0650-y.
6. Kholikov, S, Hill, F., " Meridional-Flow Measurements from Global Oscillation Network Group Data", Solar Physics, 289, 1077, (2014), doi: 10.1007/s11207-013-0394-5.
7. Kholikov, S., Serebryanskiy, A., Jackiewicz, J., " Meridional Flow in the Solar Convection Zone. I. Measurements from GONG Data", 784, 145, (2014), doi: 10.1088/0004-637X/784/2/145.
8. Kholikov, S., " A Search for Helioseismic Signature of Emerging Active Regions", Solar Physics, 287, 229, (2013), doi: 10.1007/s11207-013-0321-9.
9. González Hernández, I., Komm, R., Kholikov, S., Howe, R., Hill, F., " Meridional Flow Observations: Implications for the current Flux Transport Models", JphCS, 271a012073, (2011), doi: 10.1088/1742-6596/271/1/012073.
10. Kholikov, S., González Hernández, I., Hill, F., Leibacher, J., " Meridional-Flow Measurements from 15 Years of GONG Spherical-Harmonic Time Series", JPhCS, 271, 012052, (2011), doi: 10.1088/1742-6596/271/1/012052.
11. Kosovichev, A., Basu, S., Bogart, R., Duvall, T.~L., González Hernández, I., Haber, D., Hartlep, T., Howe, R., Komm, R., Kholikov, S., Parchevsky, K.V., Tripathy, S., Zhao, J., " ocal helioseismology of sunspot regions: Comparison of ring-diagram and time-distance results", JphCS, 271,012005, (2011), doi: 10.1088/1742-6596/271/1/012005.

12. Burtseva, O., Hill, F., Kholikov, S., Chou, D.Y., “Lifetimes of High-Degree p Modes in the Quiet and Active Sun”, Solar Physics, 258, 1, (2009), doi: 10.1007/s11207-009-9399-5.
13. González Hernández, I., Kholikov, S., Hill, F., Howe, R., Komm, R., “Subsurface Meridional Circulation in the Active Belts”, Solar Physics, 252, 235, (2008), doi: 10.1007/s11207-008-9264-y.
14. González Hernández, I., Kholikov, S., Hill, F., Howe, R., Komm, R., JphCS, 118, 012081, (2008), doi: 10.1088/1742-6596/118/1/012081.
15. Burtseva, O., Kholikov, S., Hill, F., “Latitudinal distribution of travel times in the upper solar convection zone”, JphCS, 118, 012080, (2008), doi: 10.1088/1742-6596/118/1/012080.
16. Kholikov, S., Hill, F., “Acoustic Radius Measurements from MDI and GONG”, Solar Physics, 251, 157, (2008), doi: 10.1007/s11207-008-9205-9.
17. Burtseva, O., Kholikov, S., Serebryanskiy, A., Chou, D.Y., “Effects of Dispersion of Wave Packets in the Determination of Lifetimes of High-Degree Solar p Modes from Time Distance Analysis: TON Data”, Solar Physics, 241, 17, (2007), doi: 10.1007/s11207-007-0325-4.
18. Hsiang-Kuang Chang, Dean-Yi Chou, Barry LaBonte & the TON Team, “Ambient acoustic imaging in helioseismology”, Letters to nature, 389, 825, (1997), doi: https://doi.org/10.1038/39822.

Бўлим II (part II; часть II)

19. Hughes, A, Jain, K., Kholikov, S. and the NISP Interior Group, “GONG Classic Merge: Pipeline and Producs”, eprint arXiv:1603.00836, 2016, doi: 10.48550/arXiv.1603.00836
20. Jain, K., Tripathy, S., Kholikov, S., Hill, F., “ Inhomogeneous Power Distribution in Magnetic Oscillations”, arXiv e-prints, 1003.5013, (2010), doi: 10.48550/arXiv.1003.5013
21. Kholikov, S., Roxburgh, I.~W., Vorontsov, S.~V., “ Small frequency separations as seen in the autocorrelation function of the whole-disk measurements”, Stellar Structure and Habitable Planet Finding, 539, 331, (2004), https://ui.adsabs.harvard.edu/abs/2004ESASP.538..331K.

“Fan va innovatsiyalar” xalqaro ilmiy jurnali (International scientific journal “Science and Innovation”) tahririyatida tahrirdan o‘tkazilib, o‘zbek, ingliz va rus tillaridagi matnlari o‘zaro muvofiqlashtirildi (04.05.2023).

Bosishga ruxsat etildi 19.07.2023. Qog‘oz o‘lchami 60x84 – 1/16
Hajmi 7.25 b.t. 60 nusxa. Buyurtma № 0077.
TIQXMMI bosmaxonasida chop etildi.
Toshkent 100000, Qori-Niyoziy ko‘chasi 39 uy.